

Structural Investigations of Sol-gel Glasses Using Optical Probes

Submitted for the Degree of
Master of Science

Presented to
Dublin City University

by

Gerard Joseph Ennis, B.Sc.
School of Physical Sciences
Dublin City University

Research Supervisor
Dr. Colette M^c Donagh, B.Sc., Ph.D.

July 1992

Abstract

The optical spectroscopy of the europium ion has been used as a probe of the structural changes occurring as a function of processing temperature in sol-gel derived glasses. The fluorescence and fluorescence decay times of the Eu^{3+} ion were observed and changes in the emission spectra and decay measurements were interpreted in terms of the changes taking place within the sol-gel matrix. Measurements of the fluorescence decay time indicate abnormally short lifetime measurements for sol-gel derived glasses even at relatively high fabrication temperatures. This was construed as being due to residual OH groups remaining in the glass structure. Measurements also indicated the presence of a fast lifetime component superimposed upon the slower decay of the Eu^{3+} ion. This was interpreted as concentration quenching because of rapid energy transfer within clusters of the dopant europium ion.

Acknowledgements

It is a pleasure to thank Dr Colette M^c Donagh for all her help and encouragement over the last two years. I would also like to thank my fellow postgraduates Kevin Mellon, Kevin Devlin, Kevin M^c Guggan, Pauline Marron, Brian Hurley, Jim Campion, Mark and Siobhan Daly, Charles Markham, Liam Roberts, Simon M^c Cabe, Kieran Higgins and Brian Cummins who all made contributions in various shapes and forms to this report and provided many a laugh along the way.

I would also like to thank Brendan O Kelly at Trinity College Dublin for preparing the sol-gel samples and Dr John M^c Gilp and his research group at T C D for allowing me access to his laboratory for lifetime measurements and especially Z R Tang who stayed many a late night to help me complete them.

I am deeply indebted to Dr Martin Henry for both his encouragement and the facilities he extended me in the production of this thesis, and to Marian and Barbara who let me at their printer. I would also like to acknowledge the Co Kildare Vocational Education Committee for their financial support. Finally to my housemates, this report may be finished, but without your help and encouragement it might never have been, Thanks.

Declaration

This Thesis is based on my own work

Table of Contents

Abstract	1
Acknowledgements	ii
Declaration	iii
Table of Figures	vi
Chapter 1 Conventional Glasses and Sol-gel Glasses	
1 0 Introduction	1
1 1 Conventional Glass and Sol-gel glass	1
1.2 The Glassy or Vitreous State	2
1 3 Structural Characteristics of Glass	4
1 4 Sol-gel Derived Glasses	4
1 5 Methods of Sol-gel Glass Production	6
1 6 Conclusion	8
Chapter 2 Review of Rare Earth Ions As Fluorescent Probes	
2 0 Introduction	9
2 1 Fluorescence and Fluorescence Decay	9
2.2 Optically Active Ions	10
2 3 The Interaction of Light with Optically Active Ions	11
2 4 Transition Probabilities	12
2.5 Radiative and Non Radiative Transitions	14
2 6 The Nature of Europium Fluorescence	14
2 7 Conclusion	18
Chapter 3 The Experimental Systems	
3 0 Introduction	19
3 1 Fluorescence Measurements	19
3.2 Fluorescence Data Acquisition	19
3 3 Time Resolved Fluorescence Data Acquisition	20
3 4 Lifetime Measurements	21
3 5 The Nitrogen Laser	21
3 6 The SR400 SRS Gated Photon Counter	21
3 7 Lifetime Data Acquisition	22
3 8 Lifetime Data Analysis	24
3 9 Relationship Between Mean and Half Life	24
3 10 Multi Component Decays and Component Stripping	26
3 11 Data Analysis Program for Methods 1 and 2	29
3 12 Synthesis of the Samples Studied in this Report	31
3 13 Conclusion	33
Chapter 4 Eu³⁺ Fluorescence and Decay Measurements as a Function of Sol pH in Sol-gel Glasses	
4 0 Introduction	34
4 1 Materials Preparation as a Function of pH	34

4 2	Acid and Base Catalysis of Sol-gels	35
4 3	Fluorescence Studies of Base Catalysed Samples (pH=5 6)	35
4 4	Fluorescence Studies of Base Catalysed Samples (pH=8)	38
4 5	Lifetime studies for Sol-gels at pH=5 6 and pH=8	38
4 6	Structural Implications	41
4 7	Studies of Deuterated Sample set (Sample Set No 3)	44
4 8	Conclusion	46

Chapter 5 The Fluorescence Properties of the Eu³⁺ ion in sol-gel glass as a Function of Water:TEOS Ratio

5 0	Introduction	47
5 1	Variation of H ₂ O TEOS Ratios	47
5 2	Acid Catalysed Samples	47
5 3	Base Catalysed Samples	48
5 4	Conclusion	50

Chapter 6 Investigations of Aluminium-Europium Codoped Samples

6 0	Introduction	53
6 1	Rare Earth Doping of Conventional and Sol-gel Glasses	53
6 2	Neodymium Doped Glasses	54
6 3	Results and Discussion of Experiments on Aluminium Codoped Samples	54
6 4	Conclusion	63

Chapter 7 Soaking of Sol-gel Samples in a Europium Nitrate Solution

7 0	Introduction	64
7 1	Soaked Samples	64
7 2	Results and Discussion	64
7 3	Deuteration of the Sol-gel Pores	70
7 4	Conclusion	71

Concluding Remarks 72

References 74

Appendix 1 Programme Listing "Aver2"

Appendix 2 Programme Listing "Lifet"

Appendix 3 Programme Listing "Compstw"

Appendix 4 Programme Listing "Half of 84"

Appendix 5 Absorption of Eu³⁺ in a Glass and a Liquid

Table of Figures

Chapter 1

1.1 Atomic Distribution Comparison for Various Materials	2
1.2 Temperature-Volume Diagram for Glass	3
1.3 Structural Differences in Silica Based Materials	5
1.4 Hydrolysis and Condensation in the Sol gel	7

Chapter 2

2.1 The Excitation and Emission Process	10
2.2 Radiative and Non-radiative Processes between Two Energy Levels	15
2.3 Energy Levels of Europium	16
2.4 Emission Spectra of Eu^{3+} in Three Glass Types	17

Chapter 3

3.1 The Fluorescence Measurement System	20
3.2 The Operating Principle of Time Resolved Photon Counting	23
3.3 The Lifetime Measuring System	25
3.4 Multi-Component Decay Curve Analysis	27
3.5 Triggering Problems in Lifetime Data Acquisition	30

Chapter 4

4.1 Fluorescence Spectra of Sample Set No 1 .	37
4.2 Fluorescence Spectra of Sample Set No.2	39
4.3 Hydrolysis and Condensation as a function of pH...	42
4.4 Fluorescence Spectra of Acid Catalysed Samples...	43
4.5 Fluorescence spectra of Deuterated Samples	45

Chapter 5

5.1 Fluorescence Spectra of Acid Catalysed 200° Samples	49
5.2 Fluorescence Spectra of Base Catalysed 200° Samples	51

Chapter 6

6.1 Fluorescence spectra of 1.0% Aluminium Containing Samples	57
6.2 Fluorescence Spectra of 0.5% Aluminium Containing Samples	58
6.3 Fluorescence Spectra of 0.0% Aluminium Containing Samples	59
6.4 Lifetime Measurements for 0.5% Aluminium Sample	61
6.5 Lifetime Measurements for 0.0% Aluminium Sample	62

Chapter 7

7.1 Fluorescence Spectra for Various Soaked Samples ..	66
7.2 Fluorescence Spectra for Conventionally Doped Sol-gel Glasses	67
7.3 Fluorescence Spectrum of a Europium Nitrate Solution	68

Chapter 1

Conventional Glasses and Sol-gel Glasses

1.0 Introduction

The purpose of Chapter 1 is to provide the reader with a general introduction to the science and technology of glass and to the characteristics of sol-gel glasses. This chapter commences with an introduction to conventional glasses and their qualities.

1.1 Conventional Glass and Sol-gel Glass

Glass science and technology is probably one of man's oldest attempts at cultivating what is both an art and a science. American Plains Indians used obsidian, a silicate glass formed by volcanic activity, as a cutting tool which they chipped into knives. The technique of blowing air into a gob of molten glass refined the process of glassworking to produce some of the finest examples of decorative glass seen. These techniques invented hundreds of years ago are still in use today in the production of fine crystal for decorative purposes.

The raw materials for glass manufacture are still, as they were thousands of years ago, sand and limestone. There are hundreds of different recipes for making glass, each one specific to the type of application that the glass is for. The starting mixture is ground together along with 20 to 30 % of waste glass and this mixture is melted in tank furnaces in temperatures of up to 1500°C. Special scientific glass is made from the addition of special compounds to the above mixture or can be made from completely different starting materials, e.g. borate glasses. At this point the temperature is lowered to around 1000°C and the discoloration of the glass melt is removed by the addition of various metal oxides such as antimony or manganese. Depending on the composition the thick viscous melted glass is formed to the required shapes by casting, rolling or drawing.

1.2 The Glassy or Vitreous State and its Properties

Glasses are defined by a collection of parameters that describe what each type of glass particularly resembles, ie X-ray studies show that a glassy substance has no long range order of its atomic structure. It can be seen in Figure 1.1 that the distribution pattern of atoms in a glass has a strong resemblance to that of a liquid but specifically not to that of a crystalline

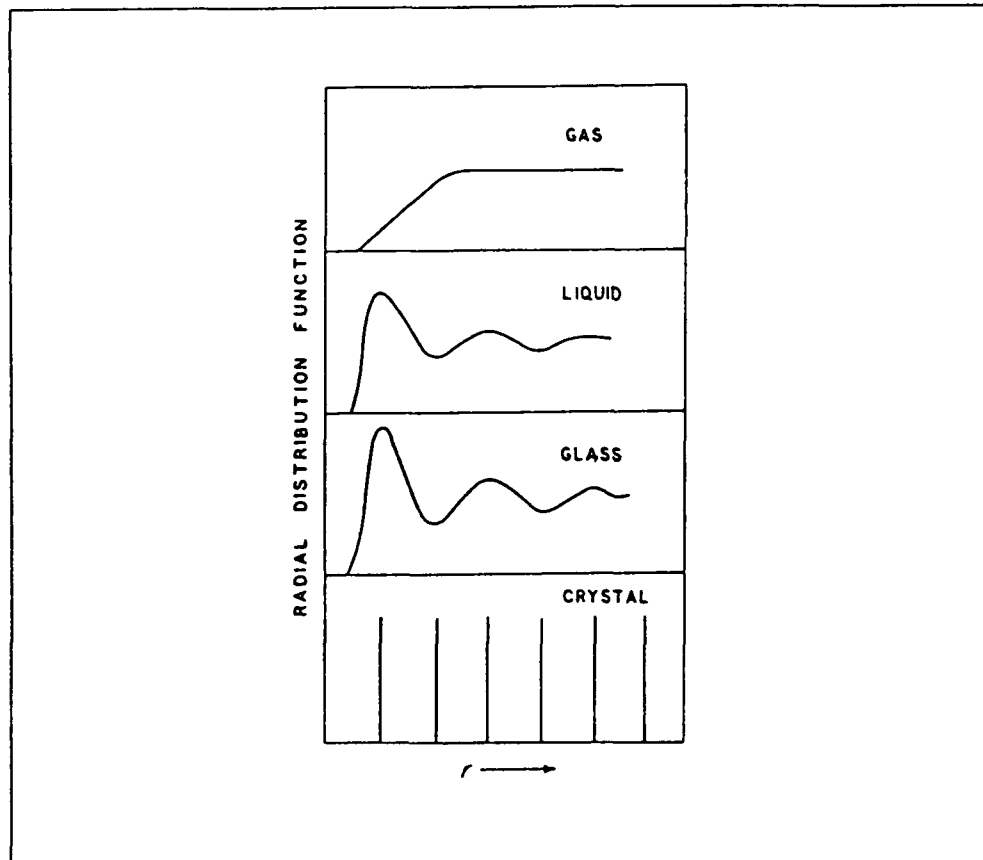


Figure 1.1 Atomic Distribution Comparisons for Various Materials

type of environment. When the contents of a glass melt start to cool its specific volume starts to decrease. When the melting point is reached a normal liquid will give up its heat of fusion and turn into the crystalline state. This does not happen to a glass melt unless the cooling rate of the melt is slow enough. The characteristic temperature volume curve of glass is of the general form shown in figure 1.2, ie, A to B to E.

If the cooling rate is fast then crystallization does not take place at the freezing temperature, T_f , but the volume decreases as the temperature is lowered, this is what is known as

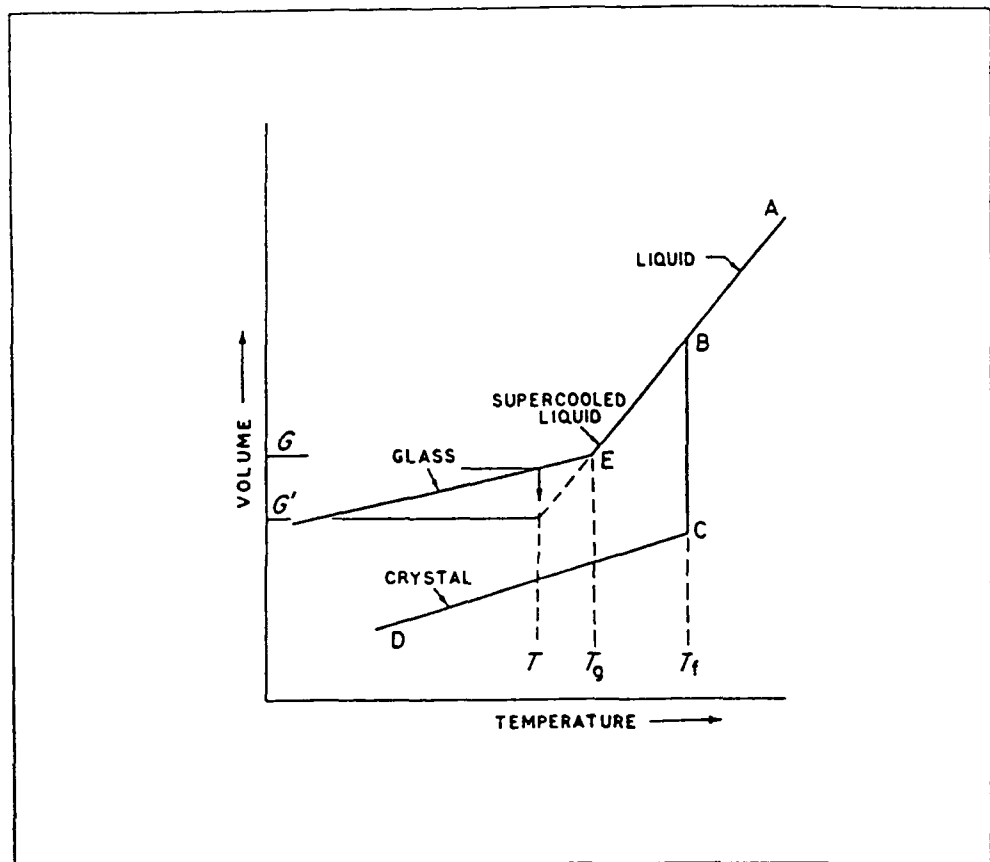


Figure 1.2 Temperature-Volume Diagram for Glass

supercooling At the point E, the glass transition temperature the volume expansion curve undergoes a change of slope It is at temperatures below T_g that the material is said to be a glass or in a vitreous state The point E on the graph does not have an exact position as it depends on the rate of cooling It is also found that if a temperature, known as the maintenance temperature, is kept fixed then the volume of glass decreases with time Eventually it reaches a certain equilibrium volume This phenomenon is called stabilization At room temperature the time required for stabilization is close to infinity At ordinary temperatures therefore glass structure shows no change with time.

To sum up this description of glassy properties, glass can be defined as a supercooled liquid which is maintained at a temperature below it's melting point so that no devitrification occurs

1.3 Structural Characteristics of Glass

Figure 1.3 shows how glass type structures can differ. The structure of a silica glass is compared to that of crystalline quartz. The structure is very similar in that both materials consist of SiO_4 tetrahedra, but in crystalline quartz, Figure 1.3(a), the bond angles are regular forming a hexagonal structure. In silica glass, Figure 1.3(b) however the bond angles are not constant and an irregular network structure is formed. Modifier ions disrupt the silicon network, Figure 1.3(c), and occupy holes so formed within the network. This is illustrated in Figure 1.3.

In order to quantify the types and characteristics of the glass forming materials Zachariasen, [1], formulated a set of rules for the structure of oxide glasses. He proposed that such glasses would have

1. An oxygen ion co-ordination number of 3 or 4 for the anions forming the structure
2. An irregular 3-D network formed by these triangular or tetrahedral structural units with the corner oxygen ions as shared points

Although there are other theories of glass structure, including some which propose some short range order, Zachariasen's theory is one of the widest held.

1.4 Sol-gel Derived Glasses

Sol-gel glasses offer many interesting advantages over conventional high temperature glasses. Perhaps the most striking of these is that a glass can be manufactured from what is initially a liquid precursor at room temperature. This negates the requirement for a high temperature processing system as the sol-gel glass need only be densified at relatively low temperatures. The method of sol-gel glass production means that the sol can be used to spin form thin glass films and coat optical fibres. These techniques have found current application in the fabrication of optical devices as chemical sensors and protective coatings, [2] [3]. Another advantage of the nature of the sol-gel process is the ease with which relatively large amounts of structure modifying ions can be added to the sol, [4] [5], thus results in the production of glasses with high enough dopant concentration to be considered as possible glass laser materials. However the major advantage of the sol-gel system is that it produces a more homogeneous glass than possible by conventional means. There are however some disadvantages to the sol-gel method for producing glass. Among these are that the sol-gel

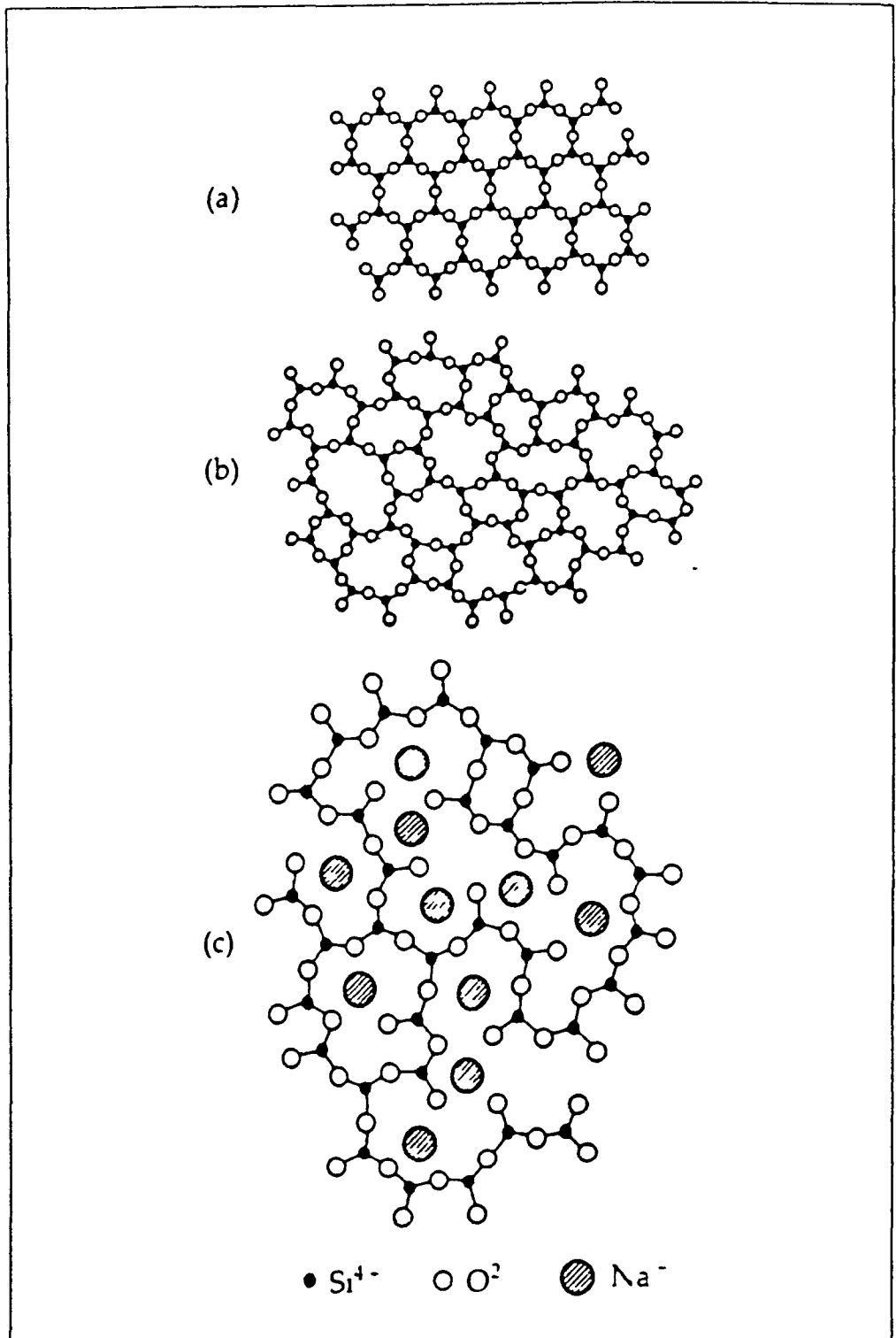


Figure 1.3 Structural Differences in Silica Based Materials

glass undergoes large scale shrinkage during drying and densification, as discussed in Section 1.5, and the production of monolithic pieces of sol-gel glass is non-trivial requiring careful drying and chemical controls, [6]

1.5 Methods of Sol-gel Glass Production

There are in general three methods of sol gel glass production. These methods are,

- (1) Gelation of a solution of colloidal powders
- (2) Hydrolysis and polycondensation of alkoxide precursor followed by hypercritical drying of the gels
- (3) Hydrolysis and polycondensation of an alkoxide precursor followed by ageing and drying under ambient pressure

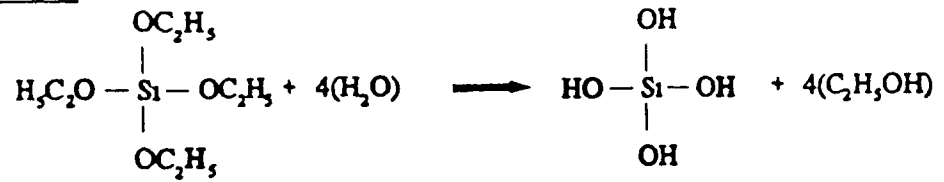
In this report all the sol-gel samples produced were manufactured by method 3. A silica gel may be formed by network growth from simultaneous hydrolysis and polycondensation of an organometallic precursor. Such a precursor is Tetraethylorthosilicate also known as TEOS. What happens is that a liquid alkoxide precursor, (TEOS) or in general any $\text{Si}(\text{OR})_4$, where the R can be CH_3 , C_2H_5 , C_3H_7 , is hydrolysed by mixing it with water,

The hydrolysed Si tetrahedra interact in a condensation reaction forming Si-O-Si bonds. Linking of additional $=\text{Si-OH}$ tetrahedra occurs as a polycondensation reaction and eventually results in an SiO_2 network. This process is illustrated in Figure 1.4.

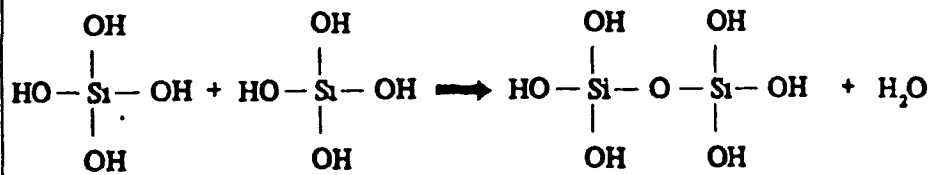
The H_2O and alcohol expelled by the reaction mechanism will eventually remain in the pores of the network now in place, until partial densification at moderate temperature and further densification at higher temperature removes the bulk of the hydrocarbon and O-H groups. As the silica network begins to link together the low viscosity fluid slowly changes until at the gelation there is a sudden increase in the viscosity and the solution takes on the shape of whatever mould it was poured into. At this stage of the process the samples used in this process were dried and variously fired at different temperatures. The term gel is often used to describe the solidified solution regardless of the following processing steps, but there is a difference. If the pore liquid, H_2O and alcohol, is removed at ambient pressure by evaporation, i.e. drying, the resultant dried gel is known as an xerogel. If the pore liquid is removed as a gas from the pore network under hypercritical drying conditions the remaining network is known as an aerogel.

The surface area of a dried gel is 100's m^2 per gramme. A dried gel still contains large concentrations of OH^- radicals chemisorbed onto the surface of the pore walls. Further heat

Hydrolysis



Condensation



Polycondensation

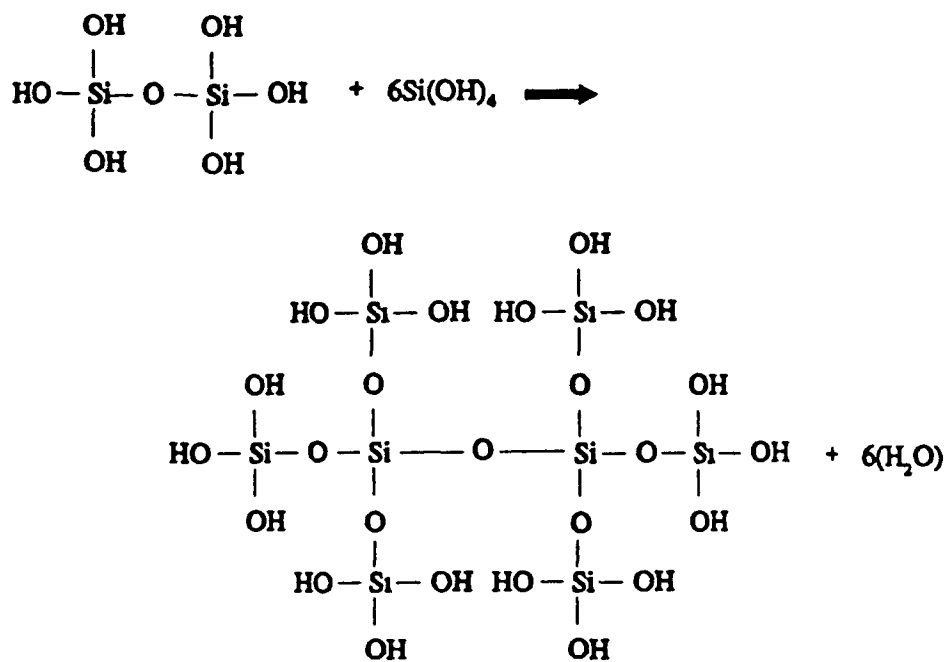


Figure 1.4 Hydrolysis and Condensation in the Sol Gel

treatment is required to remove these groups. The effect of remaining radical groups in the gel and partially densified structure is discussed in detail in Chapter 4. Heat treatment at high temperatures reduces the number of pores and their connectivity due to viscous phase sintering. This is known as densification and as it progresses the volume of the structure decreases and its density increases. The porous gel is transformed into a dense glass when all the pores have been removed. The densification temperature depends considerably on

- (A) The dimensions of the pore network and the connectivity of the pores
- (B) The surface area of the structure

Densification temperatures of the order of 1200-1500°C have been reported, with temperatures as low as 1000°C for samples produced by method 3. Silica glass produced by densification of porous silica gel is amorphous and nearly equivalent in structure and density to vitreous silica made by fusing quartz crystals or sintering of SiO₂ powders made by chemical vapour deposition (CVD) of SiCl₄.

1.6 Conclusion

This chapter has reviewed the characteristics of glassy media in general and the characteristics of sol-gel derived glasses in particular. Attention was drawn to the process of evolution of the glassy state in sol-gel materials.

Chapter 2

Review Of Rare-Earth Ions As Fluorescent Probes

2.0 Introduction

This chapter discusses the behaviour of optically active ions in glasses and glassy type materials. In order to understand the behaviour of these dopant ions it is necessary to have an understanding of some of the mechanisms of excitation, energy transfer and excited state decay that can occur in these doped insulating materials. The chapter commences with a discussion of the interaction of radiation with optically active materials and discusses absorption, luminescence and energy transfer. Next it examines the nature of europium fluorescence. Europium has been widely used as a structural probe of both crystalline and glassy environments, [1]. In this chapter the nature of the fluorescence emitted by the europium ion and the importance of the various transitions is discussed in terms of the environment experienced by the europium ion. This chapter also reviews phenomena reported by others and discusses their relevance with respect to similar results reported in Chapter 4.

2.1 Fluorescence and Fluorescence Decay

Research into optically active materials is fuelled by interest and need for optical devices such as lasers, LEDs, detectors etc at all the visible and industrial invisible wavelengths such as the near IR and the near UV. Research into optically active glasses is motivated by interest in such areas as fluorescent displays but more particularly by interest in glass lasers.

In order to understand the processes and terms discussed in this and later chapters it is important to firstly outline some of the phenomena associated with the interaction of optical radiation with an optically active material. Central to this discussion is the subject of fluorescence. Fluorescence involves the loss of energy radiatively as a species goes from a higher state to a lower energy state. There are several methods of exciting a species to a higher energy level. Photoluminescence is energy decay due to excitation by optical radiation. Other types of fluorescence are for example Electroluminescence a technology driven by the need for flat panel displays and Chemiluminescence an important source of study for chemists. The concept of luminescence is illustrated in Figure 2.1.

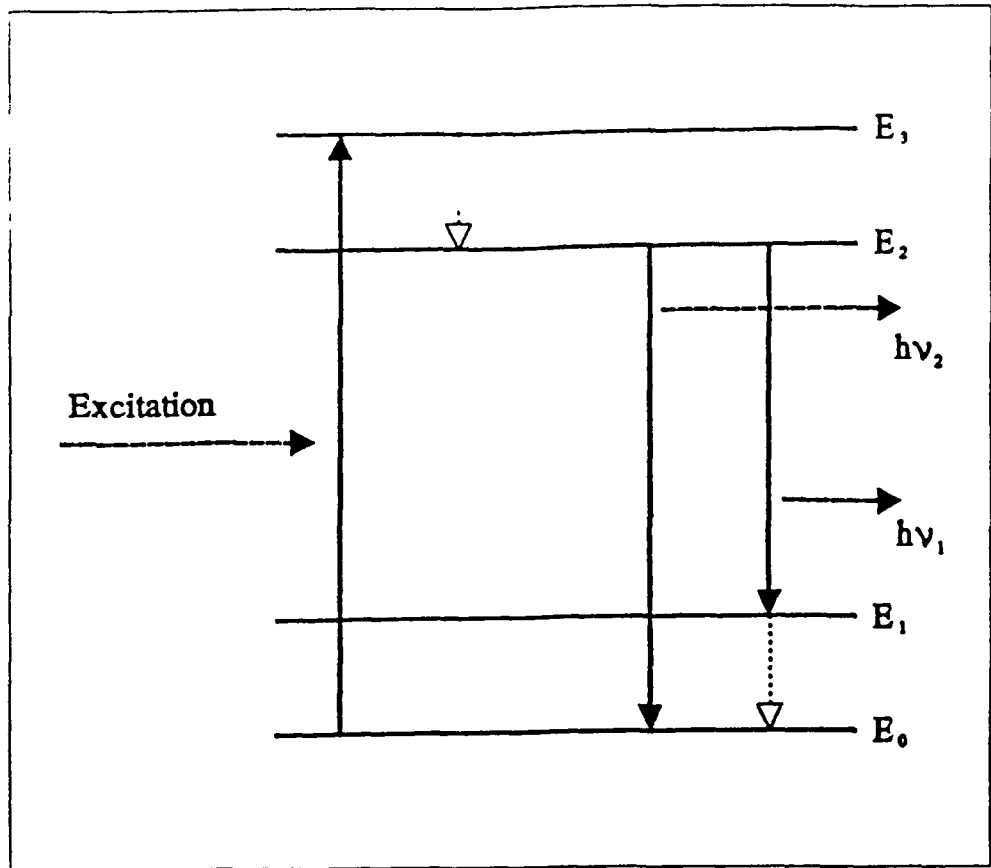


Figure 2.1 The Excitation and Emission Process

The ground state has energy E_0 and E_1 , E_2 and E_3 represent excited energy levels. Excitation of the material from E_0 to E_3 is achieved with the absorption of electromagnetic radiation. It is found that if the gap between some excited state and another state lower in energy is small, the excited state can decay non-radiatively to a lower state, [2]. Non-radiative decay takes the form of phonon vibrations through the material. In Figure 2.1 the emission is described by,

$$h\nu_1 = E_2 - E_1 \quad \text{Eqn 2.1}$$

$$h\nu_2 = E_3 - E_0 \quad \text{Eqn 2.2}$$

where ν is the frequency and h is Planck's constant.

2.2 Optically Active Ions

Many ions from the rare earth and transition metal series are optically active, by which is meant that their electronic configuration is such that they are sensitive to radiation in the "visible" region of the spectrum and can be excited to higher energy states by such wavelengths. A common example of an optically active ion in an insulator is the case of

Ruby, [2] This material is Al_2O_3 , (Aluminium Oxide), doped with a few percent of Cr^{3+} ions. The deep red is a result of the chromium having strong absorption in the blue and green. Ruby can also be pink and varying shades of red which is actually the effect of the varying concentrations of Cr^{3+} ions. The subject of dopant concentration is very important and will be discussed in detail later. Chromium, (as Cr^{3+}), in glass gives the glass a green colour, which indicates that the environment of the host matrix plays a large role in determining the emission characteristics of the dopant ion. The corollary of this is that if a deliberate doping of a glass with an optically active ion takes place then it should be possible to infer some sort of qualitative/quantitative information about the structure of the ions environment by examination of the optical properties of the activated ion.

The investigations on the optical characteristics of glasses reported in this study used Europium as an optical probe. Europium is a Rare Earth element or Lanthanide which occurs near the bottom of the Periodic Table. All these elements have unfilled 4f orbitals, which gradually fill up as the list of elements is crossed. The general form of their electronic configuration being denoted as

$$1s^2 2s^2 2p^6 3s^2 3p^6 3d^{10} 4s^2 4p^6 4d^{10} 4f^m 5s^2 5p^6 5d^m 6s^2, \quad \text{Eqn 2.3}$$

Their Atomic Numbers range from 58 for Cerium to 70 for Ytterbium. The number of electrons in the unfilled 4f shell varies from 1 to 13, while for Europium the number is 6. The electronic configuration of the triply ionised Europium ion is,

$$1s^2 2s^2 2p^6 3s^2 3p^6 3d^{10} 4s^2 4p^6 4d^{10} 5s^2 5p^6 4f^6 \quad \text{Eqn 2.4}$$

2.3 The Interaction of Light with Optically Active Ions

When an optically active ion is placed in a solid, the manner in which it interacts with visible radiation is governed by what the initial and final energy states of the ion will be and how strongly the ion interacts with the radiation. One of the commonest interactions is the process of absorption. Optical absorption occurs when an electron is optically excited from the ground state i to an excited state f . If a flux of photons N is incident upon an active medium of thickness d then, [3],

$$\frac{\delta N}{\delta x} = -Nk \quad \text{Eqn 2.5}$$

where k is the probability of absorption of a photon per meter and d is measured along the

x axis From the above then it can be seen that

$$\int_{N_{x=0}}^{N_{x=d}} \frac{\delta N}{N} = -k \int_{N_{x=0}}^{N_{x=d}} dx \quad \rightarrow \quad \ln\left(\frac{N_d}{N_0}\right) = -kd \quad \text{Eqn 2.6}$$

or in it's more usual form,

$$N_d = N_0 \exp(-kd) \quad \text{Eqn 2.7}$$

The intensity of the light I_0 is proportional to N_0 so therefore

$$I_d = I_0 \exp(-kd) \quad \text{Eqn 2.8}$$

k is called the absorption coefficient and varies with frequency of radiation, (ω) , so finally,

$$I_d(\omega) = I_0(\omega) \exp(-kd) \quad \text{Eqn 2.9}$$

The excitation from one state to another is however not random or straightforward and is discussed in terms of transition probabilities

2.4 Transition Probabilities

Visible radiation can interact with an activator ion in a number of different ways Two of the principal processes are

- 1 The Electric Dipole Process
- 2 The Magnetic Dipole Process,

Both of these interaction processes are characterised by transition probabilities If i is the initial state of a system before light is absorbed and f is the final state of the system after absorption, then the transition probability is, [4],

$$P_{(f)} = \left(\frac{2\pi}{\hbar}\right) V_{if}^2 \delta(E_f - E_i - h\omega) \quad \text{Eqn 2.10}$$

where V_{fi} is the matrix element of the transition and V is a Hamiltonian operator denoting the interaction energy of the transition between the ion and incident optical radiation. For an electric dipole transition, $V = \mathbf{p} \cdot \mathbf{E}$, where \mathbf{p} is the electric dipole moment of the transition and \mathbf{E} is the electric field intensity of the incident radiation. The value of \mathbf{p} the electric dipole moment is, [4],

$$\mathbf{p} = \sum_i e \mathbf{r}_i \quad \text{Eqn 2.11}$$

Where e is the electronic charge and the summation is over all the optically active electrons. For a magnetic dipole transition, the interaction term is $V = \boldsymbol{\mu} \cdot \mathbf{B}$, where $\boldsymbol{\mu}$ is the magnetic dipole operator and \mathbf{B} is the magnetic field strength of the radiation field. The value of $\boldsymbol{\mu}$ is given by, [4],

$$\boldsymbol{\mu} = \sum_i \frac{e}{2m} (\mathbf{l}_i + 2\mathbf{s}_i) \quad \text{Eqn 2.12}$$

where \mathbf{l}_i and \mathbf{s}_i are the orbital and spin angular momentum operators respectively. The magnetic dipole process is a much weaker process than the electric dipole process but nevertheless if a transition via the electric dipole process is forbidden then it may take place via a magnetic dipole process. The determination of what transitions may or may not take place are governed by Laporte Selection Rule, [4], [5]. What this says is that for an electric dipole transition to occur there must be a change in parity. For a Rare Earth ion all the free ion levels are formed by the same $4f^n$ configuration so transitions between these levels should only occur as magnetic dipole interactions. Admixing of states, [6], of opposite parity is required before the normally forbidden electric dipole transitions take place. This occurs with the mixing of the $4f^{n-1} 5d$ configuration into the $4f^n$ configuration, relaxing the Laporte selection rule and makes the electric dipole transition process possible. The physical requirement to allow a normally forbidden electric dipole process to occur is an asymmetric ligand field. In for example glass. The transition probabilities for intraconfigurational transitions of these Rare Earth ions in a glass host are site dependent. If the distribution of suitable sites for the rare earth ion is large the excited state decay mechanism will be highly nonexponential. This is the case in the glassy environment. Therefore it is the range of site geometries available to the dopant ion allied to the fact that the ion is in general residing in

a distorted site that is the reason the observed transitions via an electric dipole process become allowed

2.5 Radiative and Non Radiative Transitions

Many of the luminescent ions in solid/glassy environments have quantum efficiencies far below the theoretical limit of 1. An assumption can therefore be made that there exists some mechanism for radiationless decay whereby an ion can return to the ground state without emitting any radiation. The basis of this assumption is that there exists a coupling mechanism between the excited ion and the host matrix which allows an efficient transfer of energy between the ion and the host. This is achieved through phonon assisted decay.

Non-radiative transitions occur when the total energy of the phonons created in a transition equals the energy gap between the initial and final states. This is illustrated in Figure 2.2. The fluorescent decay time τ of the transition can be described as follows,

$$\frac{1}{\tau} = \frac{1}{\tau_R} + \frac{1}{\tau_{NR}} \quad \text{Eqn 2.13}$$

where τ_R is the radiative decay time and τ_{NR} is the non radiative decay or

$$W = W_R + W_{NR} \quad \text{Eqn 2.14}$$

where W_R and W_{NR} are the radiative and non-radiative transition rates.

2.6 The Nature Of Europium Fluorescence

The fluorescence of the Eu^{3+} ion in an environment can reveal a lot about its surroundings. The fluorescence spectra of Europium doped sol gel glasses were studied to elucidate the process of the sol to gel to glass transition, and to compare the fluorescence spectra with those of conventionally produced high temperature glasses, [7]. The Eu^{3+} ion, which has a configuration $4f^6 5s^2 5p^6$, has strong f-f transitions in the visible. The ground state of the ion is the 7F_0 state. The principle Europium transitions of interest are the 5D_0 - 7F_J transitions where $J=0, 1, 2$. All of these three transitions emit light within the wavelength band of 550-650nm. Fluorescence occurs from the excited D state to any level of the F multiplet. An energy level diagram is shown in Figure 2.3.

In the materials examined the fluorescence transitions studied were from the D level to the

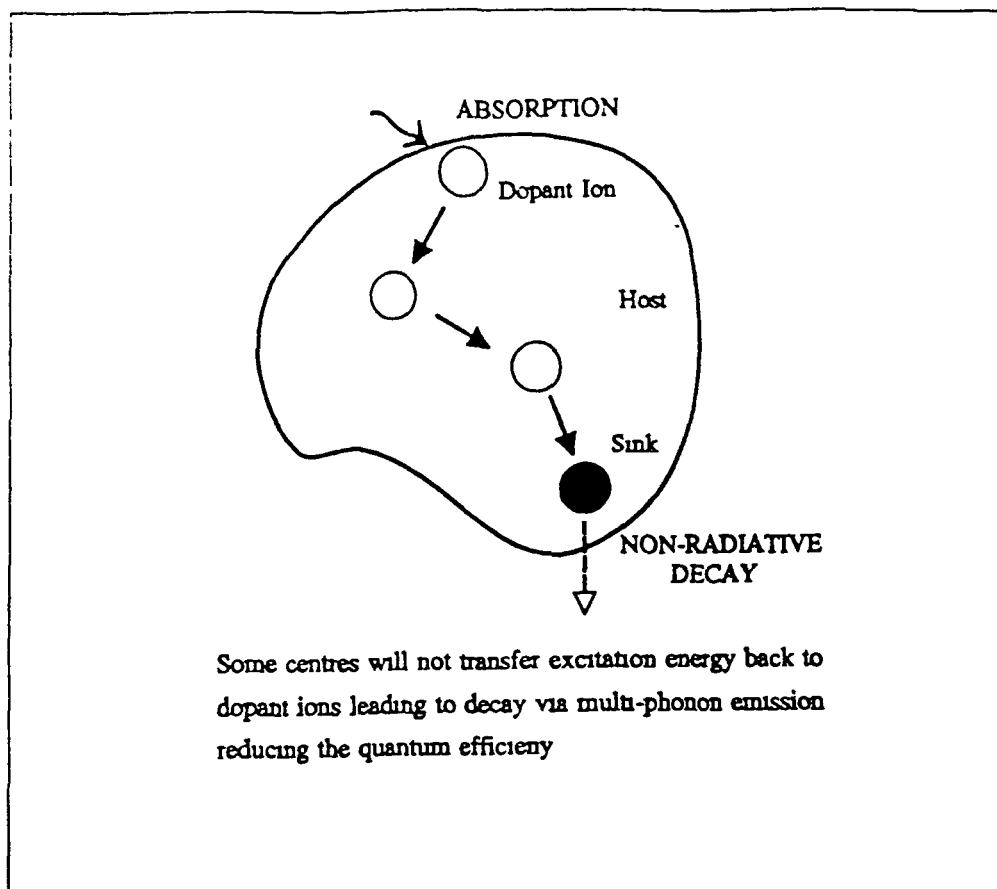


Figure 2.2 Radiative and Non - Radiative Processes Between Two Energy Levels

various levels of the F multiplet described above. In the glassy state the transitions are split by the influence of the surrounding ligand field. In a glass however, because of inhomogeneous broadening the levels are not always clearly resolvable. These levels are said to be degenerate and their number given by $2J+1$. Therefore the $J=0$ level has 1 resolvable transition, the $J=1$ level has 3 resolvable transitions and the $J=2$ level has 5 transitions not all resolvable. It should be noted that in the case of sol-gel glasses that the number of resolvable transitions depends largely on the Europium ions environment. This is especially so in the case of the sol and dried gel stage of the sol-gel glass synthesis.

In Figure 2.4, 3 fluorescence spectra, from sol-gel glass (A), conventional silicate (B) and borate glass (C) are displayed.

In Figure 2.4 the three transitions and the associated splitting for each can be seen for three types of glass. (See Appendix 5 for absorption of Eu^{3+} in a glass and a liquid). The ${}^5\text{D}_0$ - ${}^7\text{F}_0$ transition is a singlet transition and does not split under the influence of the ligand field, [8]. Its width is a result of the inhomogeneous broadening induced by a large collection of different sites made available to the ion in the glass environment. And it can be used as an

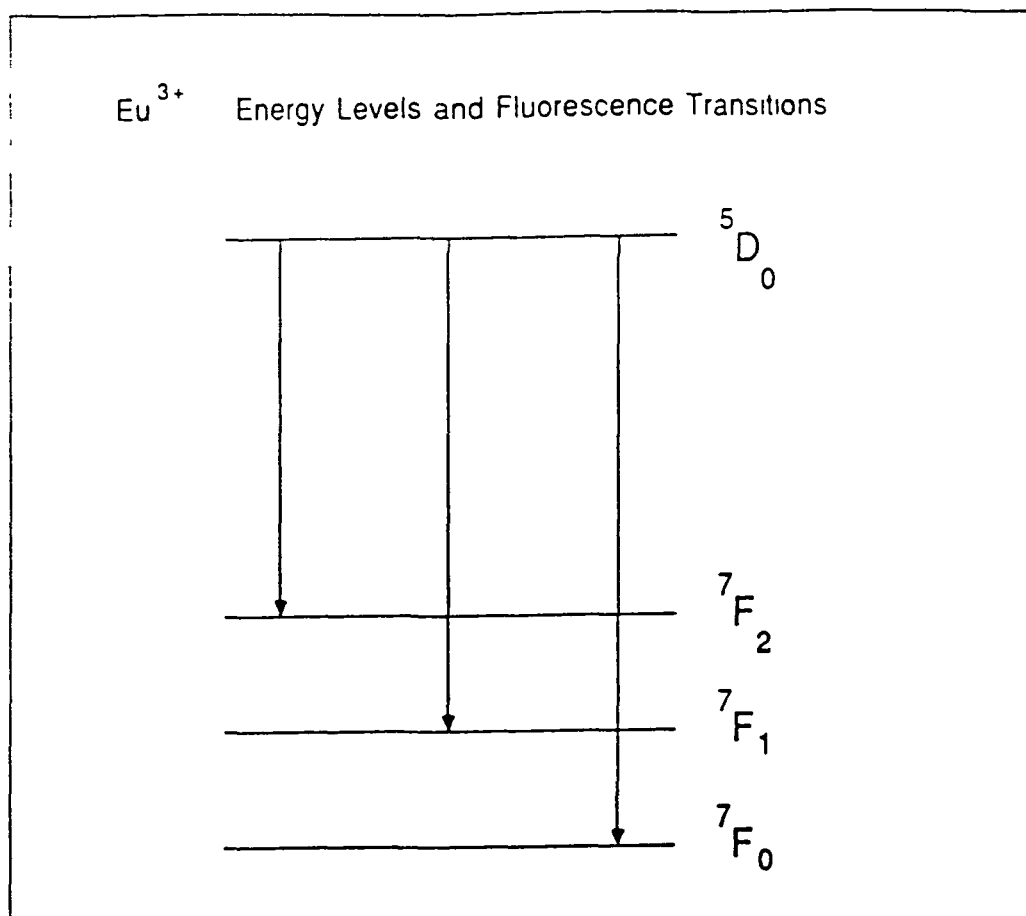


Figure 2.3 Energy Levels of Europium

indicator of the range of sites in which the ion resides. To convince oneself of this one should compare the width of the $^5D_0 \rightarrow ^7F_0$ transition in the symmetrical solvation shell of a solution, (ie very narrow), with the same broadened transition of the ion in an asymmetric, (ie glassy), environment. (See Section 7.2, Figure 7.3)

The $^5D_0 \rightarrow ^7F_1$ transition is an allowed magnetic dipole process, [6]. For a magnetic dipole transition to occur the initial and final states must have the same parity. This transition takes place within the 4f shell. The importance about this transition is that the symmetry of the environment surrounding the Eu³⁺ ion does not affect the transition probability, [6], and hence the intensity which is what we want to measure.

For an electric dipole process to occur there must be a change in parity. The $^5D_0 \rightarrow ^7F_2$ transition is an electric dipole process, [6]. This transition occurs within the 4f shell and so is forbidden by the Laporte Selection Rule. For it to occur it needs a mixing of parity which can happen if the Europium ion experiences an asymmetrical field, [8]. This is why the intensity of the transition to the 7F_2 state increases dramatically in going from the sol to the gel to the glassy

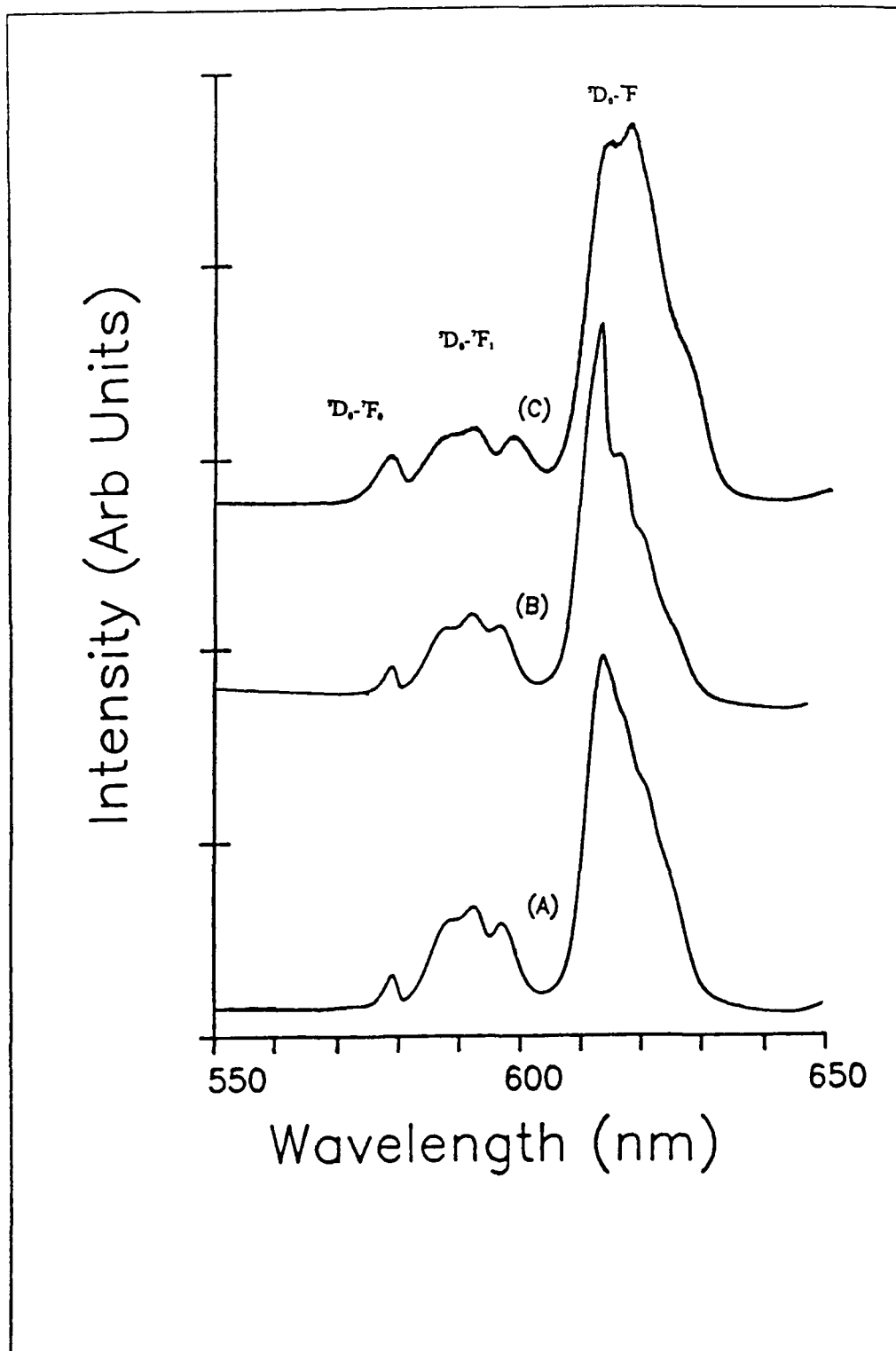


Figure 2.4 Emission Spectra of Eu³⁺ in Three Glass Types. Sol-gel glass (A), conventional silicate (B) and borate glass (C).

type matrix. The intensity of the transition is dependent on the asymmetry of the Europium ions environment.

In an attempt to quantify the asymmetry dependence of the emission intensity, Gallagher [8], proposed that a measurement of the ratio of the two transitions ${}^5D_0 \rightarrow {}^7F_2$ and ${}^5D_0 \rightarrow {}^7F_1$ should be made. This ratio, the fluorescence ratio, is called the R_{FL} ratio throughout the report.

$$R_{FL} = \frac{{}^5D_0 - {}^7F_2}{{}^5D_0 - {}^7F_1} \quad \text{Eqn 2.15}$$

As can be seen from the Equation 2.15 above, as the intensity of the ${}^5D_0 \rightarrow {}^7F_2$ transition increases the R_{FL} value increases. Therefore R_{FL} is a measure of the asymmetry of the environment surrounding the Eu^{3+} ion. The R_{FL} value is tabulated for most of the fluorescence spectra shown in this thesis.

2.7 Conclusion.

This chapter has reviewed some of the phenomena associated with optically active ions in glass and glassy type media. The discussion presented in this chapter provided an introduction to the ideas of fluorescence, radiative and non radiative transitions. These topics are the main phenomena studied in the investigation of the Europium ions behaviour in the Sol Gel type materials. Also discussed were the current ideas on the characteristics of the ions in these types of materials.

Chapter 3

The Experimental Systems

3.0 Introduction

The experimental system used in this project is outlined in this chapter. There were basically two different experimental procedures followed, one for the fluorescence measurements over a wavelength range and another to determine the lifetime of the Eu^{3+} ion in the sol-gel system. The differing excitation sources and the data acquisition techniques employed are described.

3.1 Fluorescence Measurements

The excitation source used was a 200W Applied Photophysics water cooled Xenon Arc Lamp. Light at a wavelength of 398nm, (see Appendix 5), was selected by passing the lamps output through a Minimate Monochromator, (see Figure 3.1). This was then focused onto the sample under investigation. The fluorescence from the sample was collected and focused onto the slit of a Jobin Yvon 1m focal length spectrometer, where it was detected by a Hamamatsu R928 photomultiplier tube. The Xenon lamp was not the only source used for fluorescence measurements. An Ultra Violet striplamp peaking at 368nm was also used as well as a PRA pulsed nitrogen laser. The use of the nitrogen laser was mainly confined to the measurement of excited state lifetimes. These techniques are described in the following section.

3.2 Fluorescence Data Acquisition

The fluorescence data acquisition was achieved via an Acorn Electronics Analogue Interface Board. This was connected to a BBC Master microcomputer. The experiment was controlled by the BBC Basic computer program "Aver2" (for listing see Appendix 1). Briefly this program allowed the operator to select both the starting and finishing wavelengths and the increment size. Another feature of the program was that it permitted the operator to time average the signal by explicitly requesting how many times each data point was to be sampled. This coupled with the background (ambient count) subtraction provided the operator with a greatly improved signal to noise ratio.

3.3 Time Resolved Fluorescence Data Acquisition

In order to use a pulsed source as an excitation source a different data acquisition technique was necessary. In this case the pulsed source was the Nitrogen Laser mentioned already. A programme "Lifet", (for listing see Appendix 2), was written by Devlin and Ennis, in order to enable the BBC microcomputer to analyse data from the time resolved fluorescence measurements. To control the photon counter, (described later) the nitrogen laser receives a series of trigger pulses from a function generator. Upon receipt of the same trigger pulse the photon counter enables a counting gate for a predetermined length of time. During this time period the detector signal is measured. Following this the gate is disabled until the next trigger pulse and the spectrometer is incremented by one step.

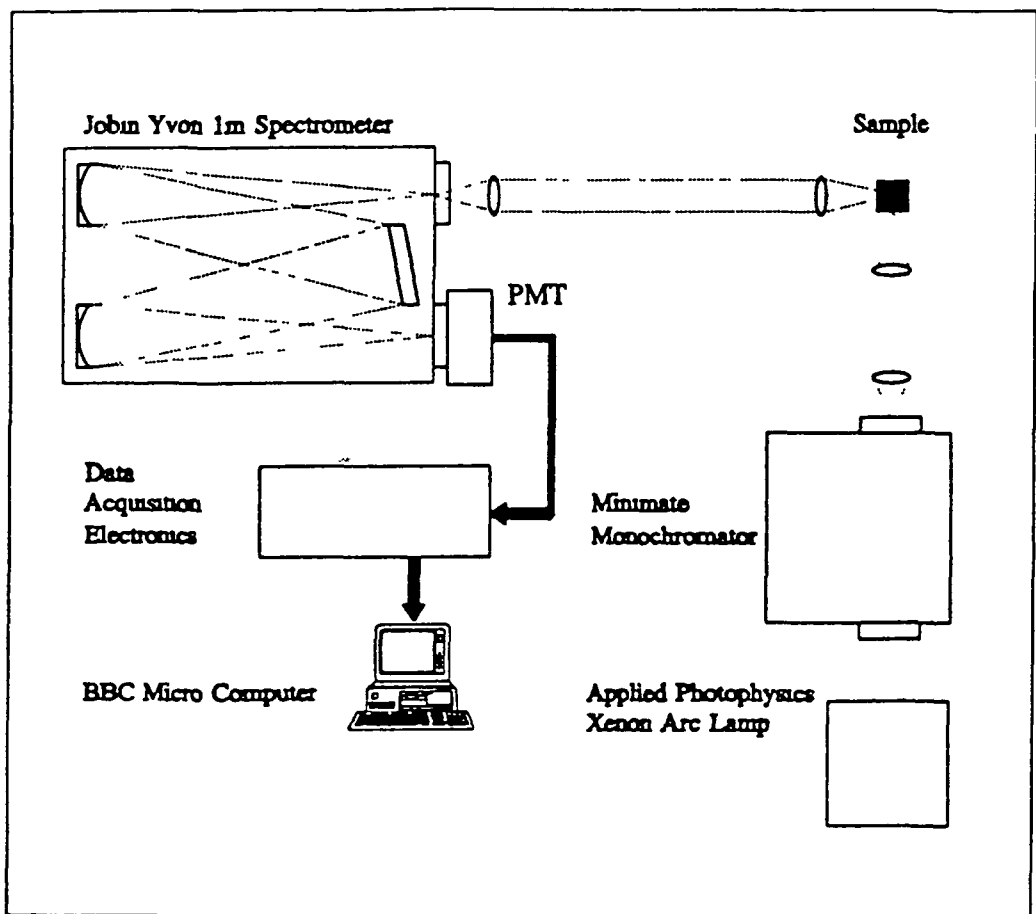


Figure 3.1 The Fluorescence Measurement System

3.4 Lifetime Measurements

The two main workhorses of the fluorescence lifetime measurement system are

- 1 The Stanford Research Instruments SR400 photon counter and
- 2 The PRA/Laser Photonics Pulsed Nitrogen Laser

3.5 The Nitrogen Laser

The main advantages of a pulsed molecular nitrogen laser are its simplicity of operation and its relatively high repetition rate. Atmospheric pressure nitrogen lasers can produce nanosecond or sub nanosecond pulses in the near ultraviolet. The 337nm output is the first choice source for many as a dye pump for wavelengths from 360nm to approx 1 μ m for experiments in dye laser spectroscopy and the study of photochemical kinetics. The laser used in these experiments was operated at 45 and 80 psi. Operating nominally at 15Kv, a very fast transverse excitation across a 6mm rectangular cross section channel produced a 0.6 nanosecond duration discharge. Triggering of the discharge was via a trigger transformer and spark gap arrangement. The physical description of what actually happens is reasonably straightforward. The Nitrogen molecules are excited by a fast high voltage discharge. This populates the upper laser level of the nitrogen molecule. This level is an excited electronic state with a lifetime of about 40ns, emitting a photon at 337nm when dropping to the lower laser level. The laser transition involves changes to both the electronic and vibrational energy levels. As a result careful examination of the neutral nitrogen spectrum at high resolution reveals that the 337.1nm transition includes many discrete lines arising because the initial and the final states have a multitude of vibrational sublevels. By laser standards Nitrogen lasers are broadband but compared to a UV lamp for example they can be considered as monochromatic.

3.6 The SR400 Stanford Research Systems Gated Photon Counter

The SR400 Gated Photon counter provides the user with the facility to repetitively measure excited lifetimes. The function generator (see Figure 3.3) simultaneously triggers both the nitrogen laser and the photon counter. The instrument is configured to count in the "A,B for Preset T" mode which means that on being enabled via a trigger pulse the counters, A and B, wait a specified time, (determined by the operator), before counting. The principle of time resolved photon counting is illustrated in Figure 3.2

The counter T is used to determine the number of times the photon count is measured at a specific delay time, in other words how many triggers of the nitrogen laser for each data point. The T counter is normally set to 100 triggers so therefore the A counter counts the photons falling within its gate width 100 times. The counting method is illustrated in Fig 3.3. Because the Nitrogen laser is a gas discharge based light source its output power can vary significantly from pulse to pulse, this can be due to a number of reasons but in our experimental setup it is due mainly to the degradation of the nitrogen gas in the triggering spark gap and the resultant fouling of the spark gap itself. This problem was overcome by forcing the spark gap to allow high pressure nitrogen gas to bleed slowly through it, this allied to careful alignment of the transverse electrodes and control of the operating pressure of the nitrogen produced a vast improvement in the pulse to pulse reproducibility of the laser's output and also in the maximum operating repetition rate to a previously unobtainable level of approximately 10 Hz. However despite this increase in reliability it was necessary to compensate for small variations in the pulse to pulse reproducibility. To that end the counter "B" was set to an initial delay of 30 μ sec's and then allowed to count for a gate width of 1msec. This in effect measured the total intensity of the fluorescence pulse. The count figure for both the A gate and the B gate was then transferred to the BBC microcomputer via the IEEE interface board and the data was normalized with respect to the intensity of the excitation pulse, ie counter A's contents divided by counter B. The Lifetime systems are depicted in Figure 3.3. In addition to the lifetime acquisition system in use at DCU some collaborative work was done at the University of Dublin, Trinity College. The experimental system used is shown schematically in Fig 3.3 and consisted of a Spectron Nd Yag pumped dye laser which was filled with Rhodamine dye. The dye laser's output was frequency doubled using a KDP crystal and the excitation wavelength used was 318nm, (see Appendix 5 for absorption spectrum of Eu^{3+}) The output of the photomultiplier tube was fed to the SR400 photon counter and the ambient count and the pulse to pulse normalization was performed as described above.

3.7 Lifetime Data Acquisition

The lifetime data acquisition was accomplished by the BBC Basic program "Lifet", (see Appendix 2 for listing). This controlled the SR400 photon counter through an IEEE Acorn 488 Board. The program saves the data, as well as all the important operating parameters such as counting mode, no of points, gate delays etc. It also provides the normalization described

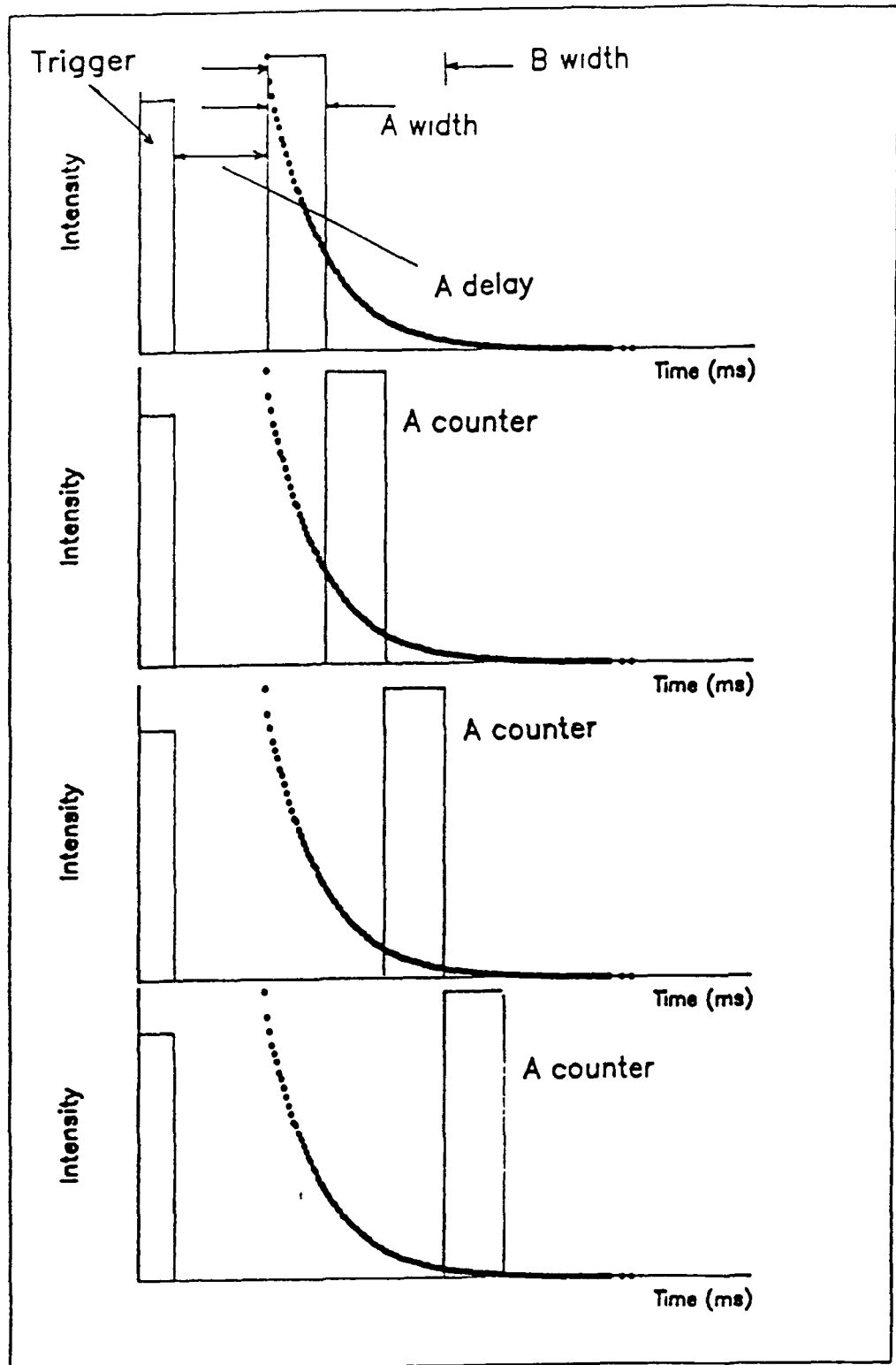


Figure 3.2 The Operating Principle of Time Resolved Photon Counting

above, (See Sec 3.6), so that the saved data file is ready to undergo the various data analysis routines that are contained in other programmes. In the acquisition programme itself provision is made to call the data analysis programme "Compstr", (see Appendix 3 for listing), this programme displays the decay curve and draws a semi logarithmic plot of the same curve. The details of this and other data analysis programmes is given in the following sections.

3.8 Lifetime Data Analysis

The analysis of the decay curve data is not unfortunately quite as straightforward as it may appear on first inspection. In glass or glassy media the analysis is further complicated by the fact that the decay process is highly non exponential due to the wide choice of sites available for the dopant ions, (See Sec 2.1). In the following section a brief description of the characteristics of transient phenomena is given, this is followed by a description of the analysis techniques used later in this report as well as suggestions about other possible analysis techniques.

3.9 Relationship Between Mean and Half Life and its Calculation

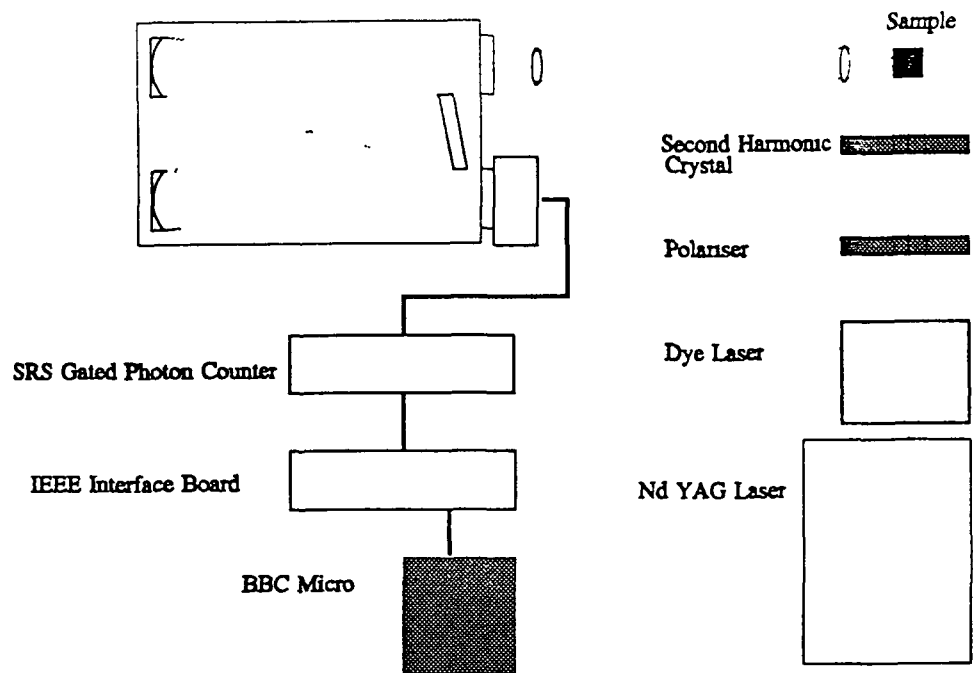
The mean life $T_{1/2}$ is generally defined as the time it takes the intensity to fall to half its original value. In excited state measurements this usually means the time required for the emission intensity to halve. Of more importance is the quantity known as the mean lifetime. If a decay is exponential the mean lifetime τ_m is equal to $1/k$, the decay rate constant. The initial excited state concentration, is reduced by a factor of $1/e$ at $t = \tau$. For an exponential decay $T_{1/2}$ and τ are related by, [1],

$$T_{1/2} = \frac{1}{k} \ln 2 \quad \text{Eqn 3.1}$$

$$T_{1/2} = .693 \tau_m \quad \text{Eqn 3.2}$$

Since $T_{1/2}$ is independent of the starting time t_0 for an exponential decay it can be used to measure how exponential a decay curve is. This is known as the $T_{1/2}$ test and is described later. In the majority of lifetime measurements the decay process is or is generally assumed to be what is known as a first order process. A first order process is one where the probability

Trinity College Lifetime System



Dublin City University Lifetime System

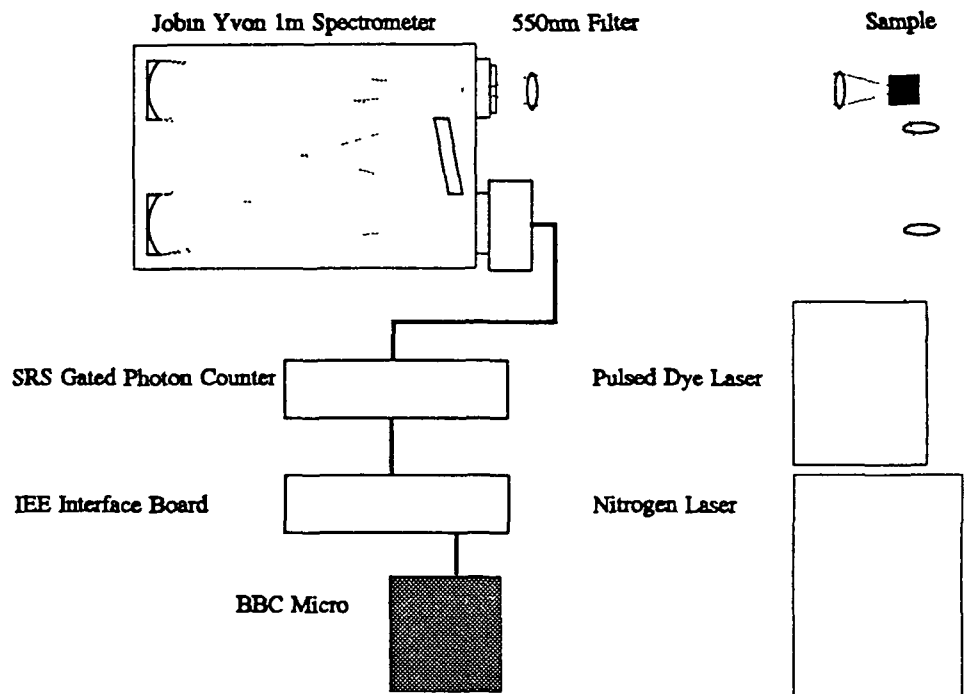


Figure 3.3 The Lifetime Measuring Systems

of decay of the excited species D^* is unaffected by the presence of like neighbours. Generally, the time dependence of the excited decay is of the form,

$$[D^*] = [D^*]_0 \exp(-kt) \quad \text{Eqn 3.3}$$

Looking at the above equation one can see that if a semi logarithmic plot of the data is taken then the resultant plot is of the form,

$$\ln [D^*] = \ln [D^*]_0 - k t \quad \text{Eqn 3.4}$$

The plot itself is linear with a slope of $-k$ and an intercept of $\ln[D^*]_0$. The above procedure is what the analysis programme "Compstw" follows. The programme produces a weighted least squares fit of the decay curve on the computer monitor as well as a semilog plot of the data. Problems arose however when calculating the lifetime from a decay curve which is not originally a single exponential decay but is actually a multi-component or sum of exponential decays. Part of the solution is given in the name of the analysis programme "Compstw", this programme also allows the user to component strip a decay curve, ie to break down a decay curve into its component lifetimes. The theory behind this technique is outlined below.

3.10 Multi Component Decays and Component Stripping

According to Demas, [1], problems begin to arise when one has to analyse a decay curve which is composed of several species each with different lifetimes which emit spontaneously and simultaneously. The classical method of representing a detector's response, $D(t)$ is,

$$D(t) = \sum_{i=1}^N K_i \exp\left(-\frac{t}{\tau_i}\right) \quad \text{Eqn 3.5}$$

Where N is the number of emitting components. In general semilog plots of $D(t)$ versus t are concave for a multicomponent decay, this is illustrated in Figure 3.4 for a multicomponent decay with its associated semilog plot. This is true unless the τ_i are equal or one of the K_i dominates, in which case the plots are nearly linear.

The diagram shows two curves $D(t)$ and $\ln D(t)$ versus t for a decay that is the sum of two

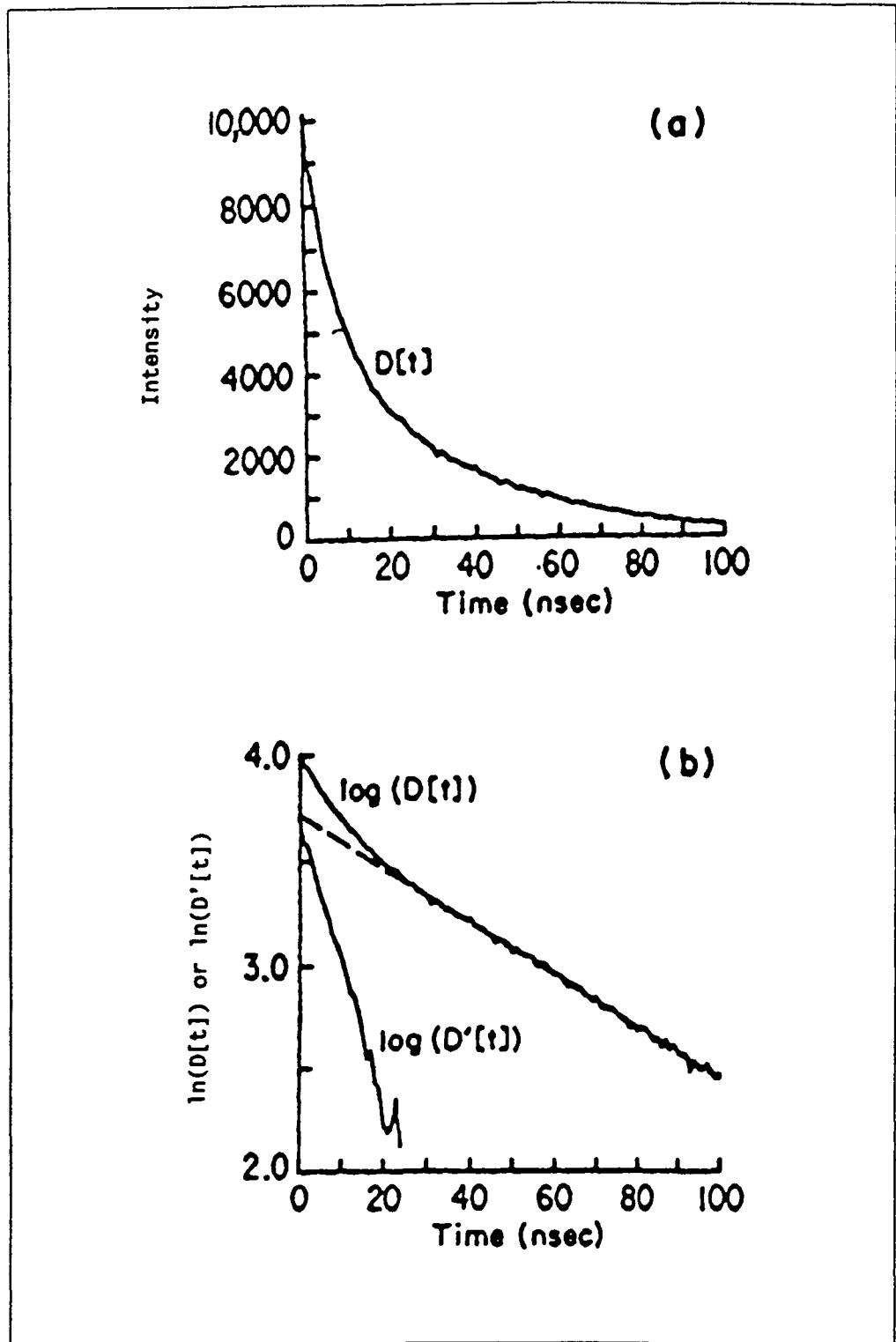


Figure 3.4 Multi-Component Decay Curve Analysis, From Demas [1].

exponentials, ($K_1=5000$, $\tau_1=35\text{nsec}$, $K_2=5000$, $\tau_2=7\text{nsec}$) That it is not exponential is readily seen by applying the $T_{1/2}$ test to different portions of the curve At $t=0$, $T_{1/2}$ is 10ns, at $t=10\text{ns}$, $T_{1/2}$ is 14ns, at $t=50\text{ns}$ $T_{1/2}$ is equal to 25ns, this corresponds to a τ value of 36ns the last value is in excellent agreement with the long lifetime component value

The result is expected because at such a long time scale the fast lifetime (7ns) makes no contribution to the decay process The differences in the $T_{1/2}$ show that the decay process is nonexponential, the semilog plot confirms it If one considers the semilog plot, (Fig 3 4(B)) one can see that on a long time base the curve will be linear with a slope of $-1/\tau$ and an intercept of $\ln K_1$ Using this K_1 and τ_1 the contribution of the slow component is subtracted from the $D(t)$ to yield $D'(t)$,

$$D'(t) = D(t) - K_1 \exp\left(-\frac{t}{\tau_1}\right) \quad \text{Eqn 3.5(a)}$$

$D'(t)$ approximates the pure decay curve for the short lived component Note that $D'(t)$ is not the difference between the observed decay and the calculated exponential decay of the long lived component. An inspection of the plot of the $D'(t)$ curve reveals a danger in the component stripping method. At longer times the $\ln D'(t)$ vs t becomes very noisy Therefore the component fitting regions must be chosen with care Component stripping provides a measurement of a second component lifetime but the increasing difficulty of the process when it is extended to more than two components makes it's use limited A more common method of analysing complicated nonexponential decay curves, such as those from a glass environment, was described by both Demas, [1], and Lempicki et al [2] This was the method that was adopted in the analysis of the nonexponential decay curves found in this study. The average lifetime τ_{Av} is defined as in Equation 3 6

$$\tau_{Av} = \frac{\int_0^{\infty} t \frac{d I(t)}{dt} dt}{\int_0^{\infty} \frac{d I(t)}{dt} dt} \quad \text{Eqn 3.6}$$

Where $I(t)$ is the experimental decay curve The quantity τ_{Av} is the summation over time of the number of excited species decayed in a time interval dt , multiplied by their age at time

of decay. This quantity is averaged over the total population. This technique is achieved through numerical integration in the case of a multicomponent decay. Another method was to use an algorithm based on Simpson's Rule, [3], for determining the area under a curve. Results obtained with both these techniques were in good agreement with each other in all measurements. In all the tables of lifetime data the three methods of lifetime calculation will be given. Method 1 will be Numerical Integration. Method 2 will be by Simpson's Rule. Method 3 will be by the semilog plot technique described earlier. Comparisons with the semilog plot were in general very good for principally exponential decays but differed considerably when multicomponent decays were considered.

3.11 Data Analysis Program for Methods 1 and 2

The data analysis program "Half of 84", (For listing see Appendix 4), performed the calculations for methods 1 and 2 above. One of the program's features was that the operator could select where on the decay curve the lifetime was to be determined from. This was necessary because of the manner in which the photon counter was triggered. It was found that the trigger pulse from the function generator wandered around its set mark space ratio. This resulted in different initial delays before counting commenced even though the initial delay had nominally been set fixed at 20 μ secs. The problems encountered because of the wavering trigger are depicted in Fig 3.5(a+b). In the diagram shown the most favourable point to commence the τ_{Av} calculation was at point "B", higher count number means higher signal to noise ratio. At point "C" the count has dropped significantly while at point "A" unless those points were disregarded the calculations would have been in error. In theory for an exponential decay it does not matter where on the decay curve the lifetime calculations begin, but this is not strictly the case for a multicomponent decay curve because information from short lived decay components can be missed or ignored. The problem with the triggering method was overcome by the use of an optical trigger placed beside the sample. This provided a trigger pulse a fixed time after the excitation pulse. The ideal case was where the A gate delay of the photon counter could be set to zero or perhaps 1 μ sec thus allowing the A gate to be enabled almost immediately after the excitation pulse. The enabling trigger was delayed only by propagation delays within the detection electronics.

The program then produced a value of the lifetime based on both methods, the results are in very good agreement and only vary for the high temperature samples where "Compstw" calculated the results as discussed above, (see Section 3.10)

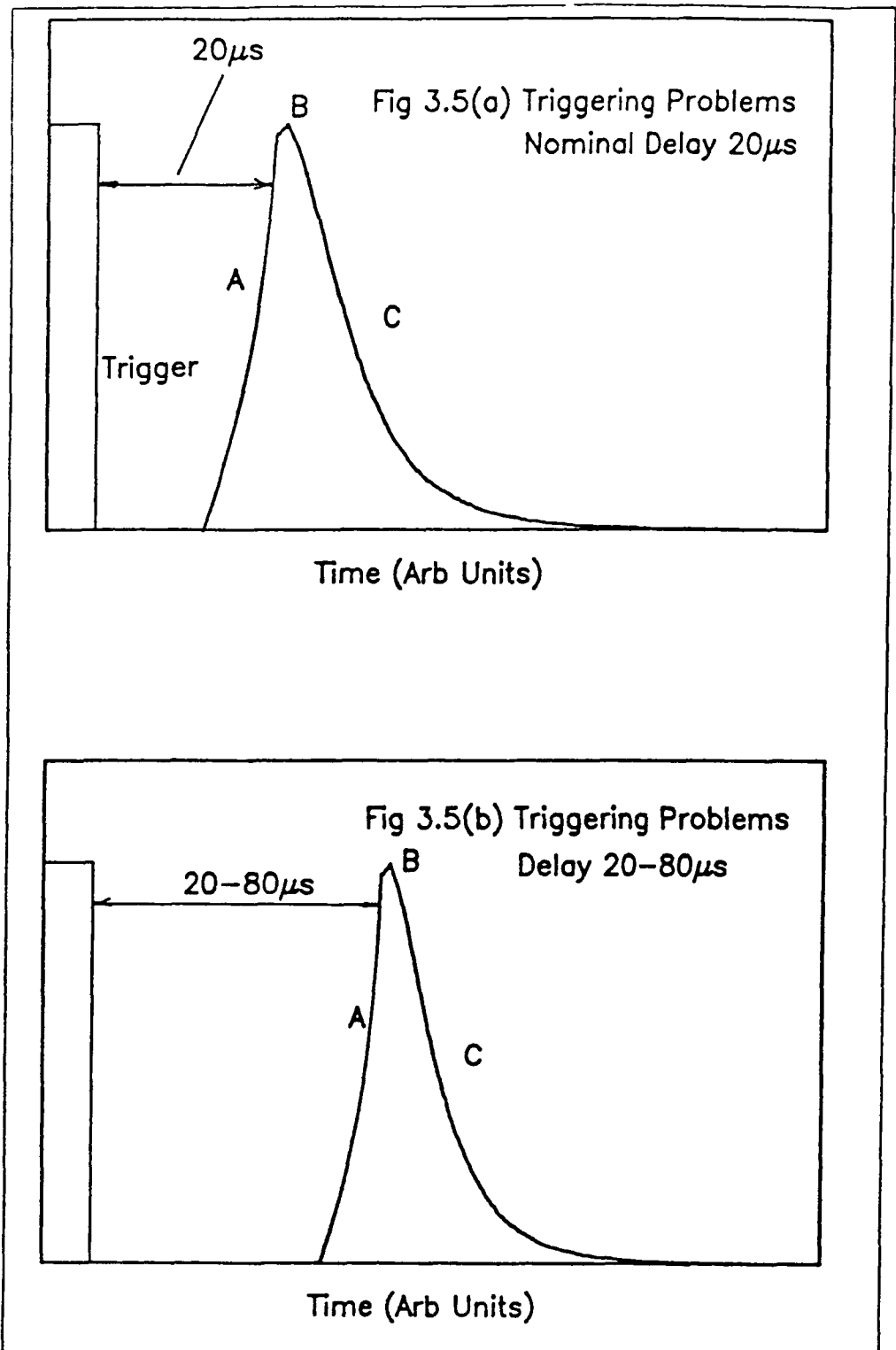


Figure 3.5 Triggering Problems in Lifetime Data Acquisition

3.12 Synthesis of the Samples Studied in this Report

All of the samples used in this study were synthesised from TEOS and water by mr Brendan O'Kelly, T C D Investigations into the character of the sol to gel to glass transitions were focused on observing how changes to the initial conditions were mirrored in the emission spectra of the dopant rare earth ions Of the initial conditions that were easily variable the following were deliberately altered the pH of the water used in hydrolysis, used to investigate two different catalysis regimes, the $H_2O/TEOS$ ratio, known as $R_{H_2O/TEOS}$, known to effect the hydrolysis rate . As well as the two conditions described above, a sample set of glasses were produced which were co-doped with Aluminium to investigate the behaviour of the optically active rare earth probes in the sol-gel glass matrix The importance of the first two processing parameters is discussed below Discussion of the other samples is left to the relevant sections in Chapters 3 and 4 to discuss

The evolution of sample history is shown below

Table 1.1 Evolution of Samples used in this Project

Sample Series No.1

Temperature	Sol, Gel, 200°C, 500°C, 800°C
$H_2O/TEOS$ Ratio	4
pH of H_2O	5.6

Sample Set No.2

Temperature	Sol, Gel, 200°C, 500°C, 800°C
$H_2O/TEOS$ Ratio	4
pH of H_2O	8

Sample Set No.3

Temperature	Sol, Gel, 200°C, 500°C, 800°C
$H_2O/TEOS$ Ratio	4
pH of D_2O	8

Sample Set No.4 $H_2O/TEOS$ Ratio for Acid Catalysis

Temperature	200°C
$R_{H_2O/TEOS}$	4, 10, 20, 40
pH of H_2O	1

Sample Set No.5 H₂O/TEOS Ratio for Base Catalysis

Temperature	200°C
pH of H ₂ O	5.6

Sample Set No.6 Aluminium Co-Doped Samples

% Aluminium	Temperature
0.0	200°C, 500°C, 800°C
0.5	200°C, 500°C, 800°C
1.0	200°C, 500°C, 800°C
pH of H ₂ O	1

Sample Set No.7 Soaked Sample Set

48 hours Soaking in 1% w/w solution of Eu(NO ₃) ₃	
Temperature	200°C, 500°C, 800°C

Sample Set No.8 Quenched Samples-Base Catalysed

Sample Name	Temperature
Sample 8(i)	Gel (72°C)
Sample 8(ii)	800°C Air Quenched
Sample 8(iii)	800°C H ₂ O Quenched
Sample 8(iv)	800°C D ₂ O Quenched

All of the samples used in this study were doped with 2% europium which was to act as a structural probe of the sol gel derived glass system. As the samples were processed from the initial sol to the gel and on to the final densified glass the changes observed in the fluorescent spectra of the samples were noted. With the exception of Sample Set no 6 none of the samples under study were codoped with any network modifying ions such as aluminium or sodium. The reason for the sample sets being designed as they are is explained again briefly below.

Sample Sets 1-3

These Sample Sets were chosen to investigate the effect of acid and base catalysis on the structural evolution as a function of temperature of the sol gel.

derived glass

Sample Sets 4-5

These sample sets were chosen to investigate the effect of the H₂O/TEOS ratio on the evolution of the sol gel derived glass. In particular how the Hydrolysis and Condensation rates effect the fluorescence properties of the Eu³⁺ structural probe

Sample Set 6

This was the only sample set where a deliberate attempt to alter the structure of the densified glass was made. It was done to determine if aggregation of Rare Earth ions in the high temperature glass stage could be overcome by the addition of the network modifying Aluminium ions

Sample Set 7

This sample set was chosen to determine the difference between incorporating the Europium in the solution stage of fabrication and soaking when already made and what effect the residual radical groups that remained in the pores of the structure could have on the luminescence characteristics of the sol gel glass. They were soaked in a Europium solution and fired to various temperatures

Sample Sets 8-9

These sample sets were chosen to investigate what the characteristics of the heating process were. They were quenched in various ways to investigate the non-radiative pathways for the Eu³⁺ fluorescence.

3.13 Conclusion

In this chapter is outlined the experimental systems used in this project. It has discussed the problems associated with analysing excited state lifetime measurements when the decay process is both exponential and highly non exponential. It outlines the history of the sol gel samples whose results are discussed in Chapters 4 to 7

Chapter 4

Eu³⁺ Fluorescence and Decay Measurements as a Function of Sol pH in Sol-gel Glasses

4.0 Introduction

This is the first in a series of results and discussion chapters. The aim of this and the following chapters is to present the results of the experimental work carried out on sol-gel silica samples which have been prepared in different ways, as discussed in section 3.12.

For all materials, the principal aim is to investigate the role played by the Eu³⁺ as a structural probe of the sol-gel material. This chapter discusses the experimental work carried out on three initial sample sets, Sample Sets Numbers 1, 2 and 3.

4.1 Materials Preparation as a Function of pH

Three sample sets were produced each having different pH conditions. Each set contained ten samples labelled A to K. The three sets were known as Sample Set Number 1, 2 and 3 respectively. For Sample Set No 1 the TEOS was hydrolysed by water at a pH of 5.6. Sample Set No 2 was hydrolysed with water at a pH of 8 and Sample Set No 3 was hydrolysed by deuterium at a pH of 8. For each pH, samples were prepared using the following heat treatments:

A Sol;

This is the original mixed solution, which had undergone no heat treatment.

B Gel;

This is the initial gelled sample, cured at 73° for 24 hours and then sealed in a clean container.

D,E Xerogel;

This is the gel cured at 73° for 189 hours and then placed in a clean container.

F,G-K Partially Densified;

Any remaining liquid was shaken off, the sample was then dried at 73° and then furnace-dried for 24 hours at,

F,G;

Furnaced for 24 hours at 200°C

H,I;

Furnaced for 24 hours at 500°C

J,K;

Furnaced for 24 hours at 800°C

The treatment described above was also applied to Sample Set No 2 in exactly the same way Any modifications are stated as they occur Both sample sets were examined and the emission spectra are displayed in Figure 4 1 and 4 2

4.2 Acid and Base Catalysis of Sol-gels.

The rapid increase in gel times for sol-gels, [1], as pH approaches 2.5, the isoelectric point of Silica, has led to the adoption of a convention in this thesis Sol-gels whose precursor pH is greater than 2.5 are termed base catalysed Sol-gels whose precursor pH is less than 2.5 are termed acid catalysed, [2] The explanation of this nomenclature is given below

The isoelectric point is defined as the point at which a sol is most likely to coagulate because the electric repulsion between particles is reduced, [3] The aggregation of colloidal particles to form a gel is essentially a base phenomenon, [4] Thus gels formed at a pH of greater than 2.5 are termed as base catalysed as their gelation characteristics are those of the gelation of a colloidal precursor solution Similarly gels formed at a pH of less than 2.5 are termed acid catalysed because they display the ramified, long chained structure which comes out of solution in a much shorter time than the base catalysed structure Thus it can be seen that a pH value of 2.5 represents a watershed in terms of describing a process as acid or base catalysed

4.3 Fluorescence Studies of Base Catalysed Samples (pH=5.6)

The evolution of the fluorescence as a function of temperature for the base catalysed sample sets can be seen in Figure 4.1 which shows how the spectrum of the sol is similar in many ways to that of the emission characteristics of the Europium ion in solution, ([5], see also Figure 7.3) The intensity is noticeably weak as evidenced by the small signal to noise ratio, however the spectral profile is similar to the ion in solution because of the narrowness of the peaks and the lack of any structural splitting or peak broadening Another feature of the sol is the width of the transition around 578nm, this transition, the ${}^5D_0-{}^7F_0$, can generally be

regarded as an indicator of the site multiplicity [6], the interpretation of the narrow peak is that the range of sites available to the Europium ion is quite limited. This is also the case for a Europium ion in solution where it is surrounded by a symmetric solvation shell, [5],[7]. Therefore the narrowness of the transition gives an indication of the "wetness" of the sample and it is surprising to note that the transition remains quite narrow even at moderately high temperatures. A measurement of the fluorescence ratio, R_{F1} as defined in section 2.6, also indicates that the environment is quite symmetrical because of its low value. The R_{F1} ratio for the samples shown is tabulated in Table 4.1. Note the decrease in R_{F1} in going from sol to gel. This would imply a more symmetrical environment for the gel. This effect was observed in acid-catalysed samples [7], both in the fluorescence data and the lifetime data and is under further investigation. In this study the effect is not corroborated by the lifetime data for pH=5.6, (Table 4.3)

Type	$R_{F1} \pm (0.5)$
Sol	3.0
Gel	1.8
200°	3.1
500°	4.2
800°	4.3

Table 4.1 Fluorescence Ratios (R_{F1}) for Sample Set 1, (pH=5.6)

As the temperature increases the spectra show the evolution of the J field splitting, (See Sec 2.6). The splitting associated with a glassy state becomes more apparent with the 7F_1 transition starting to show the development of its three levels. However from both lifetime and spectral measurements the 800°C sample, the highest treatment temperature in this sample set, has not yet acquired the same characteristics as the conventional high temperature Silicate glass doped with Eu^{3+} , [6]. The 200°C sample is interesting because as can be seen from Table 4.1, although the R_{F1} increased and the J splitting has appeared in the two lower energy transitions, the singlet transition ${}^5D_0 \rightarrow {}^7F_0$ remained relatively narrow which indicated that a wide range of sites was not available to the Europium ion in this an intermediate stage between a gel and

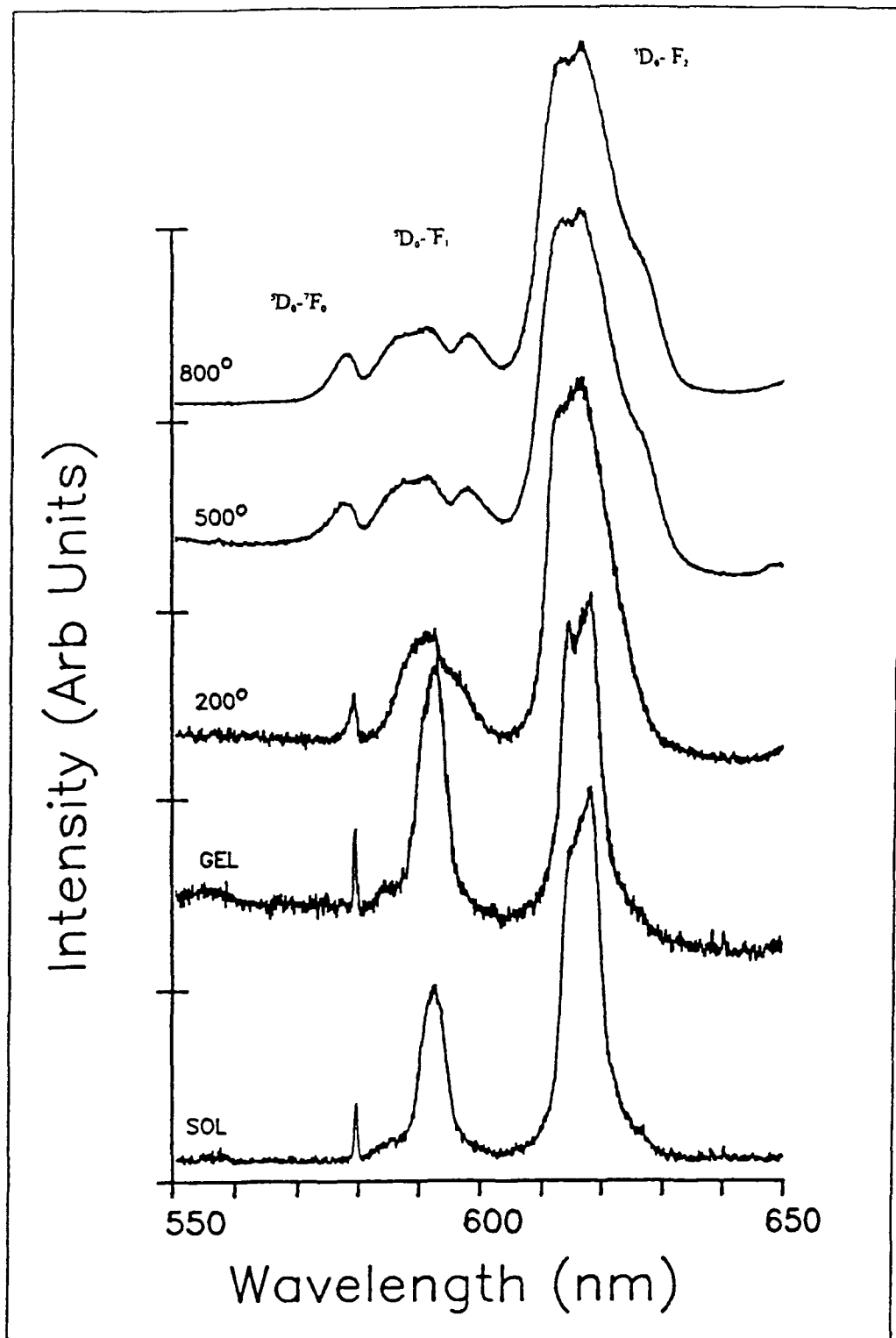


Figure 4 1 Fluorescence Spectra of Sample Set No.1, (pH=5.6 Base Catalysed, Room Temperature, λ Excitation = 398nm)

a glass This is in contrast to the 800°C sample where the wider transition widths indicate a much wider range of site geometries for the dopant ion, as is the case for a conventional glass

4.4 Fluorescence Studies of Base Catalysed Samples (pH=8)

Figure 4.2 shows the fluorescence spectra for the base catalysed, pH=8, Sample Set No 2 The spectra are very similar to those of the pH=5.6 sample set of the previous figure, Fig 4.1, except the R_{FI} measurements, within the errors indicated, increase monotonically as a function of densification temperature The R_{FI} measurements are tabulated in Table 4.2.

Type	$R_{FI} \pm (0.5)$
Sol	1.7
Gel	1.5
200°	3.2
500°	5.5
800°	7.4

Table 4.2 Fluorescence Ratio (R_{FI}) Measurements for Sample Set No.2 (Base Catalysed at pH=8)

Again the singlet transition width of the partially densified glass, the 200°C sample, is quite narrow indicating that there are still large amounts of radical groups both hydrocarbon and water based remaining within the pores of the structure, although from the lack of splitting of any of the other levels it is obvious that this stage is still far from a conventional glass

4.5 Lifetime Studies for Sol-gels at pH=5.6 and pH=8

One of the most sensitive indicators of change to the environment surrounding the Europium ion is the measurement of its fluorescent lifetime Fluorescent lifetime measurements were carried out on all samples The lifetime values for Sample Set's Number 1 and Number 2 are tabulated in Table 4.3 and 4.4

For both pH 5.6 and pH 8 the lifetime values, within the error, increase monotonically with densification temperature, (see Table 4.3 and 4.4) This increase can be attributed to the slow

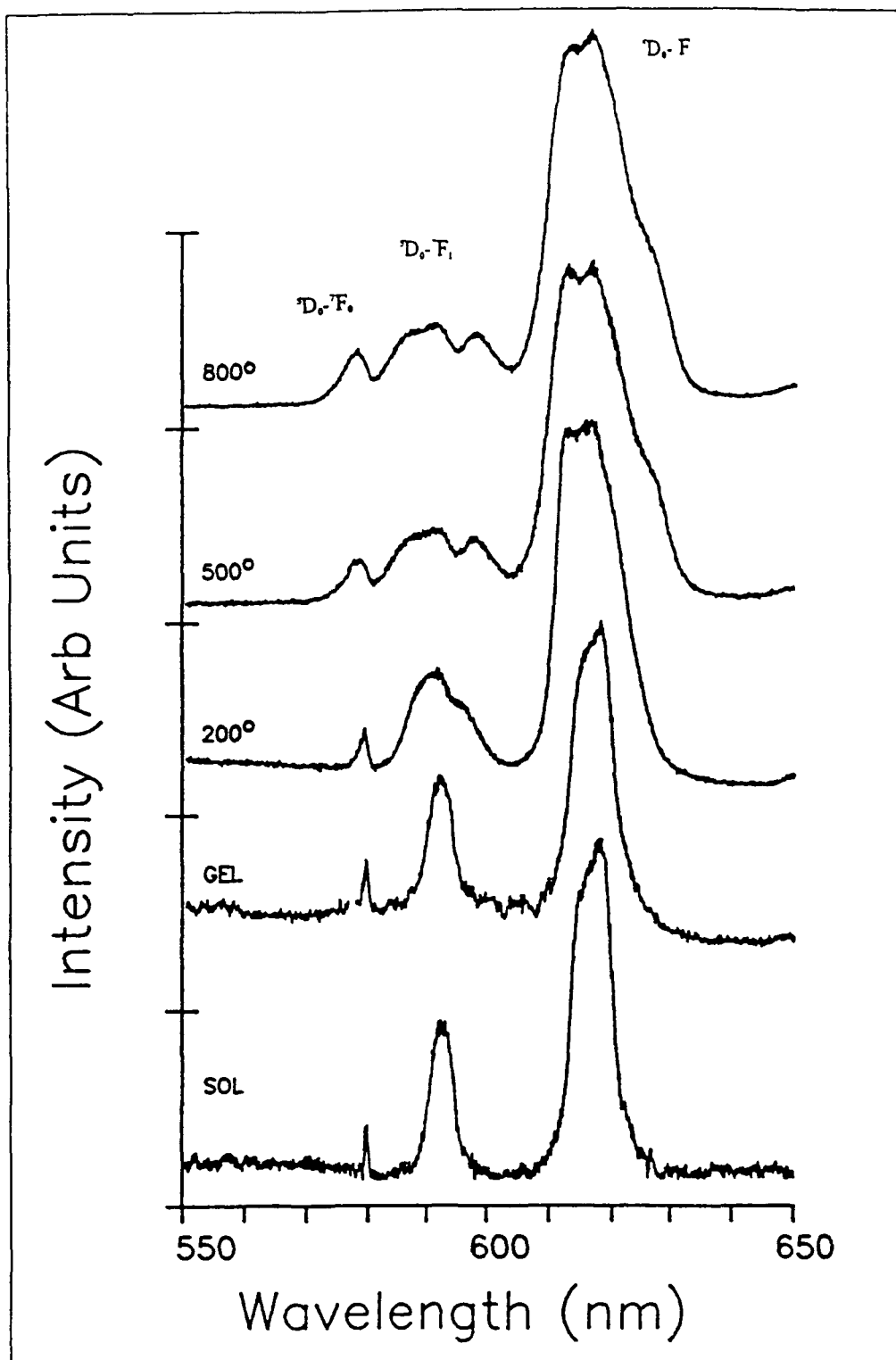


Figure 4.2 Fluorescence Spectra For Sample Set No.2 (Base Catalysis pH=8, Room Temperature, λ Excitation = 398nm)

Type	τ_{AV} Method 1 + (0.01)ms	τ_{AV} Method 2 + (0.01)ms	τ Semi-Log + (0.05)ms
Sol	0.17	0.17	0.19
Gel	0.16	0.16	0.17
200°	0.26	0.27	0.29
500°	0.75	0.76	0.87
800°	0.97	0.99	1.2

Table 4.3 Lifetime Measurements for Sample Set No.1, (pH=5.6 Base Catalysed, Room Temperature, λ Excitation = 337nm)

Type	τ_{AV} Method 1 + (0.01)ms	τ_{AV} Method 2 + (0.01)ms	τ Semi-Log + (0.05)ms
Sol	0.18	0.18	0.19
Gel	0.17	0.18	0.18
200°	0.27	0.27	0.3
500°	0.7	0.7	0.8
800°	1.0	1.0	1.2

Table 4.4 Lifetime Measurements for Sample Set No.2, (pH=8 Base Catalysed, Room Temperature, λ Excitation = 337nm)

decomposition of hydroxyl groups in the structure and the consequent reduction in the non-radiative decay paths for the Eu^{3+} ion. The low value of the lifetime measurement in the case of the partially densified sample is attributed to the presence of residual OH^- groups residing in the bulk of the sample. Previous work [8] has shown that most of the organics will have been removed by about 400°C though some can remain until considerably higher temperatures. The low value of the measured lifetime of the 800°C sample compared to the value of approximately 2.3ms measured for Eu^{3+} in a conventional silicate glass, [6], is attributed in part to the presence of residual hydroxyl ions in the matrix even at this temperature, and also to the fact that the structure of silica (SiO_2) glass is quite different to that of a mixed silicate glass, [9].

4.6 Structural Implications

It is well known that the pH of the initial components is an important factor in the synthesis of sol-gel glasses, [10] A low value of pH, ie <2, corresponds to a high hydrolysis rate and a low condensation rate, while materials with pH=8 should have a lower hydrolysis rate and a high condensation rate, [11] These trends can be seen by referring to Figure 4 3(a) which shows the hydrolysis rate as a function of pH or Figure 4 3(b) which shows the condensation rate as a function of pH

Figure 4 4 shows the fluorescence spectra of sol-gel silica at pH=1 from a previous study in this laboratory [7] From the low lifetime and R_{FL} values, Tables 4 5 and 4 6 respectively, it can be seen that this data is consistent with Eu^{3+} in a symmetric environment of mainly hydroxyl ions at the sol and gel stage This reflects the high hydrolysis rate at this pH For pH values of 5 6 or 8 the environment is less symmetrical with more organic and less hydroxyl groups, as indicated by the larger values of R_{FL} in Tables 4 1 and 4 2 The larger values for the lifetime of the sol and the gel also agree with a less symmetrical Eu^{3+} site, (see Table 4 3 and 4 4) This is consistent with a lower hydrolysis rate and a higher condensation rate. The predictions outlined above are borne out by the results of the lifetime data and fluorescence shown earlier The pH=5 6 and pH=8 sample sets, display an increase in intensity for the sol and gel compared to figure 4 4 for pH=1, resulting from the increased asymmetry of the environment due to the increased number of organic and OH groups surrounding the ion at higher pH This is a characteristic of base catalysis For acid catalysis, the high hydrolysis rate compared to the condensation rate results in more OH^- groups being present at the sol and gel stage hence giving rise to the low lifetimes and small R_{FL} values measured.

Type	τ Semi-Log msecs \pm 0 002
Sol	0 134(2)
Gel	0 123(2)
200°	0 38(2)
800°	1 05(2)

Table 4.5 Lifetime Measurements for Acid Catalysed Samples (pH=1, Room Temperature, λ Excitation=398nm, From [7])

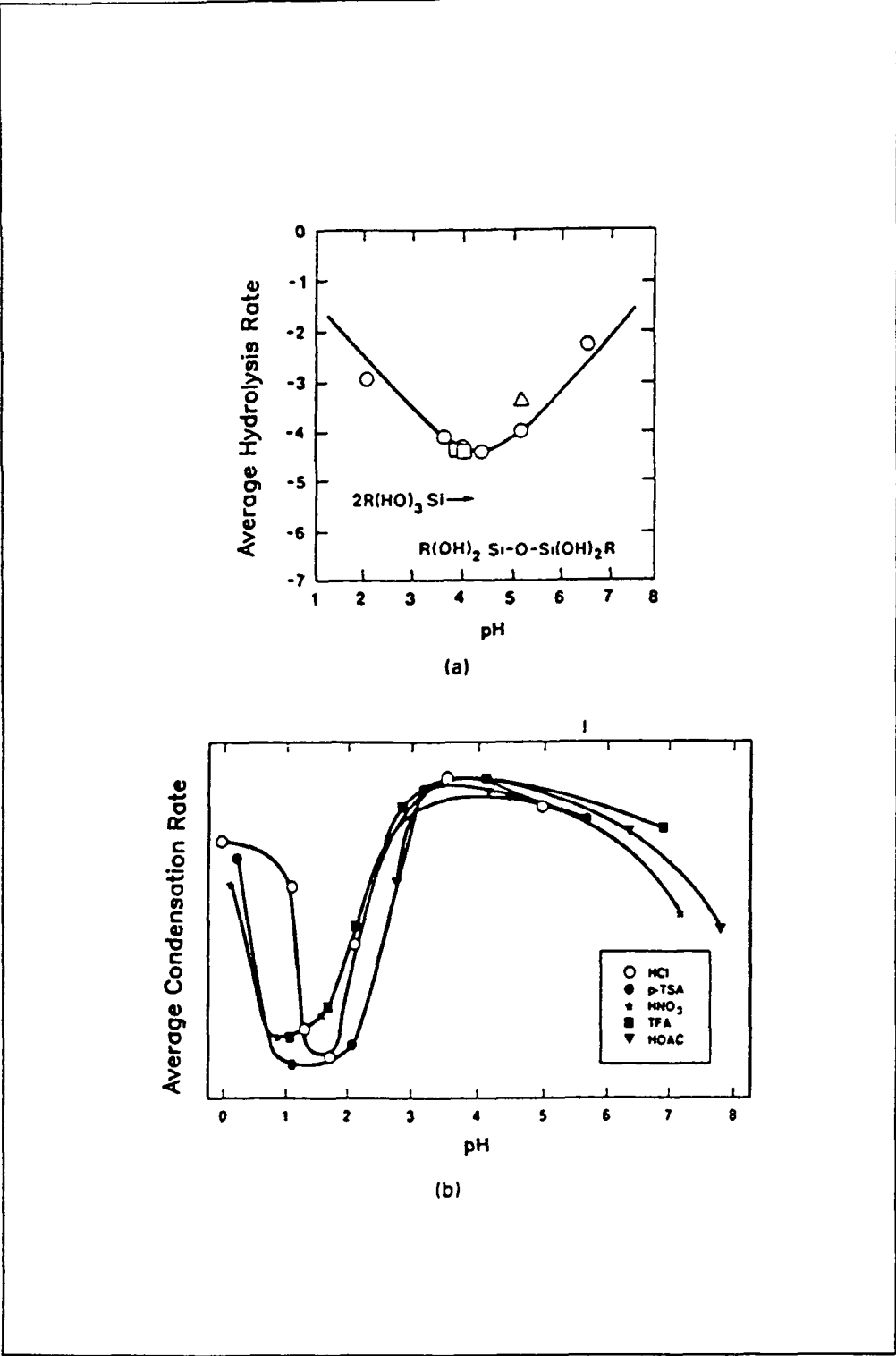


Figure 4.3(a) Hydrolysis Rate as a function of pH and (b) Condensation Rate as a function of pH From [Brinker and Scherer "Sol Gel Science"].

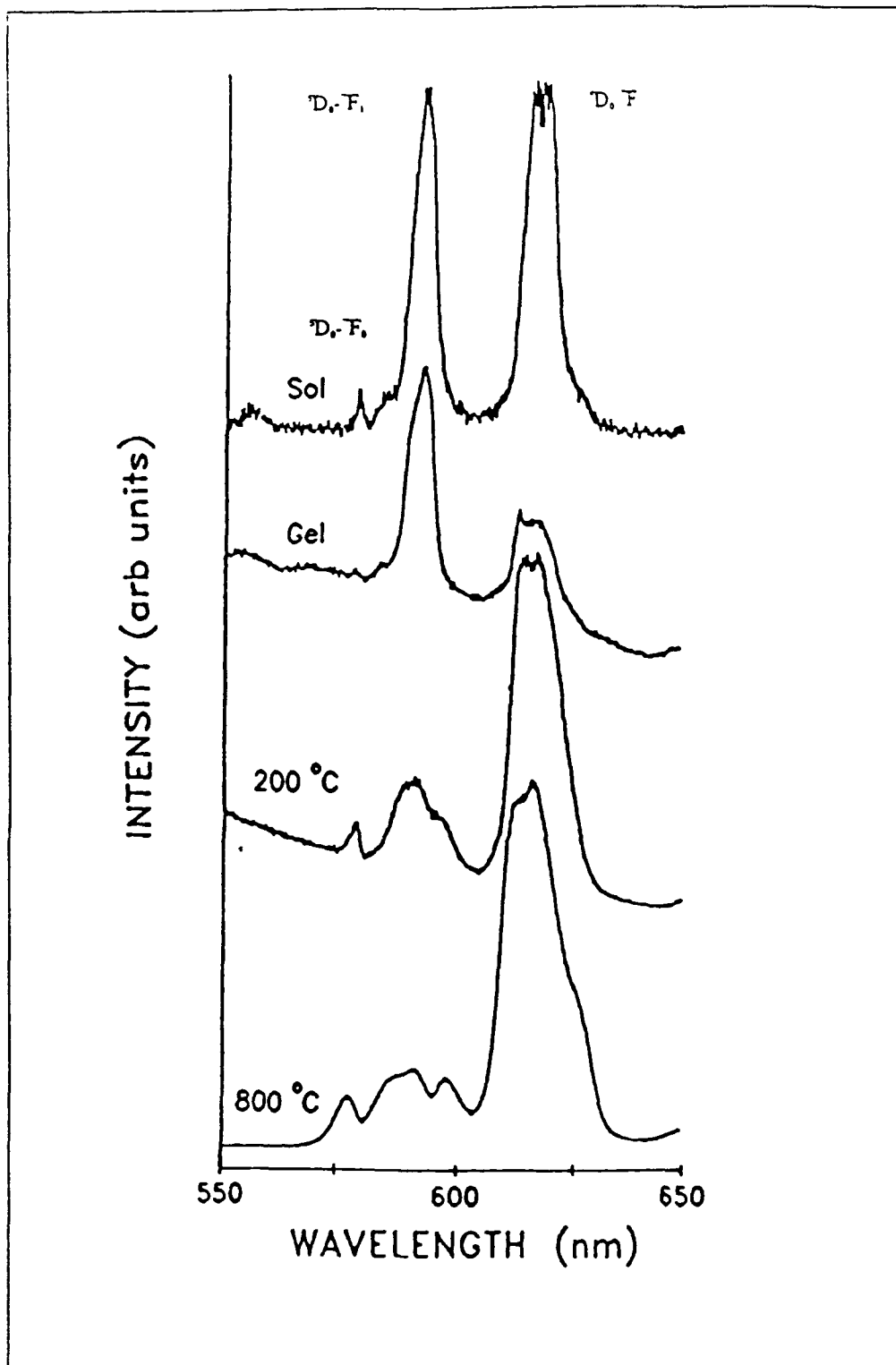


Figure 4.4 Fluorescence spectra of Acid Catalysed Samples (pH=1, Room Temperature, λ Excitation = 398nm) From [7]

Type	Fluorescence Ratio R_F
Sol	1.58
Gel	0.95
200°	3.62
800°	4.33

Table 4.6 Fluorescence Ratio, R_F , Measurements for Acid Catalysed Samples (pH=1, Room Temperature, λ Excitation=398nm) From [7]

4.7 Studies of Deuterated Sample Set (Sample Set No.3)

In previous work on rare earth fluorescence it was known that synthesis of a solution using D_2O instead of H_2O produced a much increased fluorescence yield and excited state decay times, [12]. The reason that the lifetime increases is that for a H_2O based gel the predominant energy loss is through radiationless decay via the hydroxyl groups vibration. The heavier deuterium atom has a lower frequency of vibration. The vibration energy is reduced from 3600 to 2700 cm^{-1} for the O-H stretch by Deuterium substitution for Hydrogen. Therefore as more vibrational quanta are required to fill the non radiative energy gap the probability of non radiative decay diminishes, therefore the fluorescence efficiency and the fluorescence lifetime increase. This is best described by Equation 2.13, (See Section 2.5).

$$\frac{1}{\tau} = \frac{1}{\tau_R} + \frac{1}{\tau_{NR}} \quad \text{Eqn 2.13}$$

Bearing in mind that the OH radical mentioned earlier is a possible source of fluorescence quenching it was decided to examine the properties of a sample set of sol-gel glasses synthesised with D_2O replacing H_2O . The results of the luminescence scans are illustrated in Figure 4.5

On inspection of Figure 4.5 it can be seen that the signal to noise ratio of the scans is very large. Indeed the sol could be seen to fluoresce when excited even under normal laboratory lighting conditions. The deuterated samples were compared directly with Sample Set No. 2 as they were manufactured identically except for the Deuterium substitution. Comparison with the Sample Set No. 2 reveals some very significant differences. The major difference is in the observed value of the lifetime measurement. It was approximately three times longer for the sol and gel, (see Table 4.7), than similar H_2O hydrolysed samples. This confirms the role played by OH⁻ ions in quenching the fluorescence according to equation 2.13. The presence of OD⁻ instead of OH⁻ in the sol and the gel decreases non-radiative decay and increases

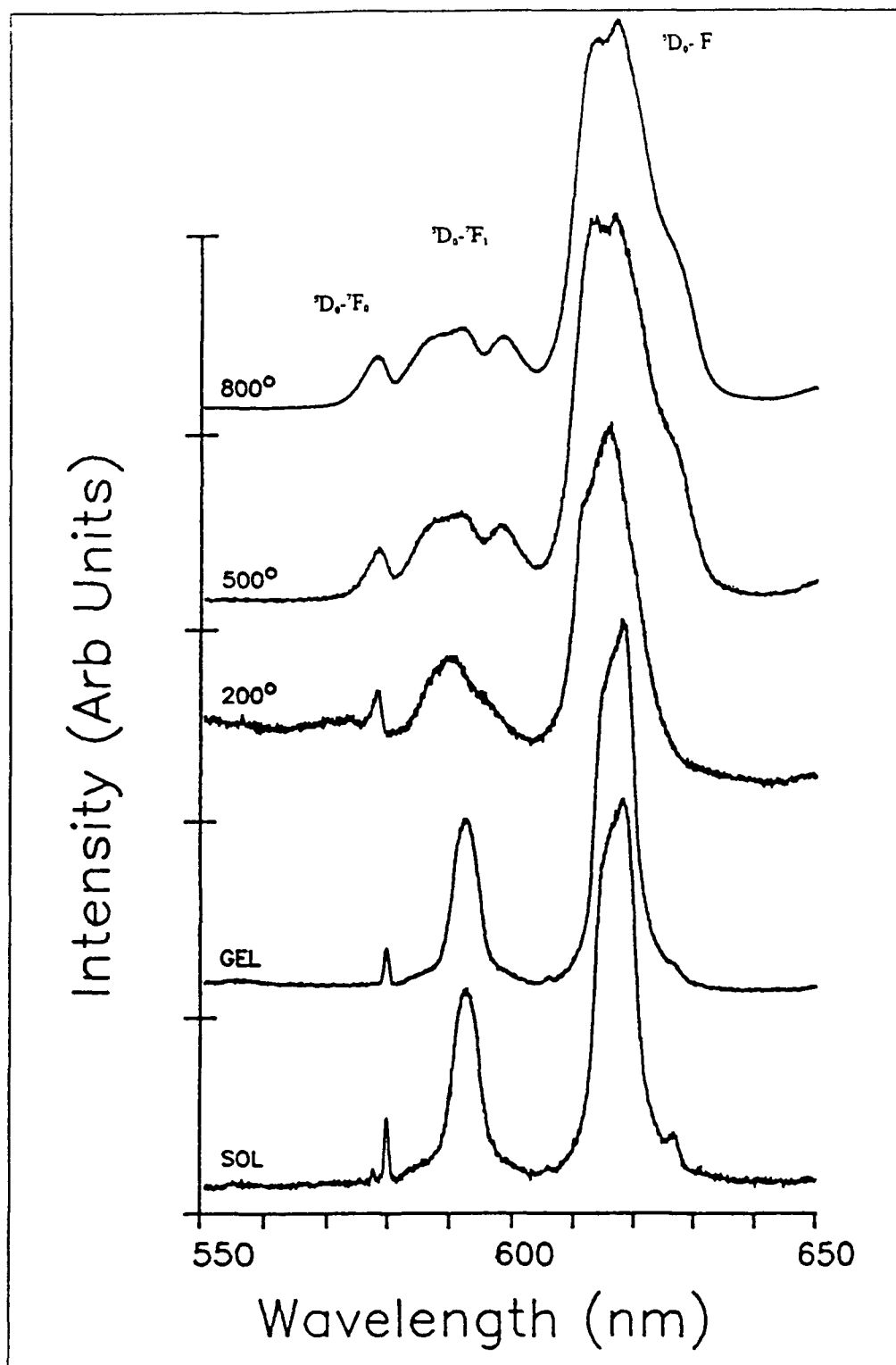


Figure 45 Fluorescence Spectra of Deuterated Samples, (pH=8, Room Temperature, λ Excitation = 398nm)

Type	τ_{Av} Method 1 + (0.01)ms	τ_{Av} Method 2 + (0.01)ms	τ Log-Line + (0.05)ms
Sol	0.48	0.48	0.48
Gel	0.46	0.45	0.42
200°	0.30	0.29	0.32
500°	0.72	0.73	0.76
800°	1.00	1.00	1.10

Table 4.7 Lifetime Measurements for Deuterated Sample Set, (pH=8, Room Temperature, λ Excitation = 337nm)

As the treatment temperature increased however the lifetime values of both sample sets, at pH=8 and the deuterated samples at pH=8 came closer together. After the gel stage, the deuterium has been used up in hydrolysis and non-radiative decay due to OH⁻ and C-H vibrations, as products of condensation continue to quench the fluorescence.

4.8 Conclusion

The lifetime and fluorescence data presented for base catalysed samples at pH=5.6 and pH=8 are consistent with predicted variation of hydrolysis and condensation rate as a function of pH. The less symmetrical environment for the gel indicated by the data needs further investigation. The data from samples hydrolysed by D₂O emphasises the large role played by non-radiative decay via OH⁻ ions in Eu³⁺ fluorescence in sol-gel materials. From the results presented it is clear that the deuterated sol and the gels have a much longer lifetime and an increased fluorescence efficiency.

Chapter 5

The Fluorescence Properties of the Eu^{3+} in Sol-gel glass as a Function of Water:TEOS Ratio

5.0 Introduction

This chapter reports the work undertaken on silica samples where the water:TEOS ratio was varied, (Sets Numbers 4 and 5, in Sec 3 13). Solution pH plays a large role in determining the eventual properties of the monolithic gel structure There is however a further factor in the evolution of the glass from the solution. The ratio of water to TEOS, known as r , determines the rate of evolution of the gel from the sol The investigation of the behaviour of the gels at varying water TEOS ratios is discussed below

5.1 Variation of H_2O :TEOS Ratios

A series of samples were produced in two pH regimes, ie pH=1 and pH=5.6. For both these series a partially densified glass, (200°), was produced For each set of samples that were produced there were four different values of the Water TEOS ratio, r . The values of the ratio were 4, 10, 20, 40

In sol gel silica the minimum number of water molecules needed per TEOS molecule for complete hydrolysis is 2, [1]. Variation of r affects hydrolysis, condensation and gel times. In the following pages the results of experiments carried out on Sample Set No 4 and 5, with varying Water-TEOS ratios are reported. The experiments were carried out on partially densified samples, (heated to 200°C)

5.2 Acid Catalysed Samples

Table 5 1 contains the lifetime measurements for the complete Sample Set Number 4, various water-TEOS ratios at pH=1 It can be seen from the Table 5 1 for acid catalysis, the $r=4$ material has a longer fluorescence decay and a larger intensity ratio The Intensity Ratio, R_{FI} , measurements are tabulated in Table 5 2 This behaviour is consistent with the model of a low pH system, which is that of a loose polymer like structure produced by fast hydrolysis, [2]. For $r>4$ however water remains in the matrix, producing shorter decay times and smaller

fluorescence ratios, due to nonradiative decay mechanisms of the OH group. At $r=4$ however, most of the water is used up in the hydrolysis stage so that the immediate environment of the Eu^{3+} ion contains fewer hydroxyl groups.

Water:TEOS	τ_{Av} Method 1 ± (0.01)ms	τ_{Av} Method 2 ± (0.01)ms	τ Log-Line ± (0.05)ms
4	0.29	0.30	0.30
10	0.24	0.25	0.25
20	0.20	0.20	0.22
40	0.23	0.23	0.24

Table 5.1 Lifetime Measurements for 200°C Samples at Various Water:TEOS Ratios (Acid Catalysed, pH=1)

Water:TEOS	R_{Fl} ± (0.5)
4	4.2
10	2.7
20	3.1
40	2.9

Table 5.2 Fluorescence Ratio, R_{Fl} , Measurements for 200° Samples at Various Water:TEOS Ratios, (Acid Catalysed pH=1)

The Fluorescence spectra of the Acid catalysed Sample set No 4 are shown in Figure 5.1

5.3 Base Catalysed Samples

At pH=5.6 the slower hydrolysis occurs due to a series of competing reactions, [3]. More water is needed for complete hydrolysis and there is a high rate of condensation, [4]. The nature of high pH synthesised sol gel glass is of an aggregation of colloidal particles, [4]. As a result the Eu^{3+} ion is not as exposed to such a large variety of environments as r changes, i.e., the colloidal particles tend to screen the ion. This should have resulted in a marked

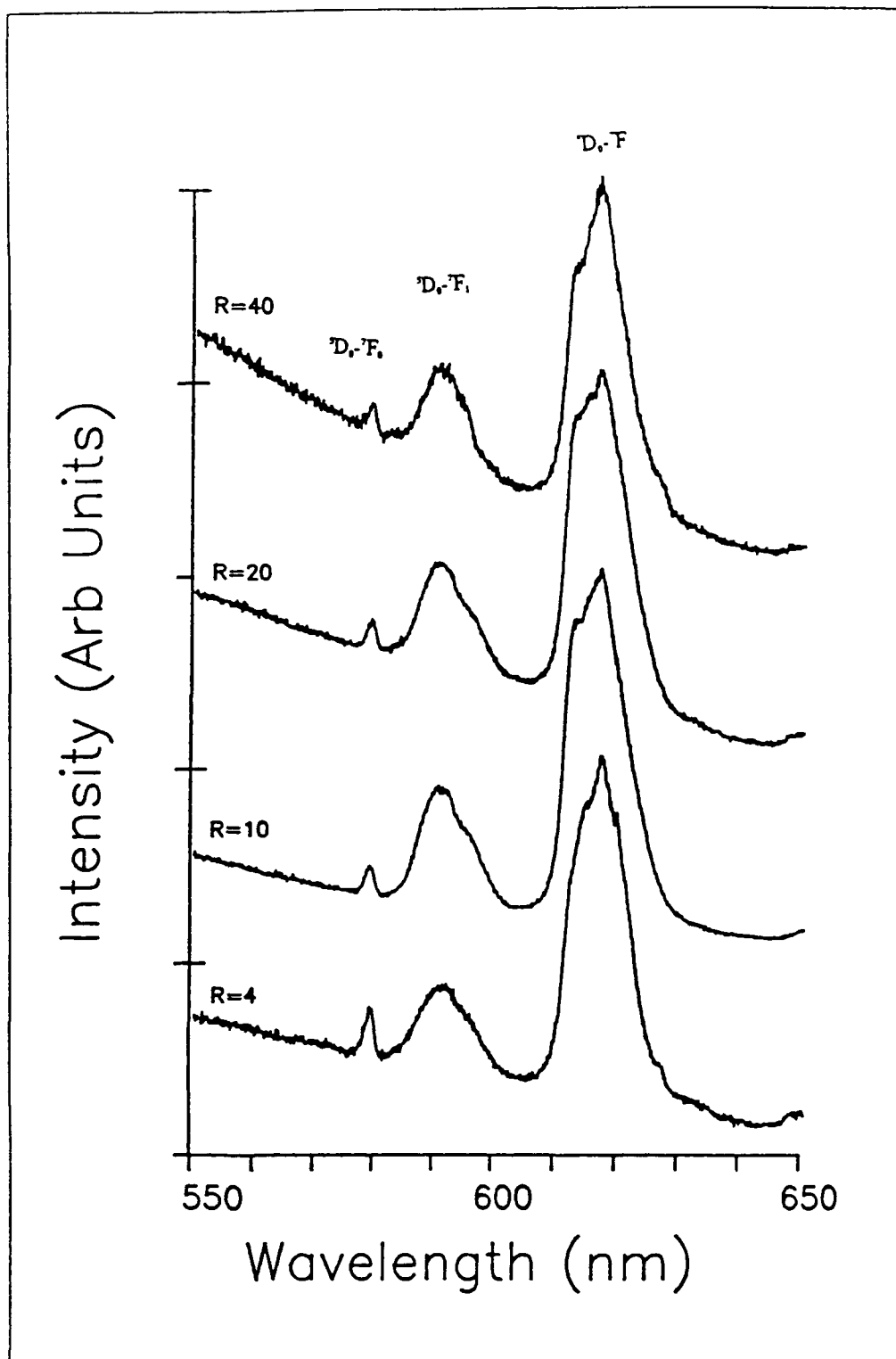


Figure 5.1 Fluorescence Spectra of Acid Catalysed 200* Samples (Sample Set No 4, pH=1, Room Temperature, λ Excitation = 398nm)

insensitivity to the excess water available at the higher R values This did indeed appear to be the case as an examination of the τ and the R_{Fl} values, within the error bounds, confirms The calculated lifetimes for the base catalysed samples of Sample Set No 4 are tabulated in Table 5.3 for the 200°C samples

As can be seen in Table 5.3 there was very little difference in the decay measurements for the pH=5.6 sample set, and this was in agreement with the model proposed above The

Water TEOS	τ_{AV} Method 1 ± (0.01)ms	τ_{AV} Method 2 ± (0.01)ms	τ Log-Line ± (0.05)ms
4	0.28	0.30	0.30
10	0.30	0.30	0.30
20	0.33	0.33	0.33
40	0.29	0.30	0.29

Table 5.3 Lifetime Measurements for 200° Samples at Various Water:TEOS Ratios, (Base Catalysed pH=5.6, Room Temperature, λ Excitation = 337nm)

Water:TEOS	R_{Fl} ± (0.5)
4	4.0
10	4.7
20	3.9
40	4.6

Table 5.4 Fluorescence Ratio, R_{Fl} , Measurements for 200° Samples at Various Water:TEOS Ratios, (Base Catalysed pH=5.6, Room Temperature)

fluorescence ratios for the 200°C samples are shown in Table 5.4

5.4 Conclusion

In conclusion it is proposed that the Fluorescence and Lifetime characteristics corroborate the theories about the mechanics of gel formation from the sol, [1], [2] These formation

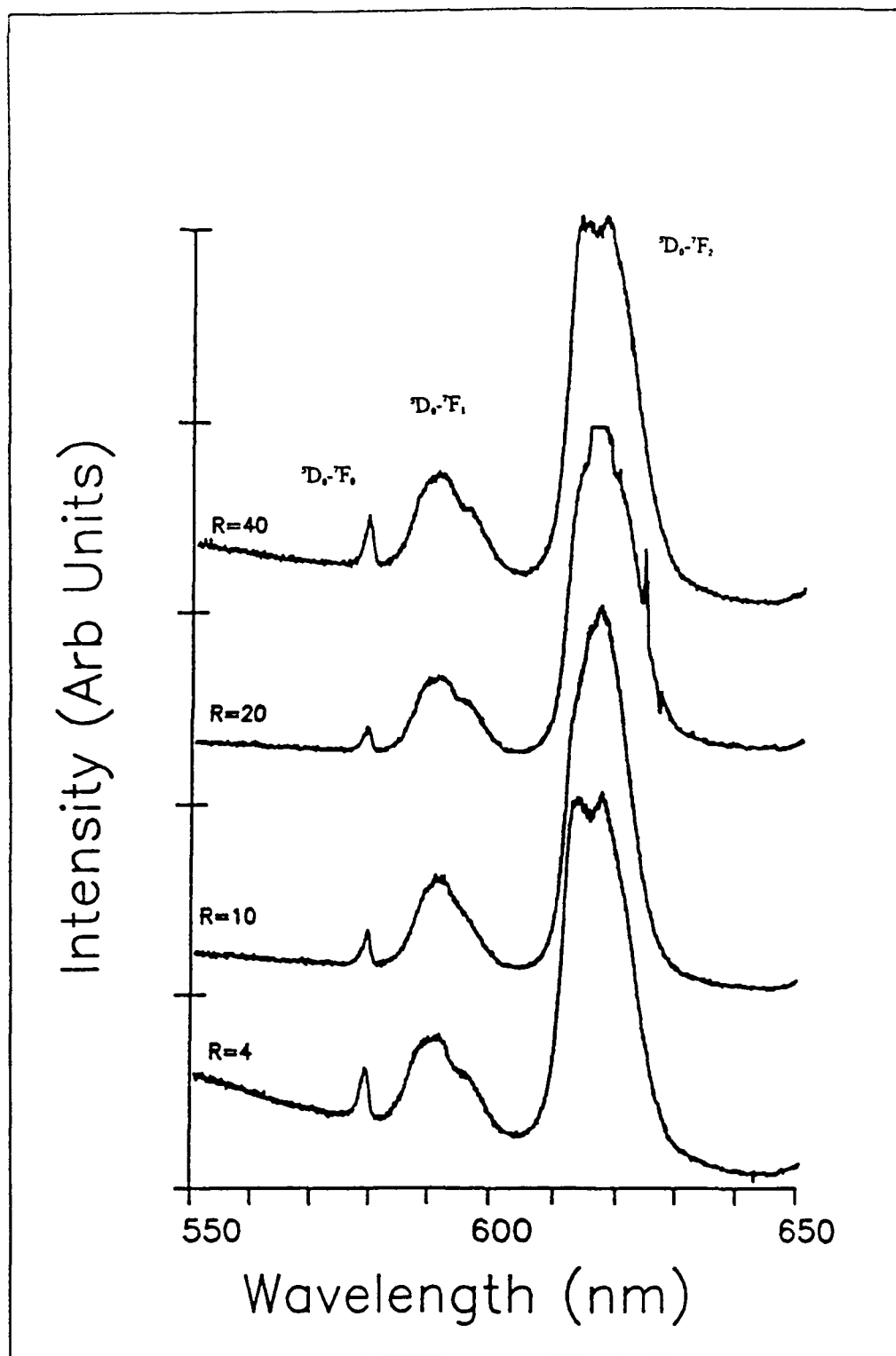


Figure 5.2 Fluorescence Spectra of Base Catalysed 200°C samples, (Base Catalysed, pH=5.6, Room Temperature, λ Excitation = 398nm)

mechanisms are seen to be pH dependent and determined by the ratio of water to the TEOS. It is proposed that the fluorescence characteristics for the Acid Catalysed Sample set show the Eu^{3+} ion to be in an environment of mainly hydroxyl ions as r increases consistent with a rapid hydrolysis rate. At higher pH, the fluorescence decay data show a marked insensitivity to the Water/TEOS ratio which is consistent with the more colloidal structure present in this pH regime where the Eu^{3+} ion is screened to a larger extent from the added water molecules.

Chapter 6

Investigations of Aluminium-Europium Codoped Samples

6.0 Introduction

This chapter reports the results of the experimental work carried out on Aluminium-Europium codoped samples, Sample Set Number 6. Aluminium-Europium codoped samples were produced to investigate the effect of a network modifying ion, aluminium, on the fluorescence characteristics of the Europium ion in a sol-gel host. The motivation behind this work was to examine the effect of the aluminium on the distribution of the Eu^{3+} ion in the sol-gel matrix. In Neodymium doped systems codoping with Aluminium dispersed the Nd ions throughout a sol gel matrix allowing higher Nd dopant concentrations and better luminescence efficiencies than had been previously thought obtainable. Sample Set Number 6 was synthesised with aluminium concentrations of 0%, 0.5%, and 1%. This, according to previous work, [1], on sol-gel systems should be enough to disperse the europium.

6.1 Rare Earth Doping of Conventional and Sol Gel Glasses

Rare earth ions are difficult to add to a simple glass network in any large quantity, [2]. Rare earth ions can enter a glass principally as a network modifier. It is frequently difficult to add more than 1% of rare earth ions to a simple oxide glass system such as SiO_2 or GeO_2 without causing the ions to cluster. The reason is that the network of these single component glasses are tightly bonded by bridging oxygens. If a network modifying ion is added then the network of the Silicon is broken and nonbridging oxygens occur. The rare earth ion can now be inserted in the gaps left by the broken structure.

Because of the method of addition, it is easier to add larger amounts of rare earth ions to a sol gel solution. It had been thought that because of the nature of the sol solution that the dopant ion would be homogeneously distributed throughout the structure. However recent experimental work here at this laboratory and in other places has indicated that the sol gel derived glass may also suffer from clustering of the dopant rare earth ion. In the case of the rare earth ions in the sol-gel, it appears that during the polymerisation process it is preferable for the dopant ion to associate and precipitate out in clusters. It had been thought that the rare

earth ion would be evenly distributed throughout the amorphous structure. The next section consists of a brief discussion of the effects of aluminum doping on Nd-doped conventional and sol-gel glasses.

6.2 Neodymium doped Glasses

It has been reported, ([1],[3]), that for both conventional and sol-gel Nd-doped SiO_2 glasses, the addition of small amounts of aluminum or phosphorous to the silica matrix serves to increase the fluorescence efficiency and the fluorescence lifetime by preventing the clustering of the Nd^{3+} ions. Neodymium doped sol-gel silica is an important candidate for new laser materials because of the superior mechanical properties of the sol-gel silica matrix compared to those of conventional mixed silicate materials, [6]. For this reason the clustering of the laser ions is a major problem that has to be overcome to achieve optimum laser performance. In pure sol-gel silica doped with Nd^{3+} the dopant ion has a tendency to cluster as discussed in the previous section. This results in low fluorescence efficiencies and reduced radiative decays, [4]. Close analysis of the decay curves showed the presence of a fast decay component, (FDC), superimposed on the longer Nd^{3+} lifetime, slow decay component (SDC). The presence of the FDC was associated with the concentration quenching of the Nd^{3+} ion due to clustering. Addition of small amounts of aluminum or phosphorous caused the FDC to decrease and the SDC to increase. Thus the presence of the aluminum or phosphorous appeared to disperse the Nd^{3+} ions hence improving the optical performance. Similar effects were seen in Nd^{3+} doped conventional SiO_2 glass prepared by plasma torch chemical vapour deposition, [3]. This work prompted a similar investigation into the phenomenon of Eu^{3+} clustering in Eu^{3+} -Al codoped SiO_2 prepared by the sol-gel method.

6.3 Results and Discussion of Experiments on Aluminium Codoped Samples

The work discussed in Section 6.2 provided the motivation for producing the sol-gel glasses with various concentrations of Aluminium as a network modifier in an attempt to corroborate the results on Nd^{3+} materials and to investigate the properties of Al- Eu^{3+} codoped samples. The results of the lifetime and fluorescence measurements show the Aluminium to have decreased the lifetime by a significant amount compared to the control sample which contains no aluminium, see Tables and Figures 6.1, 6.2, 6.3 respectively.

This was an unexpected result. It was thought that the Aluminium in its role as a network modifying ion would disperse the Eu^{3+} ion and hence increase the

Type	τ_{Av} Method 1 + (0 01)ms	τ_{2v} Method 2 + (0 01)ms	τ Log-line + (0 05)ms
Gel	0 09	0 09	0 09
200°	0 16	0 16	0 15
500°	0 73	0 74	0 73
800°	0 81	0 81	0 9

Table 6 1 Fluorescence Lifetimes for 1% Aluminium Samples (Sample Set No 6, λ Excitation = 337nm, Room Temperature)

Type	τ_{Av} Method 1 + (0 01)ms	τ_{2v} Method 2 + (0 01)ms	τ Log-line + (0 05)ms
Gel	0 08	0 08	0 09
200°	0 18	0 18	0 19
500°	0 51	0 52	0 50
800°	0 80	0 82	0 95

Table 6 2 Fluorescence Lifetimes for 0 5% Aluminium Samples (Sample Set No 6, λ Excitation = 337nm, Room Temperature)

Type	τ_{Av} Method 1 + (0 01)ms	τ_{2v} Method 2 + (0 01)ms	τ Log-line + (0 05)ms
Gel	0 10	0 11	0 12
200°	0 18	0 36	0 37
500°	0 51	0 54	0 58
800°	0 74	0 82	0 90

Table 6 3 Fluorescence Lifetimes for 0% Aluminium (Sample Set No 6, λ Excitation = 337nm, Room Temperature)

fluorescence efficiency and lifetime. This did not however appear to be the case. Both lifetimes and fluorescence efficiencies had decreased for the Aluminium containing samples. This was particularly so in the case of the gel and 200° samples for both Aluminium sets. This was interesting because it is precisely these samples that have the largest amount of hydroxyl and other radical groups. Examining the fluorescence spectra of these samples, (Figure 6 1, 6 2 and 6 3) it can be seen that the transition widths of the gel are quite narrow indicating that there is a large OH content in the samples.

In the case of the Aluminium - Europium codoped samples the problem of quenching of luminescence in the gel and partially densified stage seems to be exacerbated by the addition of Aluminium rather than eased. As the densification temperature increases the average lifetime, τ_{Av} , increases in both Aluminium containing samples. In this way the Aluminium containing samples are similar to other previously examined sample sets.

The question that must be answered is what exactly is the role of the Aluminium codopant in the sol gel system. The objective of the Aluminium addition to the sol gel system was specifically to break up the SiO_4 tetrahedra chains that formed as a result of the polymerisation of the sol. This would then allow space for the Eu^{3+} ion. As a result there would be a wider more homogeneous distribution of sites throughout the gel. Recent work on aluminosilicate sol-gel glasses, [5], indicate that even small amounts of aluminium reduces the pH of the sol thus increasing the hydrolysis rate. This would certainly explain the smaller value of the fluorescence efficiency and lifetime for the aluminium codoped samples in this study. However it is observed from the data on the 800°C aluminium codoped glasses that the behaviour is not the same as that found for the neodymium system. A measure of how effective the Aluminium was in breaking the SiO_4 polymer into shorter lengths could be achieved through a molecular weight analysis of the Si polymer, a so called chain length or N-bar analysis with for example an Ubbelohde Viscometer. This could be done at the sol stage to determine the polymer length of the Aluminium and non Aluminium containing samples, unfortunately this was not available at the sol production stage. For the Aluminium to attain its primary objective, that is the breaking up of the polymerised structure, there should be a distinct difference between the two N-bar readings. Work is presently underway in this laboratory to determine more accurately the function of the Aluminium as a network modifying ion at the sol stage. In the experiments on the aluminium doped samples, (sample Set No 6), a fast decay component was clearly observed with a τ_{FDC} of approx 0.8 μ secs, (see Figure 6 4 and 6 5). However for samples containing no aluminium a fast decay component,

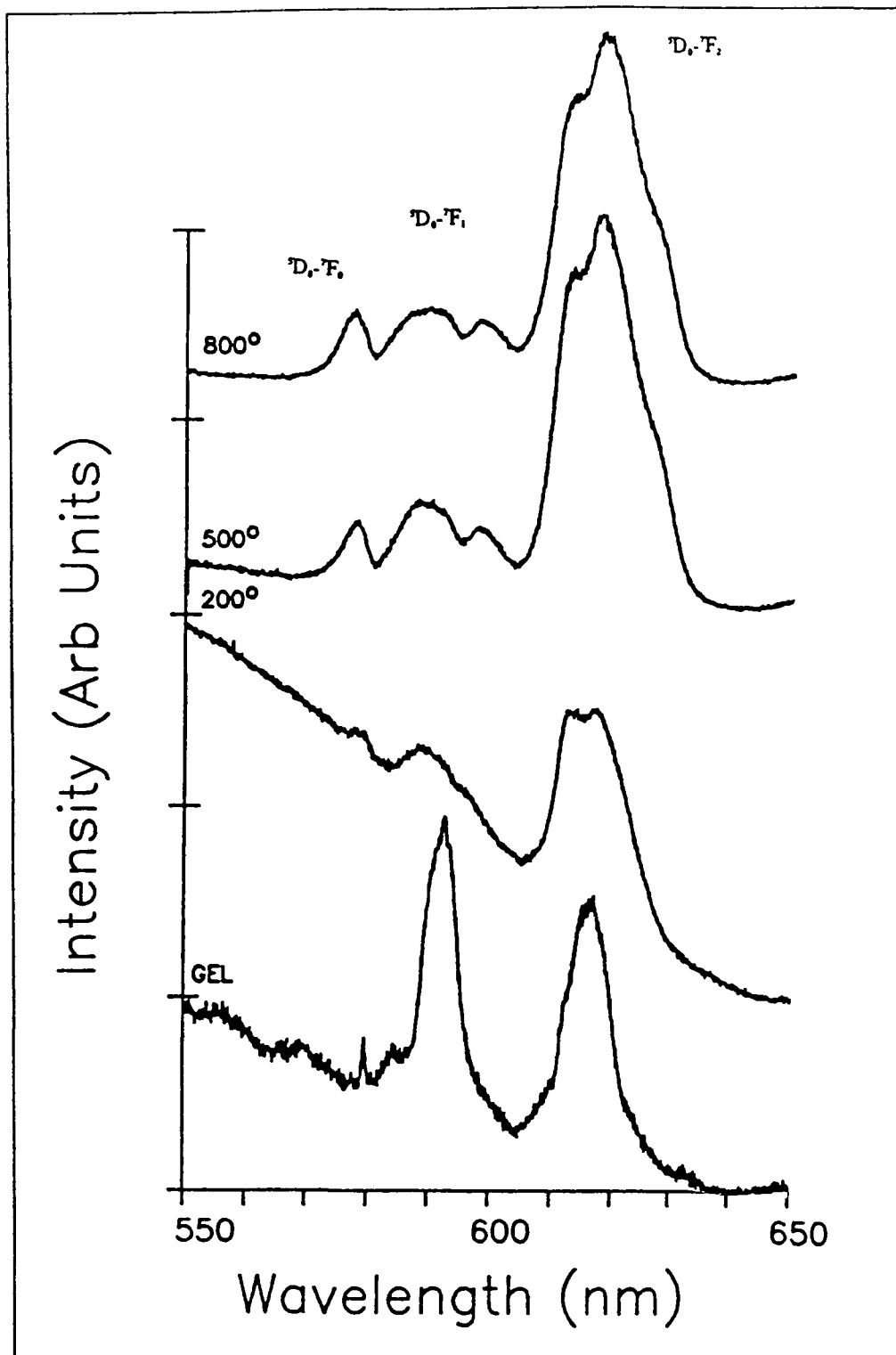


Figure 6.1 Fluorescence Spectra of 1% Aluminium Containing Sol-gel samples, (Acid Catalysed pH=1, Room Temperature, λ Excitation = 398nm)

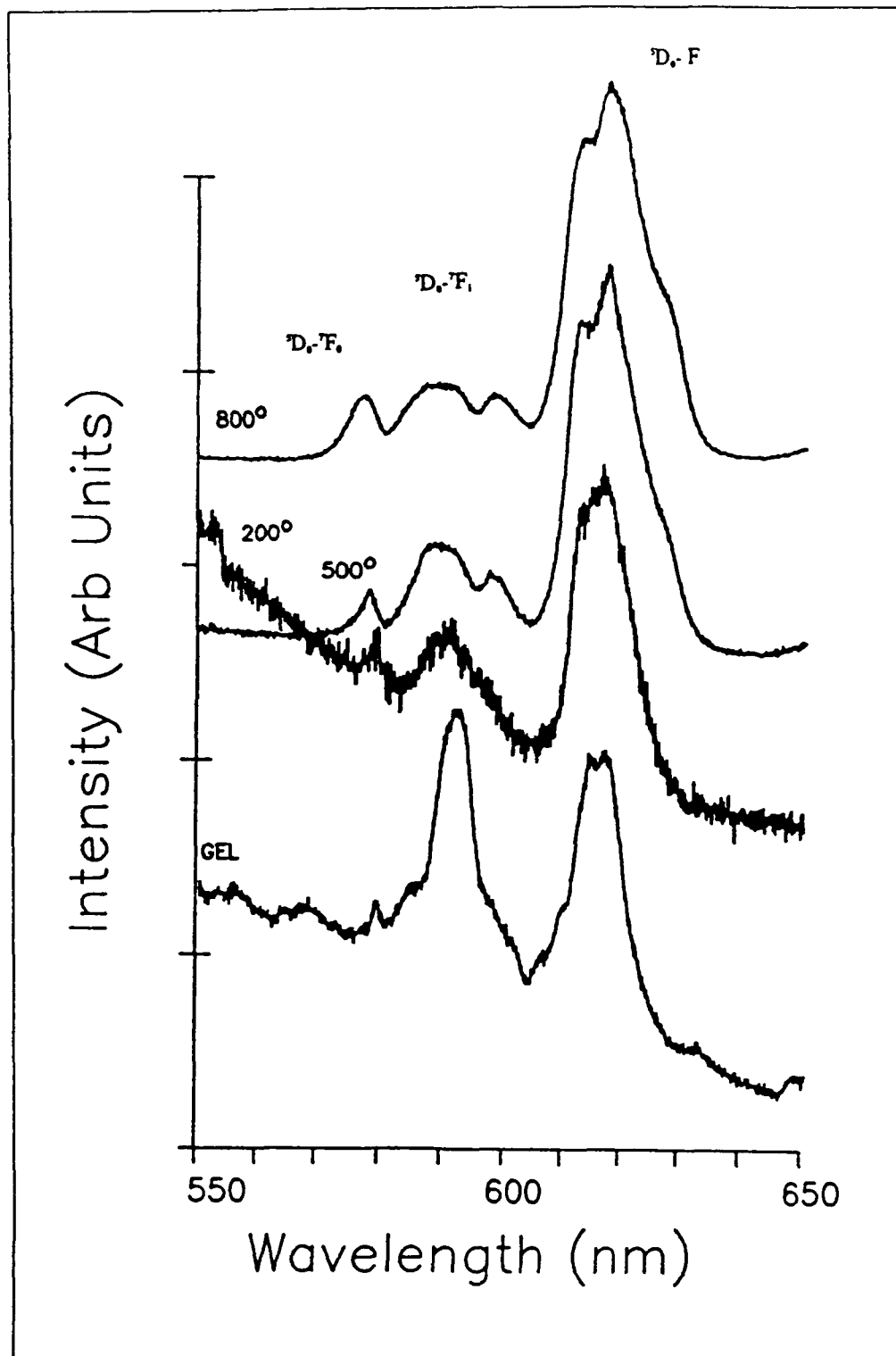


Figure 6 2 Fluorescence Spectra of 0.5% Aluminium Containing Sol-gel Samples (Acid Catalysed pH=1, Room Temperature, λ Excitation = 398nm)

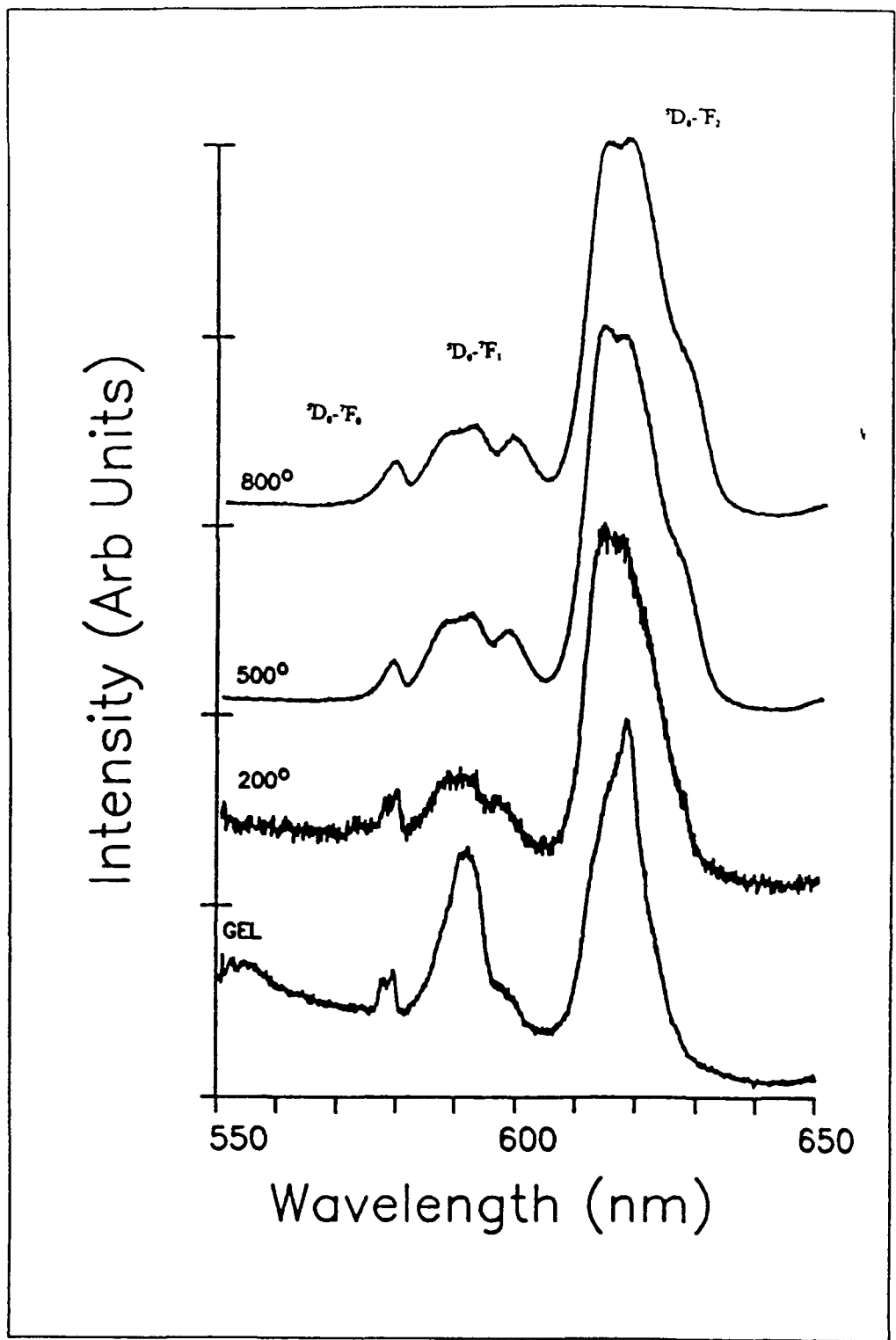


Figure 6.3 Fluorescence Spectra for 0.0% Aluminium Containing Samples (Acid Catalysed pH=1, Room Temperature, λ Excitation = 398nm)

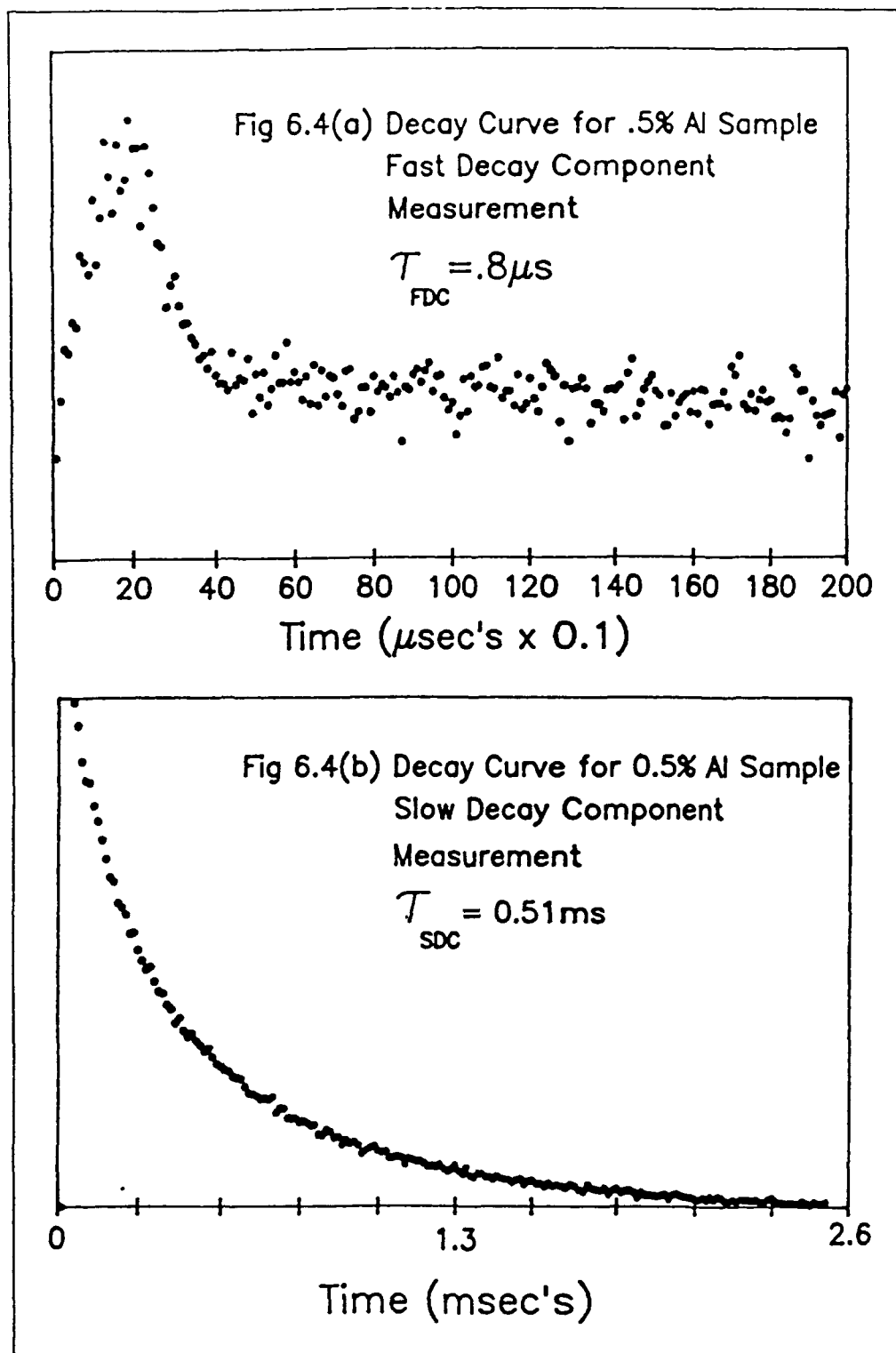


Figure 6 4 Lifetime Measurements for 0.5% Al containing sample, (A) Fast Decay Component, (FDC), (B) Slow Decay Component, (SDC). Room Temperature, λ Excitation = 337nm

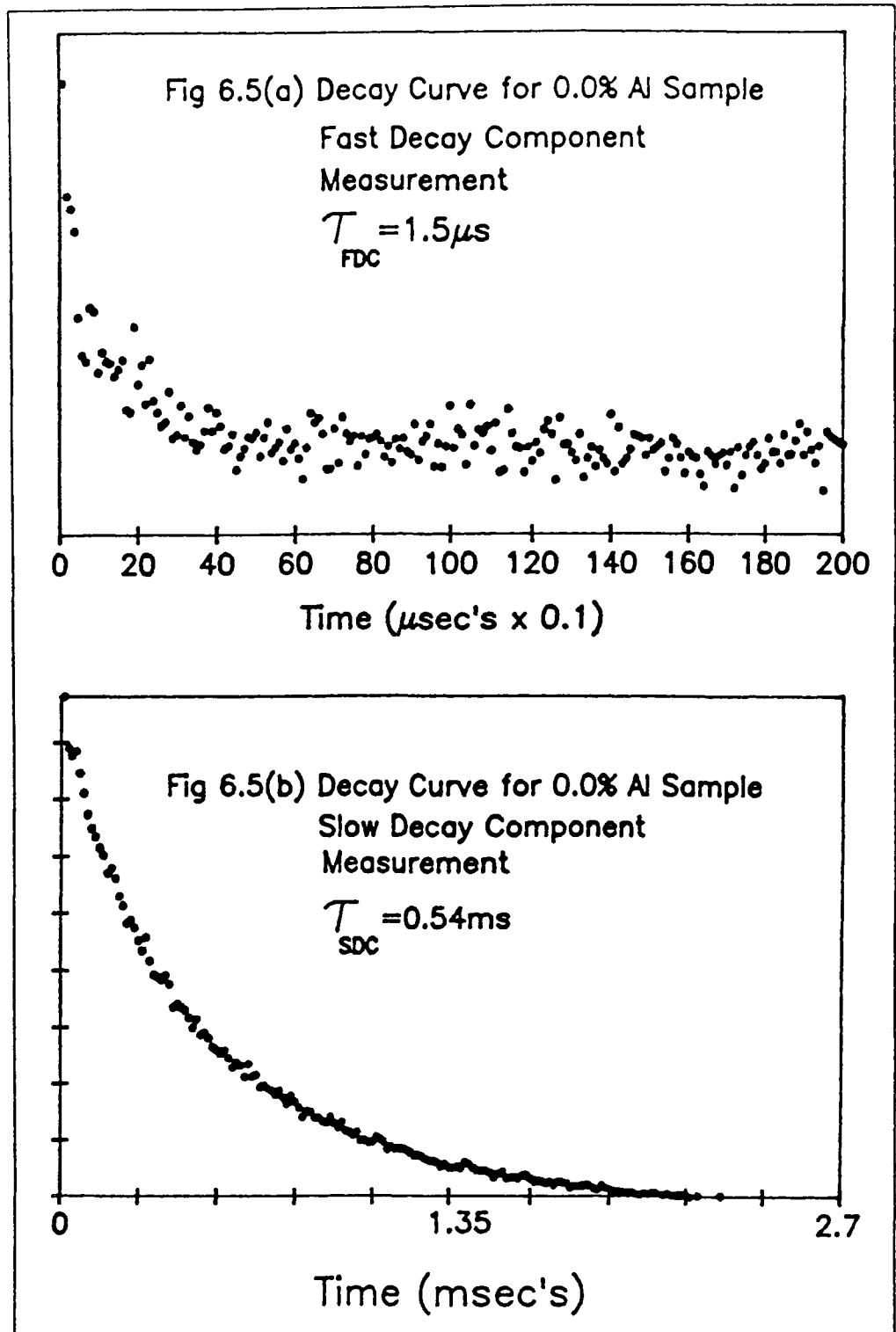


Figure 6.5 Lifetime Measurements for 0.0% Al containing sample, (A) Fast Decay Component, (FDC), (B) Slow Decay Component, (SDC). Room Temperature, λ Excitation = 337nm.

(FDC), was observed with $\tau_{\text{FDC}}=1.5\mu\text{secs}$. This is in good agreement with previous preliminary work done on the aluminium-europium codoped system examined in this laboratory, (Devlin et al [6]). It appears from this that clustering does indeed exist in these materials and that the presence of the aluminium is not dispersing the europium ions. It is proposed that the fast decay component, (FDC), is due to an alternative route for the Eu^{3+} de-excitation whereby the energy is transferred across from the excited state of ion 1 to an adjacent ion 2 in the cluster instead of de-exciting to the ground state of ion 1. This is known as concentration quenching. The excitation transfer time is shorter than the decay time to the ground state. From the data it is clear that the presence of aluminium has some effect as it reduces to some extent the fast decay component, (FDC), as compared to the aluminium free material. This could be interpreted as a reduction of the clustering effect in the presence of aluminium. It is clear that the presence of aluminium in the Eu^{3+} doped materials does not eliminate the clustering and that the aluminium affects the detailed hydrolysis and condensation rates in the process. Further work is necessary in order to (1) verify the presence of the clustering of the Eu^{3+} ions in the sol-gel matrix through other measurement techniques and (2) to investigate in detail the effect of the aluminium on both the clustering and the chemistry of the sol-gel process.

6.4 Conclusion

This chapter reported the results of the investigations into Aluminium - Europium codoped samples. It is concluded that the ad hoc addition of aluminium to a sol, hydrolysed with water at a pH=1 and a Water-TEOS ratio of 4, does not provide good dispersion of the Europium. The europium ions have a tendency to precipitate and form clusters. The presence of these clusters was confirmed by the measurement of a fast decay component in the Aluminium and non Aluminium containing samples. Based on the results presented in this and earlier chapters it is concluded that the phonon quenching due to residual OH^- ion content as well as fast decay phenomena are responsible for the quick decay of the europium ion's fluorescence. It is felt that the fast decay component measurement provides conclusive proof of the existence of the clusters of europium ions.

A problem that is not well understood is that of the form of the fast decay component. Is there just a single decay at such short timescales or are there a series, discrete or otherwise, of fast decays? It is tentatively suggested that the fast decay component may take the form of a series of discrete fast decays each characteristic of a particular cluster type in a glass environment.

In conclusion the addition of aluminium to the sol-gel samples studied in this chapter did not result in the wide dispersion of the europium ion. The gel and partially densified samples contained more residual OH groups than previously examined samples. This was one of the quenching mechanisms that are responsible for a fast decay in doped sol gel glass.

Upon heating another fast decay mechanism was observed in the sol gel system. A μsec decay time was observed in both aluminium and non aluminium containing samples. This showed that the aluminium was not able to disperse the europium ions as had been reported in the case of neodymium by Berry.

The measurement of the fast decay component corroborated earlier work by Devlin, [6], in his report of a fast decay component in europium doped sol-gel glasses. As can be seen in Table 5.3 there was very little difference in the decay measurements for the pH=5.6 sample set, and this was in agreement with the model proposed above. The fluorescence ratios for the 200°C samples are shown in Table 5.4.

Chapter 7

Soaking of Sol-Gel Samples in a Europium Nitrate Solution

7.0 Introduction

This chapter reports the work carried out on samples produced without any Europium doping and subsequently soaked in a Europium solution. Comparisons are made between the characteristics of the soaked samples and those of the conventionally doped sol-gel samples. An effort is made to infer the nature of the position of the Europium ion in the soaked sol-gel glass in order to determine whether or not the Europium ion does indeed reside in the skeleton of the sol gel glass or within the pore structure. A set of glasses, (Sample Set No 7), were produced which contained no Europium. These samples were then soaked for 48 hours in a solution of $\text{Eu}(\text{NO}_3)_3$ in ethanol and dried for 24 hours at 73°C . The samples were then furnaceed at various temperatures in order to examine the fluorescence characteristics of the soaked samples as a function of temperature.

7.1 Soaked Samples

Earlier preliminary work, [1], on soaked samples of sol gel glasses had indicated that upon soaking, the Europium ion was incorporated in a pore in the sol gel glass structure. It was suggested that the ion was attached to a pore wall and surrounded by water molecules and that as the densification temperature increased the changing emission characteristics reflected the differences between the soaked sample and a conventionally doped sol gel sample. A more comprehensive study was undertaken with a selection of glasses that were produced with no Europium and then were soaked in a manner described above. The results of both the fluorescence and lifetime measurements are shown in Figure 7.1 and Table 7.1 respectively. The dried gels were furnaceed to 200° , 500° and 800° .

7.2 Results and Discussion

The gel lifetime was measured to be 0.8ms (Method 1). This is of the order of the lifetime of 0.1ms reported by Kropp and Windsor, [2], in their study of Europium ion fluorescence in

Type	τ_{AV} Method 1 + (0 01)ms	τ_{AV} Method 2 + (0 01)ms	Log-line + (0 05)ms
Gel	0 08	0 08	0 09
200°	0 29	0 29	0 29
500°	0 31	0 31	0 37
800°	0 73	0 74	0 75

Table 7.1 Fluorescence Lifetimes for Soaked Samples (Sample Set No 7, Room Temperature, λ Excitation = 337nm)

Type	τ_{AV} Method 1 + (0 01)ms	τ_{AV} Method 2 + (0 01)ms	Log-line + (0 05)ms
Gel	0 11	0 11	0.12
200°	0 35	0 36	0 37
500°	0 51	0 54	0 58
800°	0 74	0 82	0 90

Table 7.2 Fluorescence Lifetimes for Conventionally Doped Samples, (pH=1, Room Temperature, λ Excitation = 337nm)

solution. Examining the fluorescence spectra of the gel however shows that there is a marked degree of asymmetry in the europium ions environment as in the conventionally doped gel compared with the solution, (see Figure 7.3) This can be qualitatively appreciated from the intensity of the ${}^5D_0-{}^7F_2$ transition at 615nm, (refer to figure 7.1) The narrowness of the three peaks in the spectrum of the gel show the characteristics of an ion in a liquid like environment with the relative narrowness of the low energy ${}^5D_0-{}^7F_0$ peak indicating a restricted range of site geometries for the europium ion in the pore structure of the gel. The implication is that the ion is incorporated into the pore structure and surrounded by the molecules of the solution. This would account for the quick excited decay and the mixture of solution and gel emission characteristics. In figure 7.2 the spectra of conventionally doped sol-gel glasses are displayed. Here it can be seen that the spectrum of the gel sample is also quite solution-like in its appearance. However from Table 7.2 it can be noted that the lifetime

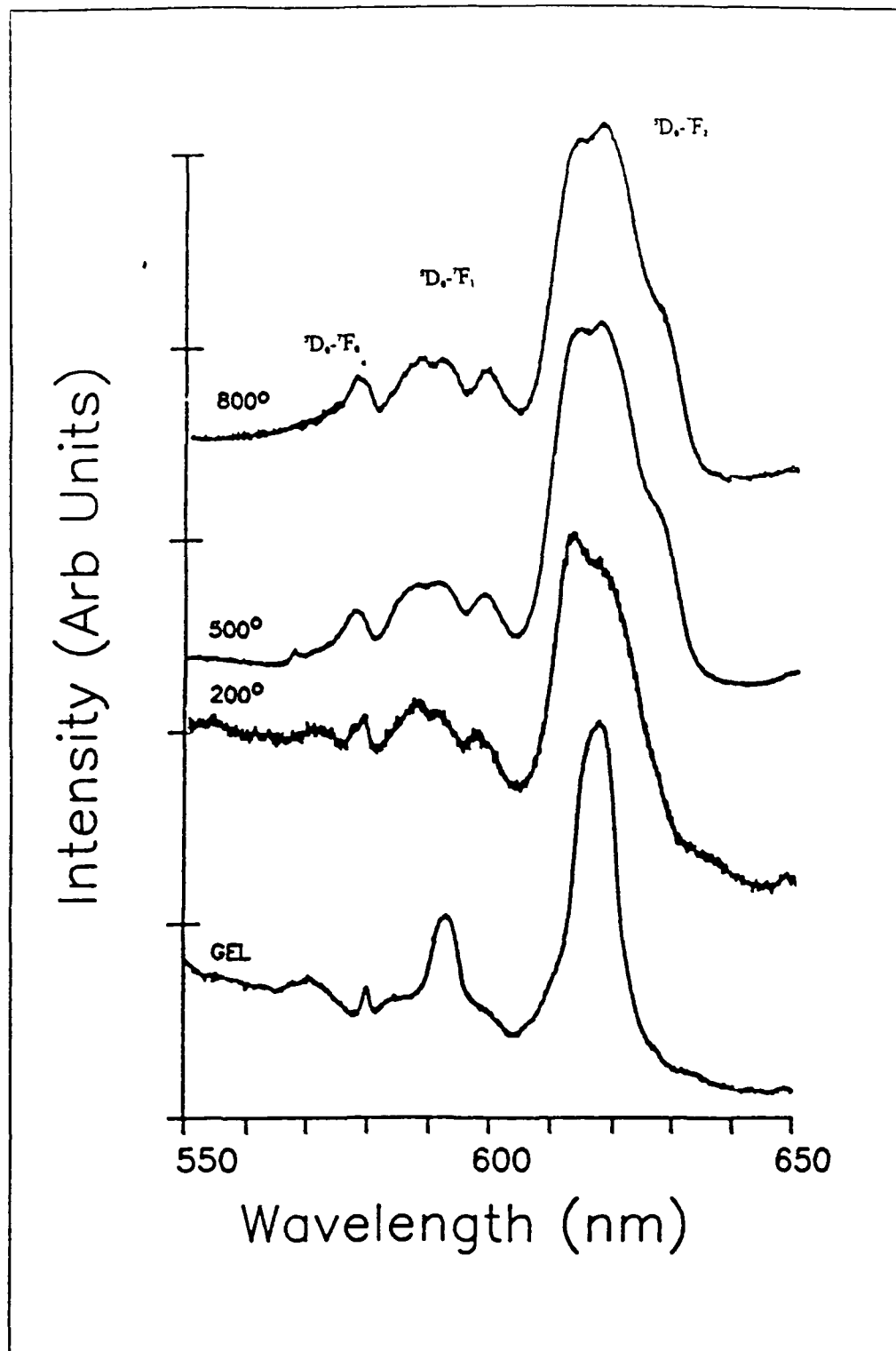


Figure 7.1 Fluorescent Spectra for Various Soaked Samples (pH=1, R=4 Sample Set No.4, Room Temperature, λ Excitation = 398nm)

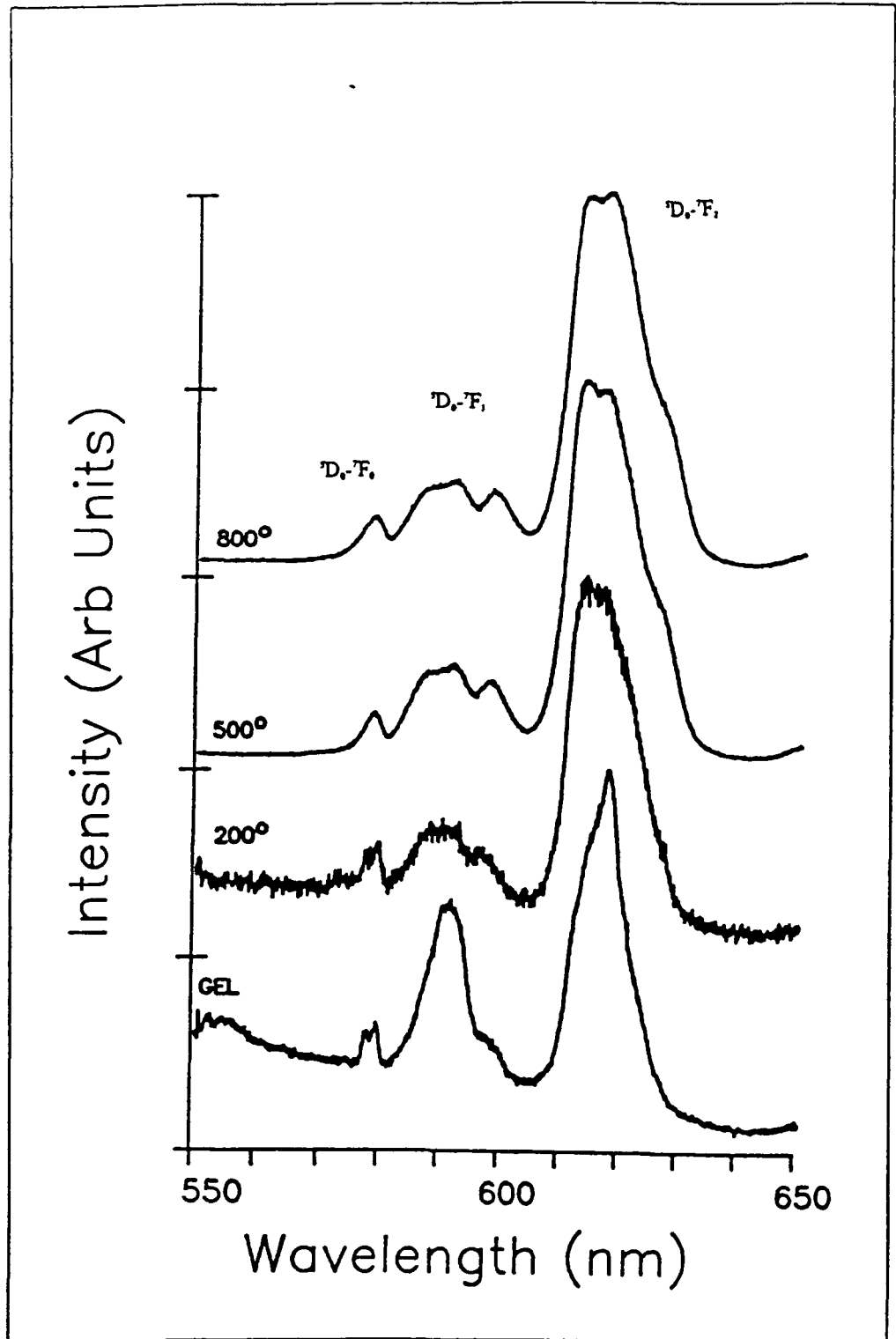


Figure 7.2 Fluorescent Spectra for Conventionally Doped Sol Gel Glasses. (pH=1, R=4, Room Temperature, λ Excitation = 398nm)

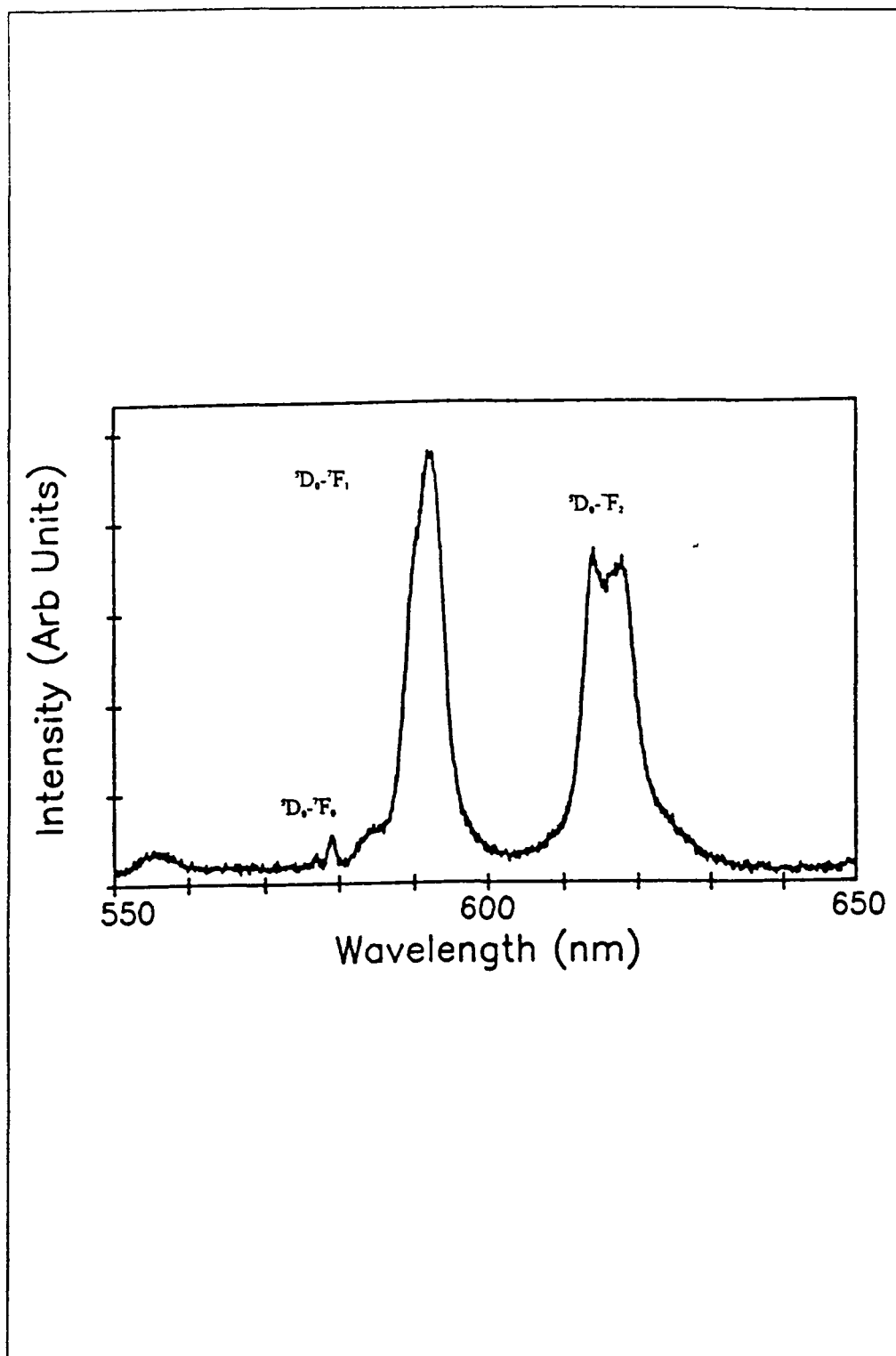


Figure 7.3 Fluorescence Spectrum of a Europium Nitrate Solution $\text{Eu}(\text{NO}_3)_3$, (Room Temperature λ Excitation = 398nm)

measurements are quite different. An explanation for the discrepancy is discussed in the next paragraph.

As the densification temperature increases the spectra of the samples furnace to different temperatures, (see Figure 7.1), acquire some of the characteristics of their conventionally doped counterparts, (Figure 7.2). The lifetime measurements at both 200°C and 500°C for the soaked samples are in no way similar to the lifetime measurements for the equivalent conventional samples. At $T = 200^\circ\text{C}$ the lifetime $\tau_{Av} = 0.29\text{ms}$ for the soaked sample and $\tau_{Av} = 0.36\text{ms}$ for the conventionally doped sample. This indicates that the Europium ion is in a much different environment from the partially densified conventionally doped sample. In conventionally doped samples the 200°C sample has been described, (see Ch. 4 Sec. 4.3), as representing a kind of intermediate step between gel and densified glass because it contains a proportionally shorter lifetime than the treatment temperature would indicate. However the soaked sample lifetime at 200°C is much shorter again and so must contain a much higher proportion of hydroxyl groups around the Europium ion. At 500°C the lifetime for the soaked sample is again less than for the conventionally doped sample. The fluorescent spectrum of the 500°C soaked sample is quite similar to the spectrum of corresponding conventional sample but the lifetime measurements indicate that the environment is still quite different in terms of hydroxyl group content. So even though the soaked sample displays the splitting associated with the high degree of asymmetry in a glassy state it must still contain a large amount of OH⁻ groups as evidenced by its comparatively fast decay time.

The 800°C soaked sample displays a fluorescence spectrum that is very similar to that of a densified gel. The broad transitions are matched by a long decay time of 0.73ms, this compares very well with a lifetime of 0.74ms for the conventionally doped 800°C sample. The high energy $^5D_0-^7F_0$ singlet transition is quite broad indicating that there are a large range of environments for the europium ion. The similarities between the soaked and conventionally doped sample are expected at a densification temperature of 800°C. This is because at such a relatively high temperature the densification process is nearly complete, [3]. The sample either soaked or conventionally doped will have adopted some or nearly all of the characteristics of amorphous SiO₂ glass. It is expected that for the soaked sample the europium ion is included into the bulk of the glass sample at this temperature as a large proportion of the pores have collapsed. This makes its optical properties appear very similar to the conventionally doped sol gel glasses where the europium is added at the solution stage of the sol gel synthesis.

7.3 Deuteration of the Sol-gel Pores

It was emphasised in Chapter 4 Section 4.6 that the maximum Eu^{3+} lifetime of approximately 1ms measured in these studies is still quite low compared to the typical lifetime measurements of approximately 2ms for Eu^{3+} in conventional glass. It is thought that a significant contribution to this small lifetime is the amount of residual OH^- still present in the materials even after densification to 800°C . To confirm this hypothesis a series of samples was prepared, (Sample Set no 8), which were quenched in either air, water or D_2O .

Base Catalysed, (pH=8), sol-gel samples were prepared at two temperature regimes, gels and 800°C . The gel was dried after soaking in D_2O and received no heat treatment and the 800°C samples were quenched in Air, Water and Deuterium respectively. They were then sealed in individual containers and lifetime measurements were carried out. The D_2O samples were sealed in an airtight container and so were impervious to degradation by water vapour. Previous work, [2], on Eu^{3+} fluorescence in deuterated solutions had reported a decrease in lifetime with time. This was attributed to the effects of water vapour coming into contact with the deuterated solution.

Lifetime measurements were performed as it was considered that they were a more sensitive indicator of the changes in the Eu^{3+} ions environment than were fluorescence spectra. The results of the lifetime measurements are tabulated in Table 7.3.

From the data presented in Table 7.3 it can be seen that the forced quenching mechanisms introduced have had a pronounced effect. One of the most notable things about these samples is that they were base catalysed at a pH=8. This should have provided the Eu^{3+} ion with a screened environment, (see chapter 5 Sec 5.3) making it less sensitive to changes in the environment surrounding it. As a guide to the lifetime measurements the decay time for the air quenched sample compares very favourably to the measured decay time of 1.0 msec for a pH=8, 800°C sample reported in Chapter 4, (Table 4.4). Using this result as a yardstick it can be seen that the effect of the water and D_2O on the decay times of 800°C samples is quite significant. The quenching in D_2O results in the doubling of the decay time and the quenching of the sample in water results in a reduction of approximately 30% in the measured lifetime. The lifetime of the water quenched sample is consistent with the presence of more water in the Eu^{3+} environment compared to the air quenched sample. The sample quenched in D_2O has a lifetime close to that expected for Eu^{3+} in conventional densified glass. The pore surface is saturated with OD^- ions which do not cause quenching of the Eu^{3+} fluorescence as discussed.

in chapter 4 Finally the deuterated gel sample has a lifetime of 0.31ms, which is approximately twice the value for the normal gel This is consistent with the presence of a layer of water on the pore surface, much of which is not displaced by D₂O on soaking It is concluded that the presence of OH ions in the sol-gel matrix is the main contributor to the reduced Eu³⁺ fluorescence lifetime Work is at present underway in this laboratory to confirm this

Sample Type	τ_{AV} Method 1 (msec + 0.01)
Gel	0.31
800° Air	0.91
800° Water	0.62
800° D ₂ O	2.0

Table 7.3 Fluorescent Decay Measurements for pH=8 Samples. (Sample Set No.8, Room Temperature, λ Excitation = 337nm)

7.4 Conclusion

Based on the experimental work carried out on the fluorescence and lifetime properties it is clear that the soaked samples have a unique combination of luminescence and lifetime characteristics. Comparison with similar conventionally doped samples show clear differences in lifetime measurements and / or fluorescent spectra. However the properties of the soaked sample at 800° are in very good agreement with the properties of the conventionally doped sol gel glass. It is suggested that at this temperature the Europium ion in the soaked sample has become incorporated into the bulk structure of the glass as the increased densification temperature causes the structure to decrease in volume collapsing the pore arrangement and surrounding the Europium ion

On the basis of the results discussed in this chapter it is concluded that when the Europium ion is added to the sol stage of the sol gel glass synthesis that it is distributed throughout the structure, bearing in mind the conclusion from Chapter 6 The europium ion does not reside in the pores of the gel structure as can be seen from the fluorescence spectra but more especially from the lifetime measurements

Concluding Remarks

This section summarizes the discussion of the properties of Eu^{3+} doped sol-gel glasses and includes various ideas for future work

Concluding Remarks

The motivation behind the work detailed in this thesis was to develop an understanding of the structure of sol-gel glasses via the optical spectroscopy of the Eu^{3+} ion in its role as a structural probe. The optical emission characteristics of the Eu^{3+} ion are a sensitive indicator of structural changes taking place within the sol-gel matrix.

This study concentrated on explaining the changes in fluorescent spectra and decay times brought about by deliberate changes to the starting materials. The modified starting materials were monitored as they were processed to different temperatures.

Areas of investigation included the role of sol pH, the confirmation of the role of OH^- groups as a large scale fluorescence quenching agent in sols and gels, this led to the investigation of the role played by Water/TEOS ratios in an attempt to determine whether there was an optimum ratio for the acid and base catalysis of sol-gel samples. Another significant area of investigation was into the role of Aluminium as a material codopant along with Europium. It was hoped to show that by addition of Aluminium, dispersion of Europium would occur thus allowing higher dopant concentration. However results indicated that the presence of Aluminium encourages large scale water retention thus causing more fluorescence quenching than in samples without Aluminium codoping. The role of Aluminium as a network modifier in sol-gel systems was also investigated following the observation of a fast decay component, (FDC), in both aluminium free and aluminium containing samples.

Studies were also carried out to determine whether or not the Eu^{3+} ion resides in the pores of the gel structure or in the glass matrix itself. On the basis of the results presented in Chapter 7 it was concluded that when dopant ions are incorporated in the sol stage that they become enmeshed in the glass skeleton as the densification temperature increased. It was also found that high temperature sol-gel samples quenched in water suffered significant reduction in decay time and those quenched in deuterium experienced significant increases in decay times.

Suggestions for Further Work

Sol-gel science and technology raises some questions that the use of the Eu^{3+} ion as a structural probe may elucidate. Based on the investigations reported in this thesis it is suggested that the following might be representative of such

From Chapter 4

What exactly is the pH dependence in the asymmetry decrease of the fluorescence transitions during the change from the sol to the gel? It appears that it may be associated with the isoelectric point of Silica at $\text{pH}=2.5$

From Chapter 5

From the deuterated sample measurements in Chapter 4 it is known that the less OH groups present in the structure the greater the fluorescence efficiency. It would be important to develop the Water-TEOS experiments specifically at the sol to 200°C stage to determine how the hydrolysis, condensation rates progress as a function of pH. What would be the effect for example of supercritical drying on high pH samples at various water-TEOS ratios?

From Chapter 6

The question of Aluminium and other metal ion codoping, for example Na, [1], raises a lot of questions about the role of the codopant as a network modifier. Based on the results presented in this thesis it would appear that the Aluminium encourages fluorescence quenching by retaining large amounts of water in the structure. It does not, again based on the results contained in this thesis, appear to disperse the Europium ions with any great degree of efficiency. This was confirmed by the observation of a fast decay component, (FDC), in both Aluminium and Aluminium free sol-gel samples. This was ascribed to clustering of the europium ions in the sol-gel matrix. It would be interesting to determine how many FDC's could be measured, [2], in a sol-gel Aluminium-Europium codoped sample. Would it be possible to discretize the time response of the decay to determine whether or not a particular cluster type is resolvable in terms of a characteristic fast decay component?

References

Chapter 1

- [1] Zachariasen, W H (1932), J Am Chem Soc 54, 38-41
- [2] M^c Craith, B D , Ruddy, V , Potter, C , O'Kelly, B , M^c Gilp, J F EElectronic Letters 27, 14
- [3] Sakka, S "Proceedings of the Winter School on Glasses and Ceramics from Gels" (1989) San Carlos Brazil p 346
- [4] Berry, A.J , King, T A , (1989) J Phys D Appl Phys 22, 1419
- [5] Brinker, C.J , Scherer, G , "Sol Gel Science" Academic Press
- [6] Hench, L , West, J (1990) Chem Rev 90 33
- [7] Klein, L C, Garvey, G.J, in "Ultrastructure processing of ceramics, glasses and composites" Hench, L L, Ulrich, D R, Eds Wiley (1984), p88
- [8] Hench, L L, Wilson M.J, Balaban, C, Nogues, J L, "Sol-gel processing of large silica optics". Proc of the 4th International Conference of Ultrastructure processing of ceramics, glasses and composites, Tucson AZ (1989).

Chapter 2

- [1] Yen, W M (1981) in Laser Spectroscopy of Solids Edited by W M Yen and P M Selzer Topics in Applied Physics Series, Vol 49 Springer-Verlag, Berlin
- [2] Imbusch, G F (1978), in Luminescence Spectroscopy, Edited by M. Lumb Academic Press
- [3] Demas, J N (1983) in Excited State Lifetime Measurements, Academic Press
- [4] Imbusch, G F (1978), in Luminescence Spectroscopy, Edited by M Lumb Academic Press
- [5] Hufner, S (1978) in Optical Spectra of Transparent Rare Earth Compounds, Academic Press
- [6] Yen, W M (1989) in Laser Spectroscopy of Solids II. Topics in Applied Physics Vol 65 Edited by W M Yen, Springer-Verlag, Berlin.
- [7] Devlin, K (1991) Ph D Thesis, Dublin City University
- [8] Gallagher, P K (1964) J. Chem. Phys , 41, 10, 3061

Chapter 3

- [1] Demas, J N (1983) in *Excited State Lifetime Measurements*, Academic Press
- [2] Lempicki et al (1981), *J Chem Phys* 74 10
- [3] Bevington, P R , in *Data Reduction and Error Analysis for the Physical Sciences* M^c Graw Hill, (1969)

Chapter 4

- [1] Iler, R K , (1979), *The Chemistry of Silica*, Wiley Interscience
- [2] Brnker, C J , Scherer, G , in "Sol Gel Science" Academic Press, (1990)
- [3] Gray, H J , Isaacs, A (1978) in *A New Dictionary of Physics*, Longman
- [4] Hench, L , West, J (1990) *Chem Rev* 90 33
- [5] Gallagher, P K , (1964) *J Chem Phys* 41 10 3061
- [6] Brecher, C , Riseberg, L.A., (1980) *J Non-Cryst Solids*, 40 469
- [7] Devlin, K , O'Kelly, B , Tang, Z R., M^cDonagh, C., M^c Gulp, J F. (1991) *J Non-Cryst. Solids*, 135, 8
- [8] James, P F , (1988) *J Non-Cryst Solids*, 100 93
- [9] Weber, M , (1981) in *Laser Spectroscopy of Solids*, Edited by W Yen and M Selzer, Springer-Verlag, Berlin
- [10] Hench, L., West, J (1990) *Chem Rev* 90 33
- [11] Brnker, C J , (1988), *J Non-Cryst Solids*, 100, 31
- [12] Kropp, J L , Windsor, M , (1965), *J Chem. Phys* 42, 5, 1599

Chapter 5

- [1] Brnker, C J , Scherer, G , in "Sol Gel Science" Academic Press, (1990)
- [2] Hench, L , West, J (1990) *Chem Rev* 90 33

- [3] Brnker, C J , (1988), *J Non-Cryst Solids*, 100, 31
- [4] James, P F , (1988) *J Non-Cryst Solids*, 100, 93

Chapter 6

- [1] Berry, A J , King, T A , (1988) J Phys D Appl Phys 22 1419
- [2] Weber, M.J , (1990) J Non-Cryst Solids, 123, 208
- [3] Arai, K , Namikawa, H , Kumata, K , Ishii, Y , Tanaka, H , Iida, I (1983), Japanese Journal of Applied Physics, 22, 7, 397
- [4] Peterson, G F , Bridenbaugh, P M , (1964), J Opt Soc Am , 54, 644
- [5] Mullins, M E , Cornilsen, B C , Kline, A A , Sokolov, Lj M , Surapanun, S (1991), Proceedings of the VII International Conference on the Physics of Non-Crystalline Solids, Cambridge, England.
- [6] Devlin, K , (1991) Ph D Thesis Dublin City University

Chapter 7

- [1] Devlin, K , O'Kelly, B., Tang, Z R , M'Donagh, C , M' Gilp, J F. (1991) J. Non-Cryst. Solids, 135, 8.
- [2] Kropp, J L , Windsor, M , (1965), J Chem Phys 42, 5, 1599
- [3] Hench, L , West, J. (1990) Chem Rev. 90 33

Concluding Remarks

- [1] Devlin, K , (1991) Ph D Thesis, Dublin City University
- [2] Arai, K , Namikawa, H , Kumata, K , Ishii, Y , Tanaka, H , Iida, I. (1983), Japanese Journal of Applied Physics, 22, 7, 397

Appendix 1: Programme Listings

Data Acquisition Programme "Aver2"

This program was used to run the fluorescence scans of the Eu^{2+} doped sol-gel glasses. It provided the spectrometer motor control and performed the data acquisition.

```
10 REM *****
20 REM **          **
30 REM **   LUMINESCENCE   **
40 REM **          **
50 REM **   SIGNAL AVERAGED   **
60 REM **          **
70 REM *****
75 CLS
77 MODE0
80 PRINT PRINT PRINT
90 PRINTTAB(5,5)"*****"
100 PRINTTAB(5,6)"          *"
110 PRINTTAB(5,7)"   DATA ACQUISITION PROGRAM   *"
120 PRINTTAB(5,8)"          *"
125 PRINTTAB(5,9)"   KEVIN DEVLIN D C U   *"
130 PRINTTAB(5,9)"*****"
132 PRINTTAB(5,12)"OPTIONS AVAILABLE"
133 PRINTTAB(5,14)"(A) Scanning Emission Spectrometer"
134 PRINTTAB(5,16)"(B) Scanning Excitation Spectrometer"
136 INPUTTAB(5,18)"CHOICE= ",CH$
140 CLS
150 CLOSE#0
160 MODE0
170 A=&FCF0
180 ?(A+11)=&C0 ?(A+2)=&70 ?(A+4)=6 ?(A+5)=0
190 C=0
200 INPUTTAB(5,5)" NUMBER OF SAMPLES PER POINT",AV
210 PRINTTAB(5,15)" CHECK TO SEE IF SLIT IS CLOSED"
220 K=GET
230 FOR T=1 TO 10
240 ?A=16 ?(A+12)=&0C ?(A+12)=&0E
250 a=(?(A+1))*16+(?(A))MOD16
260
270 C=C+a
280 PRINTa
290 NEXT
300 B=C DIV 10
310 PRINTTAB(5,15)"BACKGROUND D C SIGNAL ="B
320 K=GET
330 CLS
340
350 PRINTTAB(5,5)" ADJUST FOR MAX SIGNAL"
360 PRINTTAB(5,10)"TYPE R TO CONTINUE"
370 K=GET
380 ?(A+12)=&0C.?(A+12)=&0E
390 IN=?(A+1)*16+(?(A))MOD16
400 PRINTTAB(5,15)"MAX SIGNAL ="B-IN
410 IF K>69 AND K>82 THEN 370
```

```

420 IF K=69 THEN 380
430 PRINT
440 PRINT
450 CLS
460 *DRIVE0
470 PRINT
480 PRINT SAMPLE SPECTRUM"
490 PRINT
500 a=OPENIN"START" INPUT#a,Start
510 b=OPENIN"END" INPUT#b,End
520 c=OPENIN"Inc" INPUT#c,Inc
530 CLOSE#0
540 PRINT"Starting wavelength "Start
550 PRINT
560 PRINT"Finishing wavelength "End
570 PRINT
580 PRINT"Incremental rate "Inc
590 P=(End-Start)/Inc+1
600 PRINT
610 INPUT"Do you want to change wavelength range y/n"
620 IF GETS="Y" THEN PROCINITIAL
630 MODE4
640 DIM Y(2505) DIM K(1)
650 PROCwave
660 PROCADC
670 PROCDATA
680 PROCSAVE
690 INPUT TAB(0,8)" Do you want a copy on chart recorder y/n"
700 IF GETS="Y" THEN PROCDAC
710 PROCDRAW
720 PROCLABLE
730 *DRIVE0
740 END
750 DEF PROCINITIAL
760 PRINT PRINT PRINT
770 INPUT"Starting wavelength ",Start
780 PRINT
790 INPUT"Finish wavelength ",End
800 PRINT
810 INPUT"Incremental rate ",Inc
820 P=(End-Start)/Inc+1
830 ENDPROC
840
850 DEF PROCDATA
860 X=0
870 A1=Start.b=1 d=&FCC0 ?(d+3)=128
880 CLS M=1
890 FOR D=1 TO P
900 PROCAVERAGE
903 IF CHS="A" THEN GOTO 910
905 IF CHS="B" THEN PROCSTEP2
906 GOTO 920
910 PROCSTEP
920 PRINTTAB(5,5)A1
930 MOVE X,Y(D)/2 DRAW X,Y(D)/2
940 X=X+1200/P
950 A1=A1+Inc

```

```

960 NEXT
970 ENDPROC
980 DEF PROCDRAW
990 MOVE 0,0 DRAW 0,900
1000 DRAW 1200 900 DRAW 1200,0
1010 DRAW 0,0
1020 VDU5
1030 MOVE 250 1000 PRINT"Intensity vs Wavelength "
1040 MOVE -10,910 PRINT " MOVE 590,910 PRINT" I" MOVE 1190,910 PRINT " I"
1050 ENDPROC
1060 DEF PROCCLABLE
1070 MOVE -150,950 PRINTStart
1080 MOVE 900,950 PRINTEnd
1090 VDU4
1100 ENDPROC
1110 DEF PROCDAC
1120 A1=Start
1130 FOR D=1 TO P
1140 V=2048-(Y(D))
1150 d?b=(V)DIV16
1160 d?2=((V)MOD16)*(1+16*b)
1170 PRINTTAB(5,5)A1
1180 A1=A1+Inc
1190 FOR I=1 TO 200 NEXT
1200 NEXTD
1210 ENDPROC
1220
1230
1240 DEF PROCADC
1250 A=&FCF0
1260 ?(A+11)=&C0
1270 ?(A+2)=&70
1280 ?(A+4)=6
1290 ?(A+5)=0
1300 ENDPROC
1310 DEF PROCSAVE
1320 INPUT TAB(0,6)" Do you want to save y/n"
1330 IF GET$="N" THEN ENDPROC
1340 INPUT TAB(5,8)"Name of file " BS
1350 Y=OPENOUT(BS)
1360 PRINT#Y,Start,End,Inc
1370 FOR D=1 TO P
1380 PRINT#Y,Y(D)
1390 NEXT
1400 CLOSE#0
1410 ENDPROC
1420 DEF PROCwave
1430 a=OPENOUT"START" PRINT#a,Start
1440 b=OPENOUT"END" PRINT#b,End
1450 c=OPENOUT"INC" PRINT#c,Inc
1460 CLOSE#0
1470 ENDPROC
1480 DEF PROCAVERAGE
1490 YD1=0 YD=0
1500 FOR Q=1 TO AV
1510 ?A=16
1520 ?(A+12)=&EC

```

```
1530 ?(A+12)=-&CE
1540 YD=B-?(A+1)*16+?(A)MOD16)
1550 YD1=YD1+YD
1560 NEXT
1570 Y(D)=YD1/AV
1580 Y(D)=ABS Y(D)
1590 ENDPROC
1600 DEF PROCSTEP
1610 ?&FE62=-&03
1620 FOR L=1 TO Inc*100
1630 ?&FE60=1
1640 ?&FE60=0
1650 NEXT
1660 ENDPROC
1670 DEF PROCSTEP2
1680 ?&FE62=-&07
1690 FOR L= 1 TO Inc*6
1700 XR=254 YR=250
1710 ?&FE60=XR
1720 FOR K=1 TO 50 NEXT K
1730 ?&FE60=YR
1740 FOR K=1 TO 50 NEXT K
1750 NEXT L
1760 ENDPROC
```

Appendix 2 Programme Listings

Data Acquisition and Control Programme "Lifet"

This programme carried out all the lifetime measurements described in this report, saved the data and then called an analysis programme "Compstw", (See Appendix 3)

```
10
20 REM          DATA ACQUISITION PROGRAM
30
40 REM          FOR SR400 PHOTON COUNTER.
50
60 REM          Kevin Devlin 19/10/89 D C U
70 MODE7
90 CLS *SHADOW
100 PRINT TAB(5)"*****"
110 PRINT TAB(5)"**DATA ACQUISITION PROGRAM**"
120 PRINT TAB(5)"**FOR SR400 PHOTON COUNTER**"
130 PRINT TAB(5)"*****" PRINT
140 PRINT "PRESS C TO CONTINUE" XS=GET$ PRINT
150 IF XS="C" ELSE GOTO 90
160 INPUT"SPECTROMETER WAVELENGTH ",SWS PRINT
170 INPUT"SLIT WIDTH (mm)      ",SL$.PRINT
180 INPUT"INPUT DATAFILE NAME TO BE STORED ON DISC";F$ PRINT
190 X=OPENIN(" 2 "+F$)
200 IF X<0 THEN PRINT"**DATA FILE ALREADY EXISTS**" CLOSE#0 PRINT ELSE 230
210 PRINT"PRESS C TO CONTINUE OR ANY KEY TO RENAME" XS=GET$
220 IF XS="C" THEN 230 ELSE 90
230 *IEEE
240 cmd%=OPENIN("COMMAND")
250 data%=OPENIN("DATA")
260 ESTR$=CHR$(13)+CHR$(10)
270 PRINT#cmd%,"END OF STRING",ESTR$
280 PRINT#cmd%,"BBC DEVICE NO",0
290 PRINT#cmd%,"CLEAR"
300 PRINT#cmd%,"REMOTE ENABLE"
310 PRINT#cmd%,"UNLISTEN"
320 photon%=OPENIN("23")
330
340 REM *****INPUT OF INITIAL SETUP PARAMETERS*****
350
360 PRINT#cmd%,"LISTEN",photon%,"EXECUTE"
370 PRINT#data%,"CM,CIO,GDO,NP,DL0,GW0,GY0,CP2"
380 PRINT#cmd%,"UNLISTEN"
390 PRINT#cmd%,"TALK",photon%
400 INPUT#data%,CCM$,CCIO$,GGDO$,NNP$,DDL0$,GGW0$,GGY0$,CCP2$
410 PRINT#cmd%,"UNTALK"
420 NNP=VAL(NNP$)
425 DIM V(NNP+30),B(NNP+30),Q(NNP+30)
430
440 REM Display of parameters of significance to measurement of lifetimes
450
460 CLS
470 PRINT TAB(5)"**DATA ACQUISITION PROGRAM**"
480 PRINT TAB(5)"**FOR SR400 PHOTON COUNTER**" PRINT
```

```

490 PRINT DATA FILE "TAB(20),FS PRINT
500 REM PRINT COUNTING MODE TAB(20),CCMS PRINT
510 PRINT NO OF TRIGGERS TAB(20),CCP2S PRINT
520 PRINT NO OF POINTS"TAB(20),NNPS PRINT
530 PRINT "A DISC LEVEL"TAB(20),DDL0S PRINT
540 PRINT 'GATE A SCAN STEP TAB(20),GGY0S PRINT
550 PRINT "GATE A WIDTH"TAB(20),GGW0S PRINT
560 PRINT "GATE A DELAY"TAB(20),GGD0S PRINT
565 PRINT"Press COM on SR400 and then ESCAPE to stop scan" PRINT
570 TIME=0 REPEAT UNTIL TIME =500
580 PRINT PRINT "AT POINT NUMBER" PRINT
590 PRINT""COUNTER READING"" PRINT
600 REM*****
610
620 REM *****START OF DATA ACQUISITION *****
630
640 REM*****
650
660 REM*****Clear counters,Start scan.*****
670
680 PRINT#cmd%,"LISTEN",photon%,"EXECUTE"
690 PRINT#data%,"CR,CS"
700 PRINT#cmd%,"UNLISTEN"
710
720 REM*****Poll for data ready *****
730 SSS1=0 QQA=0 QQB=0
740 PRINT#cmd%,"LISTEN",photon%,"EXECUTE"
750 PRINT#data%,"SS1"
760 PRINT#cmd%,"UNLISTEN"
770 PRINT#cmd%,"TALK",photon%
780 INPUT#data%,SSS1$
790 PRINT#cmd%,"UNTALK"
800 SSS1=VAL(SSS1$)
810 IF SSS1=0 THEN 740
820
830 REM *****Read data value *****
840 FOR I=1 TO NNP
850 PRINT#cmd%,"LISTEN",photon%,"EXECUTE"
860 PRINT#data%,"QA"+STR$(I)
865 PRINT#data%,"QB"+STR$(I)
870 PRINT#cmd%,"UNLISTEN"
880 PRINT#cmd%,"TALK",photon%
890 INPUT#data%,QQAS,QQBS
900 PRINT#cmd%,"UNTALK"
910 PRINTTAB(20,20), I-1
920 QQA=VAL(QQAS) QQB=VAL(QQBS)
930 IF QQA=-1 THEN GOTO 850
940 D=I+9 V(D)=QQA B(D)=QQB
950 PRINT PRINT PRINT QQA
960 NEXT I
970 PRINT#cmd%,"REMOTE DISABLE"
980 CLOSE#photon%
990 CLOSE#data%
1000 CLOSE#cmd%
1010 CLOSE#0
1015 PROCDIVIDE
1020 PROCSAVE

```

```

1025 CHAIN"COMPSTW"
1030 END
1040
1050 REM*****Save data to disk.*****
1060
1070 DEF PROCSAVE
1080 *DISK
1090 Q(0)=VAL(CCMS)
1100 Q(1)=VAL(CCI0S)
1110 Q(2)=VAL(GGD0S)
1120 Q(3)=VAL(NNP5)
1130 Q(4)=VAL(DDL0S)
1140 Q(5)=VAL(GGW0S)
1150 Q(6)=VAL(GGY0S)
1160 Q(7)=VAL(SWS)
1170 Q(8)=VAL(SLS)
1175 Q(9)=VAL(CCP2S)
1180 PRINT PRINT PRINT
1190 X=OPENOUT(" 2 "+FS)
1200 FOR I= 0 TO (NNP+9)
1210 PRINT#X,Q(I)
1220 NEXTI
1230 CLOSE#0
1240 ENDPROC
1250
1260 REM*****Stop scan *****
1265
1270 DEF PROCCLEAR
1280 PRINT#cmd%,"LISTEN",photon%"EXECUTE"
1290 PRINT#data%,"CH,NE0;ET"
1300 PRINT#cmd%,"UNLISTEN"
1305 FOR I=1 TO 1000.NEXT
1310 ENDPROC
1320
1330 REM*****Calculate true signal *****
1340
1350 DEF PROCDIVIDE
1355 BMAX=-100
1360 FOR I=10 TO (NNP+9)
1370 IF B(I)>BMAX THEN BMAX=B(I)
1380 NEXT
1390 FOR I=10 TO (NNP+9)
1400 B(I)=B(I)/BMAX
1410 Q(I)=V(I)/B(I)
1420 NEXT
1430 ENDPROC

```

Appendix 3 Programme Listing

Data Analysis Programme "Compstw"

This programme analysed the decay curves using a weighted least squares semi-log plot

```
10 REM *****
20 REM ****
30 REM **** 1 Weighted Least square fit of decay curve ****
40 REM ****      semi-log plot      ****
50 REM ****
55 REM **** 2. Component stripping for two component ****
56 REM ****      lifetimes.      ****
57 REM ****
60 REM *****
80 CLEAR
90 *DRIVE2
100 MODE0
110 DIM V(12)
120 *
130 PRINT PRINT.PRINT
140 INPUT"Name of data file" ,B$
150 L=OPENIN(B$)
160 FOR I=0 TO 9
170 INPUT#L,V(I)
180 NEXT
190 CLS
200 CM=V(0) CI=V(1) GD=V(2) NP=V(3) DL=V(4) GW=V(5)-GY=V(6)
210 N=NP time=GY
220 DIM Y(N),Y1(N),Y2(N)
230 FOR I=1 TO N-1 INPUT#L,Y(I) NEXT CLOSE#0
240 B=0
250 PROCCALCULATE PROCDRAW:PROCINTENSITY.PROCRESET.PROCDUMP
260 END
270
280 DEF PROCCALCULATE          REM Calculates max
290 YMAX=0:YMIN=100          REM & min values of
300 FOR I=1 TO N-1          REM decay curve
310 IF Y(I)>YMAX THEN YMAX=Y(I)
320 IF Y(I)<=YMIN THEN YMIN=Y(I)
330 NEXT I
340 ENDPROC
350
360 DEF PROCDRAW              .REM Plots decay
370 X=100                    .REM curve on
380 FOR I=1 TO N-1          REM monitor
390 REM Y(I)=Y(I)-YMIN
400 MOVE X,(Y(I)*900/YMAX) DRAW X,(Y(I)*900/YMAX)
410 X=X+1200/N NEXT
430 ENDPROC
440
450 DEF PROCINTENSITY
460 VDU4 VDU 29,50;950; X=50
```

```

470 Y1max=-100 Y1min=100
480 PROCCALC2
490 FOR I=1 TO N-1
500 Y=Y1(I)*-900/Y1min
510 MOVE X+2,Y+2 DRAW X-2 Y-2
520 MOVE X 2,Y+2 DRAW X+2,Y-2
530 X=X+1200/N NEXT I
540 PROCZOOM
550 STA=S FIN=F
560 T=STA*time P=FIN -STA P=P+1
570 w=0 w1=0 w2=0 w3=0 w4=0
580 REM SLOPE OF SLOW COMPONENT
590 FOR O=STA TO FIN
600 PROCSUM T=T+time NEXT O
610 PROCSLOPE PROCEQ
620 w=0 w1=0 w2=0 w3=0 w4=0
630 PROCCALCULATE2
640 T=0 X=50 FOR O=2 TO N
650 Y1(O)=LN(Y2(O)/Imax)
660 Y=Y1(O)*-900/Y1min MOVEX,Y DRAW X,Y
670 P=N PROCSUM T=T+time
680 X=X+1200/N NEXT O PROCSLOPE
690 w=0 w1=0 w2=0 w3=0 w4=0
700 PROCZOOM
710 STA=S.FIN=F T=(time)*STA
720 FOR O= STA TO FIN
730 Y1(O)=(Y(O)-Y2(O))
740 IF Y1(O)<=0 THEN GOTO 770
750 Y1(O)=LN(Y1(O)/(YMAX-Imax))
760 PROCSUM
770 T=T+time.NEXT O
780 PROCSLOPE PROCEQ ENDPROC
790
800 DEF PROCSUM
805 WEIGHT=(1/(Y1(O)*(-1)))
860 w=w+WEIGHT REM sum w
870 w1=w1+WEIGHT*T*Y1(O) .REM sum t*y
880 w2=w2+WEIGHT*T REM sum t
890 w3=w3+WEIGHT*Y1(O) REM sum y
895 w4=w4+WEIGHT*T*T REM sum sqr t
900 ENDPROC
910
920 DEF PROCSLOPE
935 Slope=((w*w1)-(w2*w3))/((w*w4)-(w2*w2))
940 Intercept=((w4*w3)-(w2*w1))/((w*w4)-(w2*w2))
950 PRINTTAB(0,20)Slope
960 LIFT=-1/Slope
970 PRINTTAB(0,25)LIFT
980 ENDPROC
990
1000 DEF PROCEQ
1010 T1=0 X=50 FOR p=1 TO N
1020 Y1(p)=T1*Slope+Intercept Y=Y1(p)*-900/Y1min
1030 MOVE X,Y DRAW X,Y X=X+1200/N Y2(p)=EXP(Y1(p))*YMAX
1040 T1=T1+time NEXT p
1050 ENDPROC
1060

```

```

1070 DEF PROCZOOM
1080 *FX4,1
1090 C=400 hold=0 M=0 UZ=0
1100 MOVE C,50 PLOT 6,C,-900
1110 PRINT TAB(0,0),"
1120 PRINT TAB(0,0), Slow [ ,CHRS(200), 'CHRS(201),"] Fast[<>] HOLD(H) EXPAND (E) REMOVE
(R)".
1130 XS=GETS
1140 IF XS=CHRS(136) THEN PROCBAR(-1200/N)
1150 IF XS=CHRS(137) THEN PROCBAR(1200/N)
1160 IF XS="H" THEN PROCHOLD
1170 IF XS=">" ORXS=" " THEN PROCBAR(10*1200/N)
1180 IF XS="<" ORXS="," THEN PROCBAR(-10*1200/N)
1190 IF XS="R" THEN PROCREMOVE
1200 IF XS="E" THEN PROCEXPAND
1210 IF M=1 THEN GOTO1230
1220 GOTO 1130
1230 ENDPROC
1240
1250 DEF PROCBAR(I)
1260 MOVE C,50 PLOT 6,C,-900
1270 C=C+I
1280 IF C>1250 THEN C=50
1290 IF C<50 THEN C=1250
1300 MOVE C,50-PLOT 6,C,-900
1310 ENDPROC
1320
1330 DEF PROCHOLD
1340 PRINTTAB(0,0)"
1350 IF hold =1 THEN PRINT TAB(0,0),"Point already held press R to remove " XS=GETS GOTO 1450
1360 UZ=1200/N POINT=((C-50)/UZ)
1370 F=POINT
1380 VDU5
1390 PLOT 4,C,-900
1400 PLOT0,2,-4
1410 PRINT CHRS(202),
1420 VDU4
1430 hold=1
1440 C=C+UZ MOVE C,50 PLOT 6,C,-900
1450 ENDPROC
1460
1470 DEF PROCREMOVE
1480 IF hold=0 THEN GOTO 1570
1490 J=C
1500 C=INT(POINT)
1510 hold=0
1520 GCOL4,1 PROCHOLD
1530 MOVE C,50 PLOT 6,C,-900 C=C+UZ.MOVE C,50.PLOT 6,C,-900
1540 hold=0
1550 C=J
1560 GCOL0,1
1570 ENDPROC
1580
1590 DEF PROCEXPAND
1600 PRINTTAB(0,0),"
1610 D=((C-50)/UZ)
1620 S=D

```

```

1630 IFS>F THEN TEMP=S S=F F=TEMP
1640 PRINT S,F
1650 M=1
1660 W=1
1670 ENDPROC
1680
1690 DEF PROCRESET
1700 *FX4,0
1710 ENDPROC
1720
1730 DEF PROCCALC2
1740 FOR I=1 TO N-1
1750 IF Y(I)<=0 THEN 1790
1760 Y1(I)=LN((Y(I))/YMAX)
1770 IF Y1(I)>Y1max THEN Y1max=Y1(I)
1780 IF Y1(I)<=Y1min THEN Y1min=Y1(I)
1790 NEXT I
1800 ENDPROC
1810
1820 DEF PROCDUMP
1830 DS=GETS IF DS="D" THEN CALL D%
1840 ENDPROC
1850
1860 DEF PROCCALCULATE2
1870 Imax=-100 Imin=100
1880 FOR I=1 TO N
1890 IF Y2(i) > Imax THEN Imax=Y2(i)
1900 IF Y2(i) <= Imin THEN Imin=Y2(i)
1910 NEXT I.ENDPROC

```

Appendix 4 Programme Listing

Programme Listing "Half of 84"

This programme analysed the decay curve data, to determine an average lifetime, in two ways
Numerical Integration and Simpsons Rule

```
10 *SHADOW
11 REM*****
12 REM*****          *****
13 REM***** THIS PROGRAM CALCULATES THE LIFETIME BY TWO *****
14 REM*****      SEPERATE METHODS          *****
15 REM*****          *****
16 REM***** 1 NUMERICAL INTEGRATION          *****
17 REM***** 2 AREA UNDER THE CURVE SIMPSONS RULE *****
18 REM***** GER ENNIS, D C U 1991          *****
19 REM*****
20 CLEAR
30 *DRIVE0
40 MODE0
50 DIM V(12)
60 *
70 PRINT PRINT PRINT
80 INPUT"Name of data file" ,B$
90 L=OPENIN(B$)
100 FOR I=0 TO 9
110 INPUT#L,V(I)
120 NEXT
130 CLS
140 CM=V(0) CI=V(1) GD=V(2) NP=V(3) DT=V(4) GW=V(5)·GY=V(6)
150 N=NP
160 time=GY
170 DIM Y(N),J(N),K(N)
180 FOR I=1 TO N-1 INPUT#L,Y(I) NEXT CLOSE#0
190 B=0
191 REM*****
192 REM*****          *****
193 REM***** PROC THE PROGRAMS "FUNCTIONS"          *****
194 REM*****          *****
195 REM*****
200 PROCCALCULATE PROCDRAW PROCBACKGROUND·PROCZOOM ST=F EN=K
205 PROCMEANLIFE PROCMEANLIFE1 ST2=F·EN2=K PROCSILPHO PROCSILPHO1 PROCINFO
210 PROCSILPHO PROCSILPHO1 PROCINFO
220 END
224 REM*****
225 REM*****          *****
226 REM***** PROCCALCULATE MAX+MIN VALUES          *****
227 REM*****          *****
228 REM*****
230 DEF PROCCALCULATE
240 YMAX=0 YMIN=100
```

```

250 FOR i=1 TO N-1
260 IF Y(i)>YMAX THEN YMAX=Y(i)
270 IF Y(i)<=YMIN THEN YMIN=Y(i)
280 NEXT i
290 ENDPROC
294 REM *****
295 REM *****
296 REM ***** PROCDRAW DRAW ON SCREEN *****
297 REM *****
300 DEF PROCDRAW
310 X=50
320 FOR I=1 TO N-1
330 REM Y(I)=Y(I)-YMIN
340 MOVE X,(Y(I)*900/YMAX) DRAW X,(Y(I)*900/YMAX)
350 X=X+1200/N NEXT
360 ENDPROC
370 REM*****
380 REM*****
390 REM***** PROCEDURE TO CALCULATE LIFETIMES STARTS HERE *****
400 REM*****
410 REM*****
420 REM
430 REM
440 REM
441 REM *****
442 REM *****
443 REM ***** PROCMEANLIFE *****
444 REM *****
445 REM *****
450 DEF PROCMEANLIFE
460 K1=0
470 FOR C=ST TO EN
480 J(C)=K1*Y(C)*tunc
490 K1=K1+tunc
500 NEXT
510 FOR G=ST TO EN
520 X = J(G)
530 X1 =X1+X
540 NEXT G
570 MEAN =X1
580 ENDPROC
590 REM
600 REM
610 REM
620 REM *****
630 REM *****
640 REM ***** PROCMEANLIFE 1 *****
650 REM *****
651 REM *****
652 REM
653 REM
660 DEF PROCMEANLIFE1
670 FOR C=ST TO EN
680 J(C)=Y(C)*tunc
690 NEXT
700 FOR H=ST TO EN
710 H1=H1+J(H)

```

```

720 NEXT H
740 MEAN1=H1
750 PRINT PRINT PRINT
760 REM THESE ARE THE TWO SUMS NEEDED*****
780 PRINT PRINT
800 PRINT
810 ENDPROC
820 DEF PROCBACKGROUND
830 Q1=NP-30 B=0
840 FOR I=1 TO 20 B=B+Y(I+Q1) NEXT
850 B=B/20
860 FOR I=1 TO NP
870 IF Y(I)<=B THEN GOTO 890
880 NEXT
890 NP=I
900 ENDPROC
910 DEF PROCHECK
920 I1=YMAX/EXP1
930 FOR I= 1 TO NP
940 IF Y(I) <I1 THEN GOTO 960
950 NEXT
960 EP1=I*time PRINT "1/EXP1 ",EP1
970 PRINT
980 I2=YMAX/EXP2
990 FOR I=1 TO NP
1000 IF Y(I)<I2 THEN GOTO 1020
1010 NEXT
1020 EP2=I*time PRINT "1/EXP2 ",EP2
1030 PRINT
1040 I3=YMAX/EXP3
1050 FOR I=1 TO NP
1060 IF Y(I)<I3 THEN GOTO 1080
1070 NEXT
1080 EP3=I*time PRINT "1/EXP3 ";EP3
1090 ENDPROC
1095 REM*****
1096 REM *****
1097 REM ***** REM DEF PROCZOOM *****
1098 REM *****
1099 REM*****
1100 DEF PROCZOOM
1110 *FX4,1
1120 C=50 HOLD=0 M=0 UZ=0
1130 MOVE C,0 PLOT 6,C,900
1140 PRINT TAB(0,0),"
1160 XS=GET$
1170 REM*****
1171 REM *****
1180 REM SELECTION OF GRAPH POINTS BEGINS HERE
1181 REM *****
1190 REM*****
1200 IF XS=CHRS(136) THEN PROCBAR(-1200/N)
1210 IF XS=CHRS(137) THEN PROCBAR(1200/N)
1220 IF XS="H" THEN PROCHOLD
1230 IF XS=">" OR XS="." THEN PROCBAR(10*1200/N)
1240 IF XS="<" OR XS="," THEN PROCBAR(-10*1200/N)
1260 IF XS="E" THEN PROCEXPAND

```

```

1270 IF M=1 THEN GOTO 1290
1280 GOTO 1160
1290 ENDPROC
1295 REM*****
1296 REM *****
1310 REM DEFINITION OF PROCBAR
1320 REM *****
1330 REM*****
1340 DEF PROCBAR(I)
1350 MOVE C,0 PLOT 6,C,900
1360 C=C+I
1370 IF C>1250 THEN C=50
1380 IF C<50 THEN C=1250
1390 MOVE C,0 PLOT 6,C,900
1395 POINT= (C-50)*N/1200
1400 PRINT TAB(0,0),"POINT NO " POINT
1410 ENDPROC
1420 REM*****
1421 REM *****
1430 REM SETTING THE CURSOR
1440 REM SETTING UP THE LINEHOLD
1444 REM *****
1445 REM*****
1446 DEF PROCHOLD
1450 PRINT.PRINT.PRINT
1470 UZ=1200/N.POINT=((C-50)/UZ)
1480 F=POINT
1500 PLOT 4,C,900
1510 PLOT 0,2,-4
1550 C=C+UZ MOVE C,0 PLOT 6,C,900
1560 ENDPROC
1565 REM*****
1566 REM *****
1567 REM ***** PROCEXPAND THE SECOND NUMBER *****
1568 REM *****
1569 REM*****
1570 DEF PROCEXPAND
1580 K=((C-50)*N/1200)
1590 PRINT F,K
1591 @%=&20207
1592 PRINT Y(F), Y(K)
1595 M=1
1600 ENDPROC
1601 REM*****
1602 REM *****
1603 REM ***** PROCINFO PRINTS THE ANSWERS *****
1604 REM *****
1605 REM*****
1610 DEF PROCINFO
1620 PRINT TAB(56,0)"FILENAME ",B$
1630 PRINT TAB(59,1)" "
1635 @%=10
1636 PRINT TAB(56,2)"NUMERICAL INT"N",
1640 PRINT TAB(56,4)"LIFETIME= ",X1/H1
1650 ENDPROC
1655 REM*****
1656 REM *****

```

```

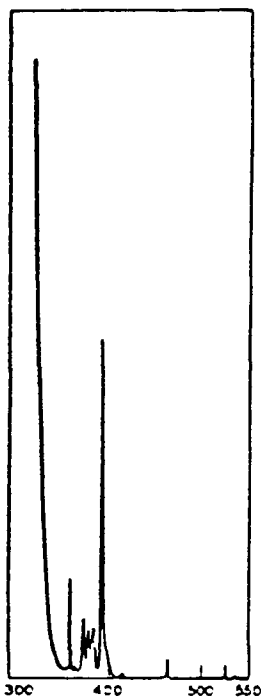
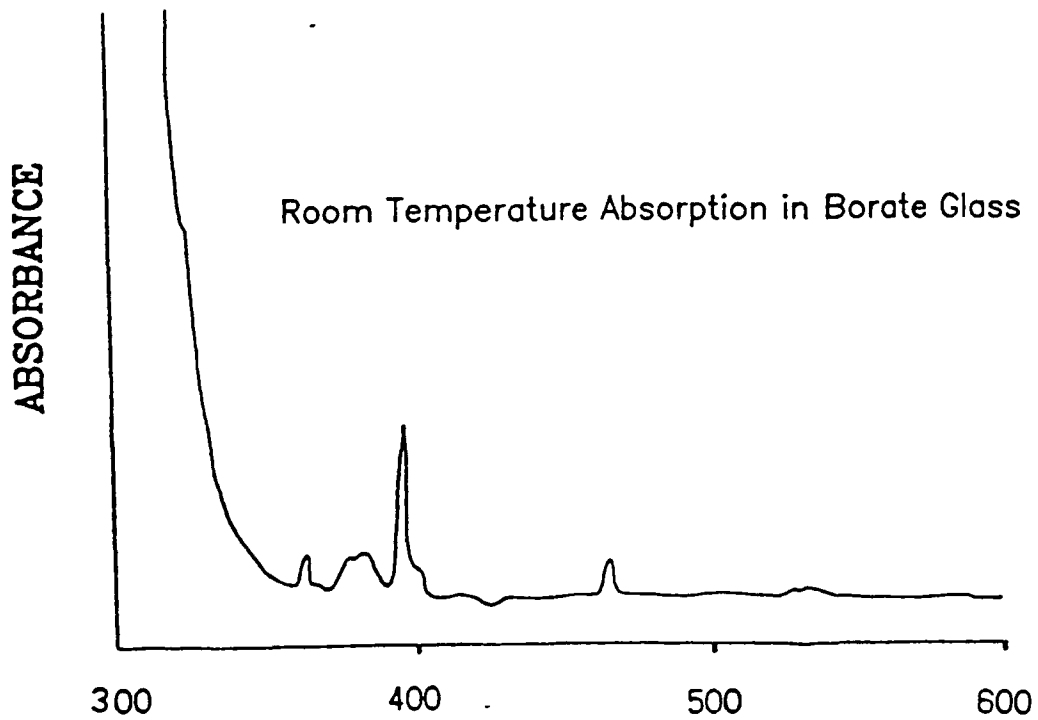
1657 REM ***** PROCSILPHO SIMPSONS METHOD *****
1658 REM *****
1659 REM*****
1660 DEF PROCSILPHO
1670 K1=0
1680 FOR C=ST2 TO EN2
1690 J(C)=K1*Y(C)*tume
1700 K1=K1+tume
1710 NEXT
1720 S=tume FL=J(ST2) LF=J(EN2) ER1=0 RE1=0 MEAN=0
1730 FOR Z=(ST2+1) TO (EN2-2) STEP 2
1740 ER=J(Z)
1750 ER1=ER1+ER
1760 NEXT Z
1770 FOR B=(ST2+2) TO (EN2-1) STEP 2
1780 RE=J(B)
1790 RE1=RE1+RE
1800 NEXT B
1810 MEAN=(S/3)*((FL+LF)+(4*ER1)+(2*RE1))
1820 ENDPROC
1821 REM*****
1822 REM *****
1823 REM ***** PROCSILPHO1 SECOND SIMPSON NUMBER *****
1824 REM *****
1825 REM*****
1830 DEF PROCSILPHO1
1840 FOR C=ST2 TO EN2
1850 J(C)=Y(C)*tume
1860 NEXT
1870 S=tume FL=J(ST2) LF=J(EN2) ER1=0 RE1=0 MEAN1=0
1880 FOR Z=(ST2+1) TO (EN2-2) STEP 2
1890 ER=J(Z)
1900 ER1=ER1+ER
1910 NEXT Z
1920 FOR B=(ST2+2) TO (EN2-1) STEP 2
1930 RE=J(B)
1940 RE1=RE1+RE
1950 NEXT B
1960 MEAN1=(S/3)*((FL+LF)+(4*ER1)+(2*RE1))
1966 @%=10
1967 PRINT TAB(56,8)"SIMPSONS MTH'D",
1968 PRINT TAB(56,10)"LIFETIME =", MEAN/MEAN1
1970 ENDPROC

```

Appendix 5

Absorption of Eu^{3+} in a Glass and a Liquid

This appendix contains absorption scans of Eu^{3+} in two different environments



Room Temperature Absorption in $\text{Eu}^{3+}(\text{NO}_3)_3$

Pump Wavelengths 318nm and 398nm